TECHNISCHE UNIVERSITÄT MÜNCHEN
Lehrstuhl für Makromolekulare Stoffe

Functionalization of poly(2-oxazoline)s with cyclic RGD peptides

Sonia Cesana

Vollständiger Abdruck der von der Fakultät für Chemie
der Technische Universität München zur Erlangung des akademischen Grades eines

Doktors der Naturwissenschaften

genehmigten Dissertation.

Vorsitzender:	Univ-Prof. Dr. St. J. Glaser
Prüfer der Dissertation:	1. Univ-Prof. Dr. O. Nuyken
	2. Univ-Prof. Dr. H. Kessler

Die Dissertation wurde am 22.09.04 bei der Technische Universität München eingereicht und durch die Fakultät für Chemie am 21.10.04 angenommen.

This work was performed from February 2001 to September 2004 at Lehrstuhl für Makromolekulare Stoffe at the Technische Universität München under the guidance of Prof. Dr.-Ing. Oskar Nuyken.

First of all I would like to thank *Prof. Dr.-Ing. Oskar Nuyken* for giving me the possibility to work by his research group, for completely supporting this work during the critical phases and for the interesting ideas during the development of the project.

I would also like to thank *PD Dr. Rainer Jordan* for the interesting research subject and for the discussions about the development of the project.

I would like to express my gratitude to *Prof. Dr. Horst Kessler* and his research group for the good cooperation, for giving me the possibility to access to their equipments and for the good atmosphere and hospitality. Especially of this group, I am grateful to *Dr. Ulrich Hersel*, *Dr. Claudia Dahmen*, *Dipl. Ing. Jörg Auernheimer* for the successful discussions about the work and for the help in the development of the ideas.

Dr. Roland Haubner I would like to thank for the peptide I received and for starting the cooperation.

I am very grateful to *Dr.-Ing. Heidi Samarian* for her help during the time spent at "Lehrstuhl" and for her availability.

Special thanks are for my labor colleagues, *Dr. Marcel Heller*, *Thomas Kotre*, *Eva Lichnerova*, *Martin Bortenschlager* and the "half present" *Dr. Ralf Weberskirch* for the nice atmosphere and for the music-fun we had in the lab besides the discussions about poly(2-oxazoline)s and chemistry in general.

I am very grateful to many collegues at the "Lehrstuhl für Makromolekulare Stoffe" not only for the work but also for the friendship I could build during these years with most of them. I hope I do not forget anybody… *Valérie Wiederhirn*, *Ursula Schmelmer*, *Christine Strissel*, *Doris Kaufmann*, *Annalisa Giró*, *Karin Lüdtke*, as the

"Frauenfraktion", *Bernhard Lerche*, *Steffen Jungermann*, *Tomaž Kos*, *Martin Mayershofer*, *Benjamin Roßbach*, *Mario Vierle*, *Erwin Bacher*, *Lars Friebe*, *Anton Förtig*, *Andreas Junger*, *Thomas Komenda*, *Daniel Käsmayr*, *Jens Krause*, *Robert Luxenhofer*, *Daniel Schönfelder*, *Alexander Wörndle*, *Tobias Zarka*, *Dr. Nicolas Stöckel*, *Dr. Dirk Schön*, *Dr. Harald Braun*, *Dr. Philipp Wieland*.

I would like to thank all the members of the NMR-crew, computer-crew, GPC-crew who made possible to measure the samples and *Brughard Cordes*, co-worker of Prof. Kessler's research group, for the ESI-MS measurements.

I am particularly grateful to *Ute Schnöller* and *Elsa Locardi* for their friendship in Munich, to my family *Paolo* and *Fabio Cesana*, *Alessandra Viganó* and to my extended family, my best friends, *Massimo Ferronato*, *Giorgia Bovati* (and family), *Francesca Villa*, *Lorenzo Santucci*, *Francesco Tedesco*, *Paolo Viola*, *Marco Mirenda*, *Giulia Mella*, *Giulia Gerosa*, *Mirko Riboldi* and *Alessandra Casiraghi* with whom I deeply kept in touch even if there are the alps in-between, *Ryan Clarke* and *Rafael Pena* even if there is the Atlantic ocean in-between.

Last but not least I am particularly grateful and indebit with *Helga Brebeck* and *Kuni Schindler* for giving me important advices, they were a great "mother-support" during my staying here in Munich and of course for their efficient work at "Lehrstuhl".

List of abbreviations

Ac	acetyl
Ahx	ε-aminohexancarboxylic acid
ACN	acetonitrile
BOC	*t*-butoxycarbonyl
CAM	chorioallantoic membrane
CDI	*N*,*N*-carbonyldiimidazol
DCC	dicyclohexylcarbodiimide
DCM	dichloromethane
DIPEA	diisopropylethylamine
DMAc	*N*,*N*-dimethylacetamide
DMF	dimethylformamide
DMSO	dimethylsufoxyde
ECM	extracellular matrix
EDCI	*N*-ethyl-*N*,*N'*-(dimethylaminopropyl)-carbodiimide
E.F.	end functionalization
EPR	enhanced permeability and retention
ESI-MS	electrospray ionization – mass spectroscopy
GPC	gel permeation chromatography
HEPES	2-[4-(2-hydroxyethyl)-1-piperazine]-ethane sulfonic acid
HOBt	1-hydroxybenzotriazole
HPLC	high performance liquid chromatography
HPMA	(*N*-(2-hydroxypropyl)methylacrylamide))copolymer
ICAM	intracellular adhesion molecule
M_n	numeral average of the molecular weights
M_w	weight average of the molecular weights
MALDI-TOF	matrix assisted laser desorption/ionization – time of flight
MES	2-morpholine ethane sulfonic acid
MeOH	Methanol
MeOTf	trifluoromethanesulfonate

MP	maximum peak
NCS	neocarzinostatin
NHS	*N*-hydroxysuccinimine
NMR	nuclear magnetic resonance
Pbf	2,2,4,6,7-pentamethyldihydrobenzofuran-5-sulfonyle
PDI	polydispersity index
PEG	polyethyleneglycol
PET	positron emission tomography
PMMA	polymethylmethacrylate
PyBOP	benzotriazole-1-yl-oxy-tris-pyrrolidino-phosphinium hexafluorophosphate
ppm	parts per million
RT	room temperature
S.C.F.	side chain functionalization
SMA	styrene maleic anhydride
SMANCS	styrene maleic anhydride – neo carzinostatin
SPECT	single photon emission computed tomography
^{t}Bu	*tert*-butyl
TEA	triethylamine
TEOA	triethanolamine
TFA	trifluoro acetic acid
THF	tetrahydrofuran
% -wg.	weight percentage

Index

1 Introduction

In the last 20 years, synthetic polymer chemistry entered in the field of medical chemistry,[1-5] and especially, in cancer research.[6,7]

In industrial countries, cancer is one of the most frequent causes of death. Referring to the data given by the American Cancer Society Inc., cancer is the second cause of death in the USA (data referred to year 2001) with 22.9 % of all deaths (553.768 No. of deaths).[1] Among the causes of this disease cigarette smoke, not healthy nourishment habits and the use of chemicals can be named.[8]

An isolated abnormal cell that does not proliferate more than its normal neighbors does not significant damage, but if its proliferation is out of control, it will give rise to a tumor, or neoplasm. As long as the neoplastic cells remain clustered together in a single mass, the tumor is said to be benign, and a complete cure can usually be achieved by removing the mass surgically. A tumor is counted as cancer only if is malignant, that is, only if cells have the ability to invade surrounding tissue. Invasiveness usually implies an ability to break loose, enter the blood stream and form secondary tumors or metastases at other sites in the body. The more widely a cancer metastasizes, the harder it becomes to eradicate.[9]

Both, the inner working of cells and their social interactions must be understood, to understand cancer and to device rational ways to treat it. This disease has a great importance in cell biology because it reflects the disturbances of the most fundamental rules in a multicellular organism. A much wider area of medical knowledge than that of cancer alone has profoundly benefited of the efforts put in cancer research.[9]

The approach followed in this work is the intervention in the angiogenesis process by using RGD peptides, which selectively interact with $\alpha_v\beta_3$-intergrin cell receptors.[10-13]

Tumor cells stimulate endothelial cells for the formation of new blood vessels,[14,15] which are necessary for its survival[16.17] but they also allow invasive cells to migrate in other parts of the body and to form metastasis. The formation of these new blood vessels is called angiogenesis.

[1] http://www.cancer.org/docroot/STT/stt_0.asp, 2004

The purpose of this work was to design a new molecule and to introduce it in diagnosis of tumor. Poly(2-oxazoline)s should be used as polymeric carrier for pharmaceutically active molecules, therefore, they should be functionalized with cyclic RGD peptides, as targeting molecule. Afterwards, the newly formed peptide-polymer conjugate should be radio labeled and examined with the common techniques used in the radio diagnosis of tumors.

This work was performed in cooperation of Prof. Kessler's research group (TU München) and Dr. Haubner's research group (Klinikum Rechts der Isar, TU München) who synthesized the cyclic RGD peptides.

2 Background

2.1 Integrins

Cell adhesion is the process how cells recognize and bind to one another as they move and assemble into tissue organs. The extracellular matrix (ECM) and the cell surface receptors are involved in this process: cells use cell receptors to bind to the ECM.
The ECM is composed of a variety of proteins and polysaccarides that are locally secreted by the cells and assemble to an organized network in close association with the surface of the cells that produced them. The ECM has two main functions: it provides a scaffold which stabilizes the physical and mechanical structure of the tissues, and it also regulates the cellular behavior of the cells in contact with the ECM, i.e. it influences their survival, development, migration, proliferation, shape and function.[9]

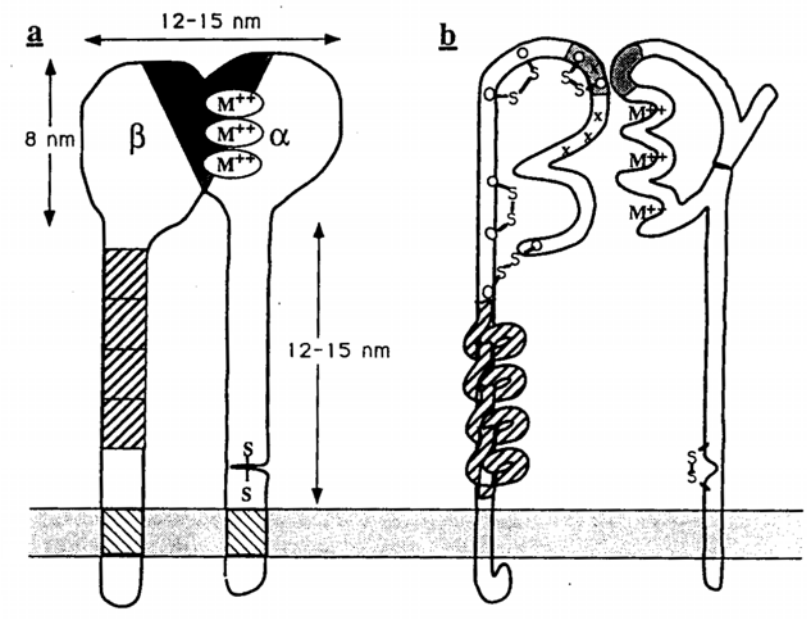

Fig. 2.1 Schematic representation of integrins. Taken from [18]

Cell receptors can be cathegorized into four classes: integrins,[18] cadherines,[19,20] immunoglobine-superfamilies[21,22] and selectins.[23,24]

Integrins are heterodimeric proteins composed of α and β subunits, which are not covalently bound. Up to date 18 α and 8 β subunits are known in mammals and their association form 24 different heterodimers.[18,25-27] The α subunits are sequences of 1100 amino acids which can be divided into two long chains connected together by S-S bridges,[28] whereas β subunits are composed of less than 800 amino acids (except for β4, ca. 1750 amino acids).[29] The structure within each subunit is stabilized by disulfide bridges, introduced by cysteine, and by divalent cations (such as Ca^{2+}, Mg^{2+}, Mn^{2+}),[30] (Fig. 2.1).

Integrins were originally characterized as a family of cell surface receptors responsible for anchoring cells to the ECM, but further studies showed the impact on dynamic processes in cells such as intracellular signaling and gene expression that leads to cell migration proliferation, differentiation and survival.[31,32] A crucial characteristic of integrins is that their activation is of equal importance as their inactivation. In case of cell adhesion, the inactive state of integrins allows cells not to bind at the wrong time and place. Inappropriate adhesion of platelets and leukocytes, for example, leads to thrombosis and inflammation. In case of cell migration, the inactive state of integrins allows cells to detach from the ECM they previously attached to.[18] (Fig. 2.2)

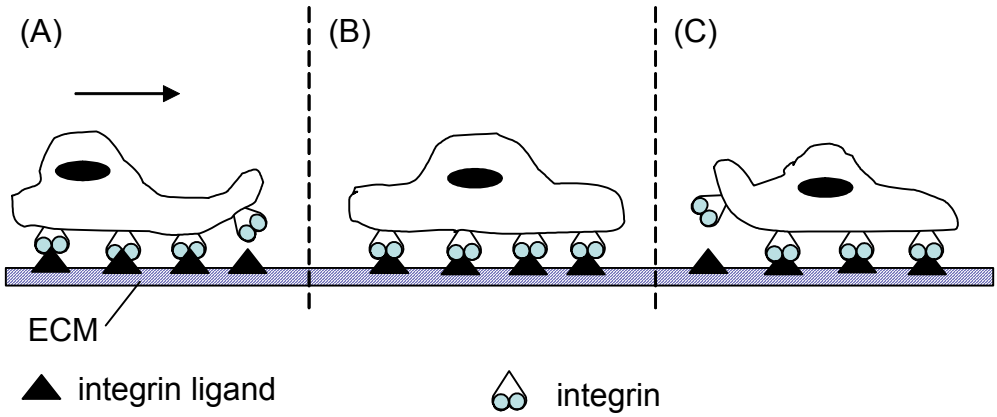

Fig. 2.2 Cell migration. (A) the cell stretches in the direction of the next integrin receptor of the ECM (extracellular matrix), (B) binding of the integrin with the integrin receptor of the ECM, (C) detachment of the integrin with the integrin receptor of the ECM. Taken from [33].

Most integrins are expressed in a wide variety of cell types and most cells express different integrins. However, the function of many integrins is still not clear and currently under investigation.[18]

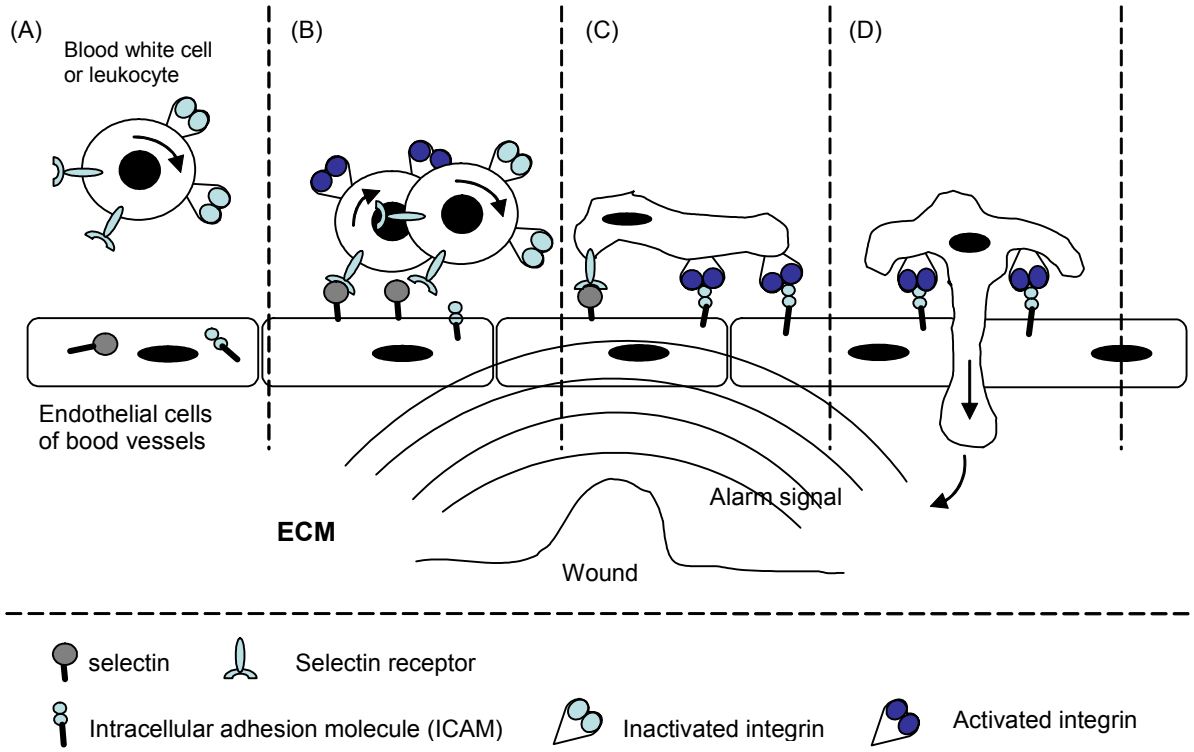

Fig. 2.3 Cell adhesion in case of wound. Endothelial cells are activated by the alarm signal given by the wound, they express selectine and ICAM (intracellular adhesion molecules) (A). Selectins bind to selectin receptors and integrins are activated (B). Activated integrins bind to ICAM (C) and leukocytes migrate to repair the wound (D). Taken from [33].

It has been demonstrated that integrins are involved in several human genetic diseases, such as thrombosis, inflammation and cancer. This supports their importance in various physiological and pathological processes. A schematic representation of integrins behavior in case of inflammation is presented in Fig. 2.3. Leukocytes roll in the blood vessels. Endothelial cells, which constitute the walls of blood vessels, are activated by the alarm signal given by the wound. They express selectine and ICAM (intracellular adhesion molecules) (A). The first binding is between the selectine and selectine-receptors on the leukocytes (B) and the simultaneous activation of integrins. Selectine binding is weak and the cell could soon detach. Activated integrins bind to ICAM molecules (C) and the leukocytes migrates to repair the wound (D).[33,34]

The ability to interfere with integrin functions using antibodies or peptides offers many opportunities for a therapeutic intervention in diverse diseases.[18,25]

2.2 RGD Peptides

As briefly introduced, the possibility to interact with integrins using antibodies or peptides represented a big challenge for scientists in the last two decades. In the '80s *Pierschbacher* and *Ruoslahti* tested different amino acid sequences taken from fibronectin, one of the most important ECM proteins, and demonstrated that the amino acid sequence responsible for the integrin binding could be reduced to three amino acids: arginine (R), glycine (G) and aspartic acid (D) (Fig. 2.4).[35,36]

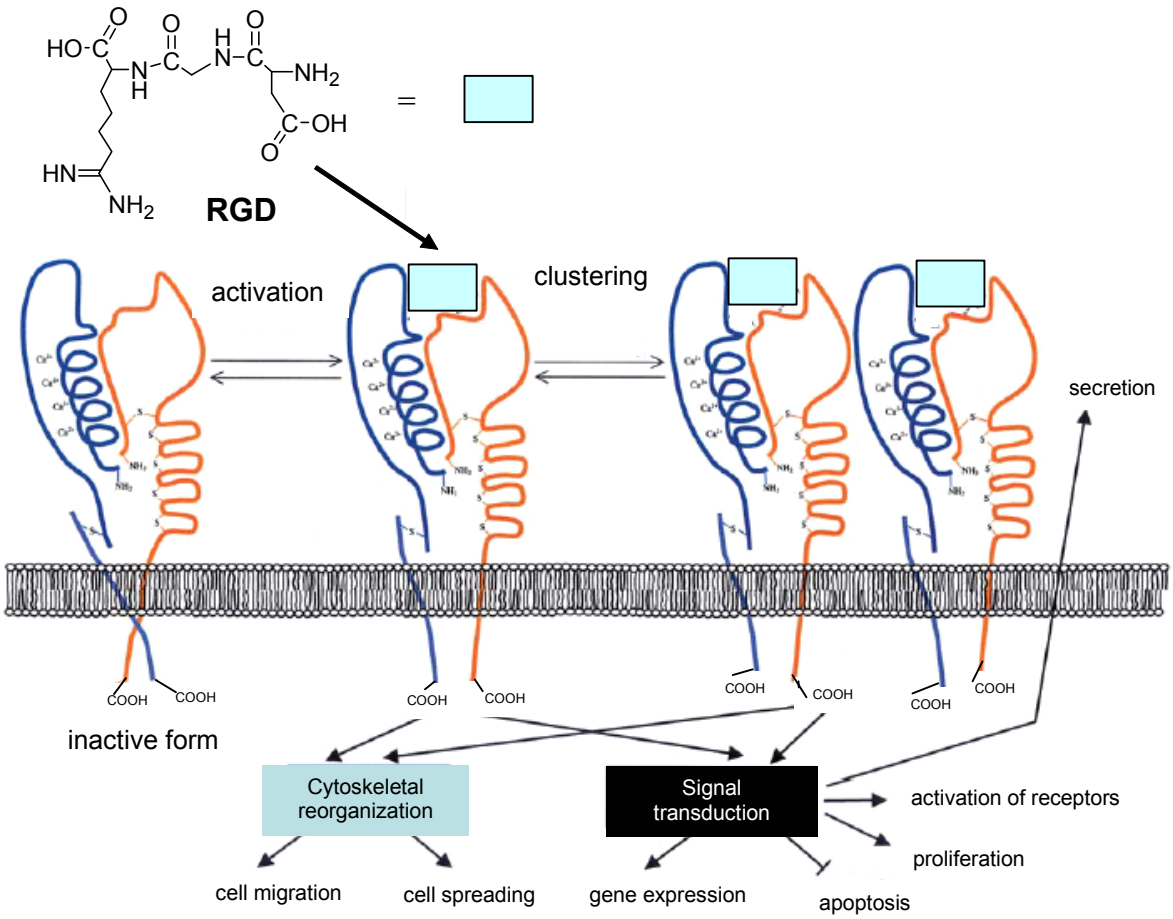

Fig. 2.4 Interaction between RGD peptides and $\alpha_v\beta_3$-integrins. Taken from [37]

In the last 20 years RGD peptides occupied a central role in cell adhesion biology as the prototype adhesion signal, because of its small size the RGD sequence could be easily reproduced and investigated. Short peptides containing the RGD sequence can mimic cell adhesion proteins in two ways: when coated onto a surface, they promote cell adhesion, whereas in solution they act as inhibitor preventing adhesion.[38]

Several variations of the RGD system were also studied:[35,39]

- Small changes in the side chains of the amino acids, e.g. glutamic acid instead of aspartic acid or alanine instead of glycine, reduce the activity of the peptide in cell attachment assays 100-fold or more.[38,40]
- The conformation of the amino acid alters the binding specificity if aspartic acid is in the D-form but has no effect if arginine is in the D-form.[38,41]

Further developments of these studies led to cyclic peptides, where the RGD sequence is flanked by other amino acids to build a ring system, it confers more stability and selectivity.[37,42]

Prof. *Kessler´*s research group was the first who introduced the cyclic pentapeptide as small integrin antagonist.[45,46] Giving a detailed characterization of penta- and hexapeptide conformations (spacial screening) and supporting the results with biological tests, Prof. *Kessler´*s research group was able to conclude that the pentapeptide sequence RGDfX (see Fig. 2.5) was high selective to $\alpha_v\beta_3$ integrins.[45-47]

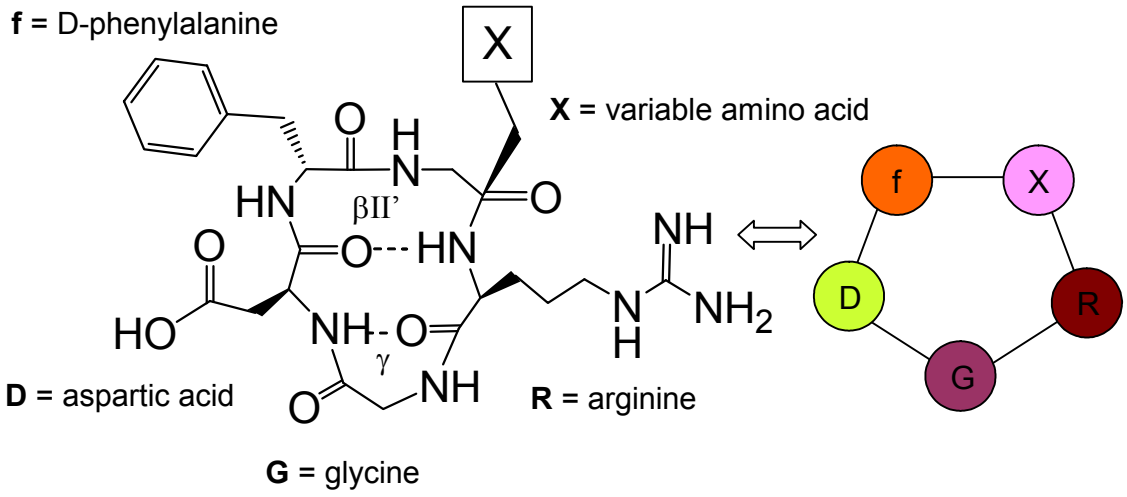

Fig. 2.5 Structure of the cyclic RGDfX peptide, the carbon atoms in alfa position of each amino acid are symbolized with a circle and the schematic representation of the cyclic pentapeptide on the right side will be used in this work.

The stereoisomerism has a great influence on the biological activity of cyclic peptides. On the basis of previous results, which showed that hydrophobic phenylalanine increases the receptor binding affinity,[48] a conformational control in the cyclic hexapeptides and cyclic pentapeptides was introduced by incorporating D-amino acid. In cyclic pentapeptides the introduction of a D-amino acid induces a characteristic turn motif. The D-amino acid strongly prefers the i+1 position of a βII' turn and gives rise to a βII-γ turn arrangement. as shown in Fig. 2.5. The fifth amino acid X was demonstrated to produce only a slight effect on the biological activity.[45,49]

Together with RGD peptides also other systems such as peptide mimetica have been developed.[37,50-52]

Cyclic RGD peptides have been developed for various purposes: fibrogen receptor antagonists, selective $\alpha_v\beta_3$ integrins antagonists for treatment of human tumor and tumor-induced angiogenesis, phagocytosis of cells undergoing apoptosis, bone remodeling and osteoporosis, diabetic retinopathy and actual renal failure.[37]

This work is focused on cyclic RGDfX peptides as highly selective $\alpha_v\beta_3$-integrins ligands and their application in radionuclide diagnostic as well as for the treatment of human tumor tissue.

2.3 Angiogenesis in tumor cells

Angiogenesis is the growth of new blood vessels by sprouting from existing ones. Angiogenesis and neovascularization are critical for normal physiological processes, such as embryonic development and wound repair. However, angiogenesis also facilitates tumor growth, retinopathy and various inflammatory disorders.[9]

The growth and the metastatic properties of solid tumors are directly influenced by the process of angiogenesis. Primary tumor growth depends on nutrients supplied by blood vessel infiltration while these same vessels will also serve as channel for invasive cells and thereby the metastatic process will be much faster.[53,54]

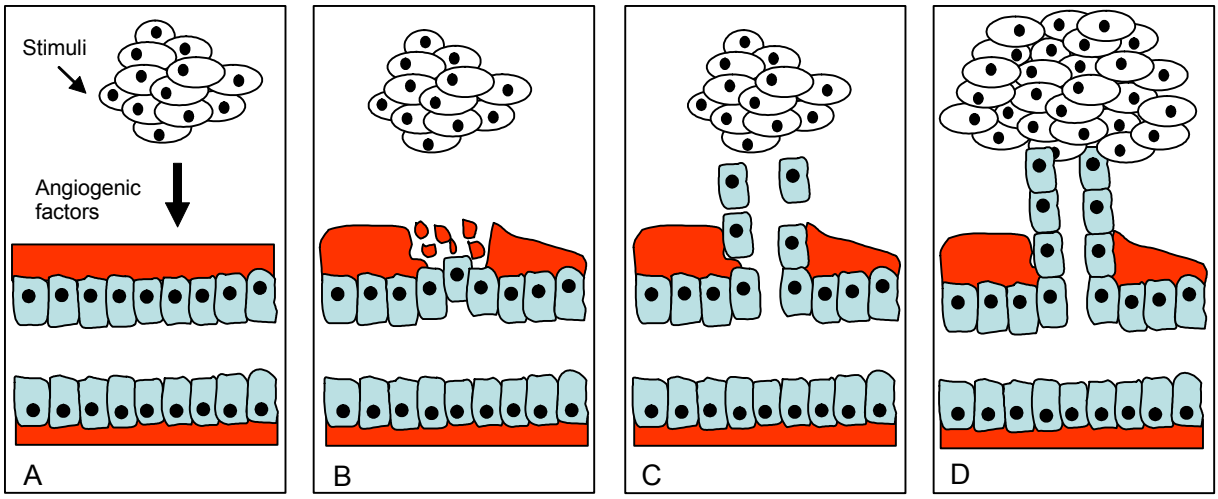

Fig. 2.6 Schematic representation of the different phases in the angiogenic process. A)Tumor cells are activated by different stimuli (e.g. hypoxia, stress, genetic mutations). Excretion of angiogenic factors subsequently activates endothelial cells of existing vessels; B) proteolytic enzymes secreted by endothelial cells degrade the basement membrane; C) activated endothelial cells express adhesion receptors (e.g. $\alpha_v\beta_3$ integrins) allowing migration through the extracellular matrix during the vessel formation; D) capillary organization and stabilization of the cells. Finally the endothelial cells reorganize by forming tight junctions. Taken from [14].

Tumor angiogenesis is a multi-step cascade process involving activation of endothelial cells by angiogenic stimulators resulting in endothelial cell proliferation, endothelial cell migration and tube formation. The tumor cells, activated by different stimuli, excrete angiogenic factors, which subsequently activate endothelial cells of existing vessels. Proteolytic enzymes secreted by endothelial cells degrade the basement membrane and activate the endothelial cells, which express adhesion receptors (e.g. $\alpha_v\beta_3$ integrins) allowing migration through the ECM during the vessel formation. Finally, endothelial cells reorganize by forming tight junctions (Fig. 2.6).[14]

The multi-step process of angiogenesis offers several potential targets for therapeutic strategies, some of these steps have been characterized, but the whole process is still not understood.[54,55] Integrins, as cell receptors, play an important role in tumor-induced angiogenesis, as briefly described, endothelial cells exposed to growth factors, or those undergoing angiogenesis in tumor, wounds, or inflammatory tissue, express high levels of $\alpha_v\beta_3$ integrins.[56,57] The use of blocking reagents (antibodies, peptides and peptomimetics) to inhibit the functions of various integrins has been used most intensively to investigate functions of α_v integrins but they also represent a strategy against tumor growth, consequently, antiangiogenic treatment strategies have been

developed.[38] Different kind of experiments demonstrated that inhibition of angiogenesis, achieved by antibodies against $\alpha_v\beta_3$-integrins or RGD-containing peptides for blocking integrins–binding sites, resulted in decreasing of blood vessel formation in a mouse Matrigel model of angiogenesis,[58] apoptosis of antiangiogenic blood vessel in a melanoma model on chick allantoic membrane,[52] regression of preestablished human tumors growing in laboratory animals[59] and a reduction of tumor progression in a chemically induced colon carcinoma in model rats.[60] An example about these studies is presented in Fig. 2.7. *Brooks et al*.[52] examined the ability of the cyclic pentapeptide, RGDfV, as an antagonist of $\alpha_v\beta_3$-intergrins to disrupt angiogenesis when injected intravenously. In this experiment angiogenesis was initiated with fragments of $\alpha_v\beta_3$-negative human melanoma tumor cells (M21-L) on chick chorioallantoic membranes (CAMs) of 10 day old embryos. After one day the embryos received a single intravenous (IV) injection of the cyclic peptide (RGDfV) or of the control peptide (RADfV)[2] and after three days the tumor was removed, analyzed and photographed with a stereo microscope. Within two days the cyclic RGD peptide disrupted tumor induced angiogenesis, as shown in Fig. 2.7A (middle panels) yet had no effect on preexisting adjacent vessels within these same CAMs (right panels). In contrast, the control cyclic peptide had no effect on tumor-induced angiogenesis (left panels). Examination of tumor treated with the active peptide revealed that angiogenesis had been stimulated; however, the few vessels remaining appeared disrupted and discontinuous. (Fig. 2.7B)

[2] RADfV: Peptide composed of arginine, alanine , aspartic acid phenylalanine and valine, it does not interact with $\alpha_v\beta_3$ integrins

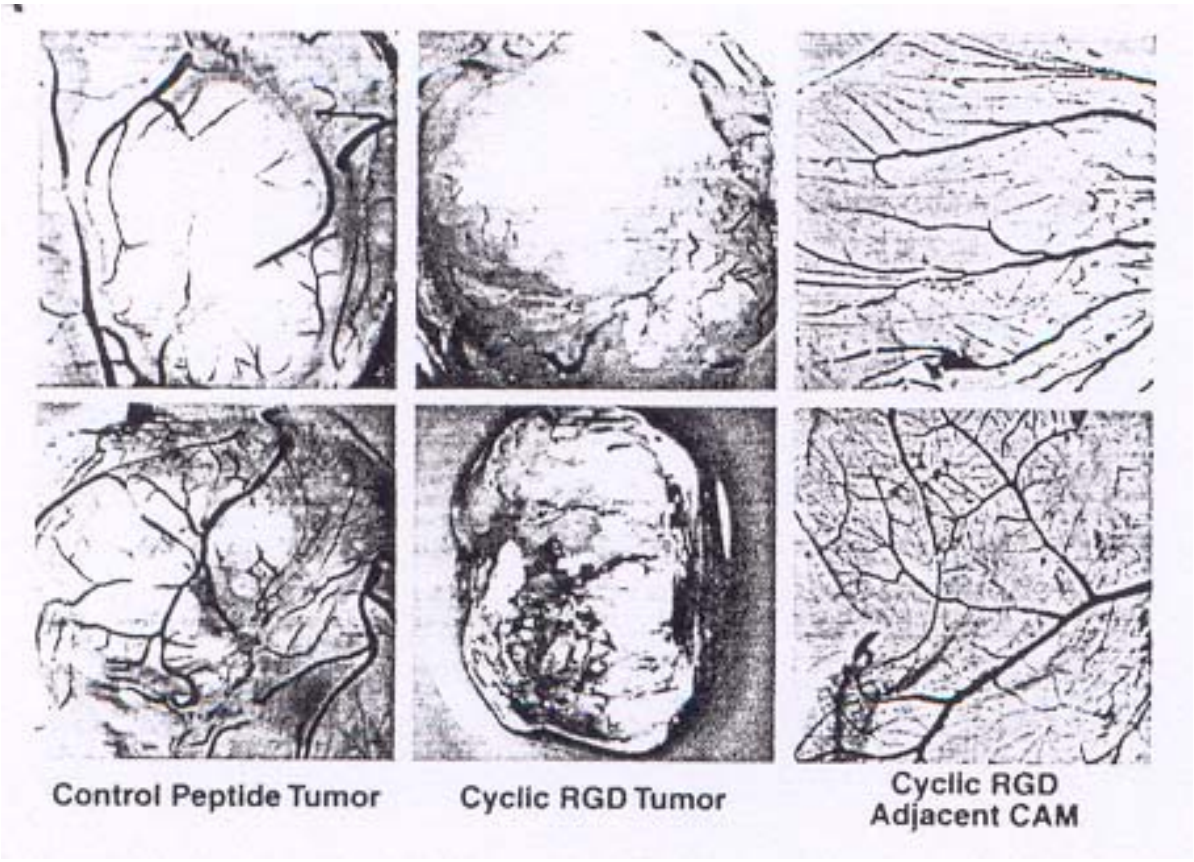

Fig. 2.7 Intravenous administration of $\alpha_v\beta_3$-antagonists inhibit tumor-induced angiogenesis. Human M21-L melanoma tumor fragments were implanted on the CAMs (chick chorioallantoic membranes) of a 10 old embryos. After two days the tumor was removed, analyzed and photographed with a stereo microscope. (A) control cyclic RAD peptide, left panel; cyclic RGD peptide, middle panel; adjacent CAMs tissue taken from the same embryos treated with cyclic RGD peptides, right panel. (B) High magnification of peptide-treated tumor. The left panel represent normal vessel from control-treated tumor, and the right panel represents examples of disrupted blood vessels treated with the control peptide (arrows). Taken from [52].

2.4 Radiodiagnosis of tumor

The usual procedure against cancer is to surgically remove the primary tumor or to irradiate it with a strong beam, locally directed, until the tumor disintegrates. As second step, further irradiation and chemotheraphy are necessary to destroy the remaining cancerous cells in the body that survived the first step.[8]

Therapeutic doses of radiations can be delivered to sites of desease, such as cancer, in three ways: external beam radiation, implantable "seeds" or systemic administration. The systemic administration of radiopharmaceuticals provides the opportunity for the treatment of disseminated diseases. Therapeutic radiopharmaceuticals are radiolabeled molecules designed to deliver therapeutic doses of ionizing radiation to specific disease sites. A schematic representation of such molecules is given in Fig. 2.8.[61]

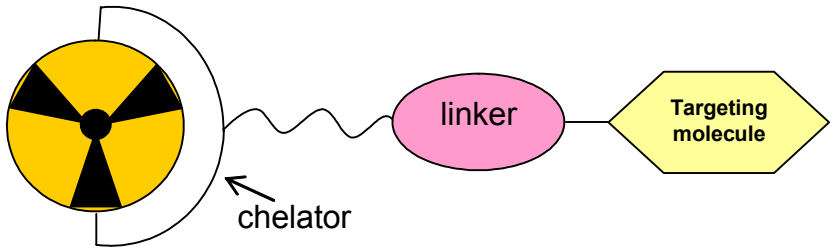

Fig. 2.8 Radiopharmaceuticals are composed of a targeting molecule, a linker, a chelator and a radio nuclide. Taken from [62].

The four parts which constitute a metallopharmaceutical are: a targeting molecule, a linker, a chelator and a metallic radionuclide. Combining biochemistry, as it concerns the targeting molecule and the linker, and radiochemistry, as it concerns metal isotopes and their corresponding chelators, a number of radiolabeled small peptides have been studied for their potential use in tumor therapy and diagnosis. These studies incremented the research in the synthesis of new therapeutic radionuclides, as well as of new bifunctional chelators.[61]

The same concept of molecule as it concerns the radiopharmaceuticals can be applied for the radio therapy as well as for the radio diagnosis of cancer. A variety of

radionuclides have been employed to expand the choice of emission characteristics and half lives for diagnostic (γ and β^+ emitters) and therapeutics (β^- and α emitters) applications.[62-64]

The usual techniques used for tumor imaging are positron emission tomography (PET) and single photon emission computed tomography (SPECT), the spatial resolution of nuclear medicine imaging can delineate tumor voxels[3] whose dimension approach 0.5 cm on a side.[65-67]

Linear RGD peptides have been labeled with ^{99m}Tc, ^{188}Re, ^{90}Y and ^{111}In, whereas the cyclic RGD peptides have been labeled with ^{125}I, ^{111}In and ^{18}F. Radiolabeled cyclic RGD peptides are able to target tumor tissue after intravenous injection in a xenograft mouse model.[73]

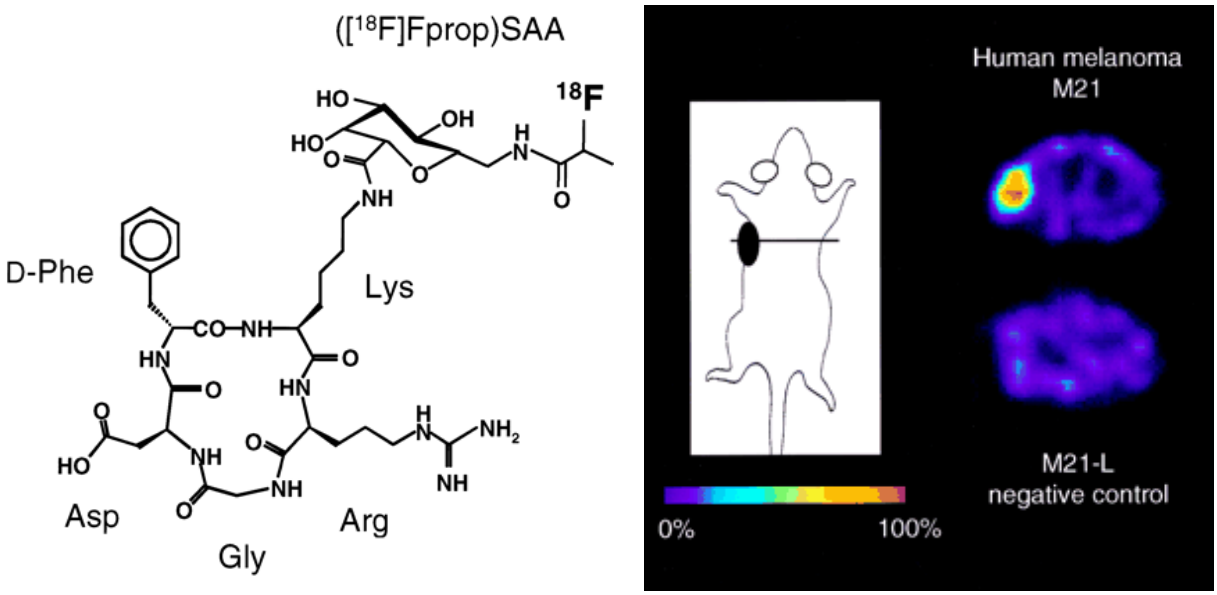

Fig. 2.9 The radiolabeled RGD, [^{18}F]galacto-RGD, on the left side. On the right side, transaxial small animal PET (positron emission tomography) images of nude mice bearing human melanoma xenografts. Images were acquired 90 min after injection of the [^{18}F]galacto-RGD. The top right image shows selective accumulation of the tracer in the $\alpha_v\beta_3$-positive (M21) tumor on the left flank. In contrast, no focal tracer accumulation is visible in the $\alpha_v\beta_3$-negative (M21-L) control tumor (bottom right image). Taken from [66].

[3] Volume rendering, or more generally spoken volume graphics, is a sub-specialty of 3D computer graphics which is concerned with the discrete representation and visualization of objects represented as sampled data in three or more dimensions. A volume/*voxel* data set is a three-dimensional array of *voxels*. The term *voxel* is used to characterize a volume element; it is a generalization of the notion of *pixel* that stands for a picture element.

In Fig. 2.9 an example of the application in tumor imaging is presented. *Haubner et al.* synthesized [^{18}F]Galacto RGD (the structure is presented on the right side of the figure) and demonstrated that this compound is suitable for noninvasive imaging of $\alpha_v\beta_3$-integrin expression using PET. The top right image shows selective accumulation of the tracer in the $\alpha_v\beta_3$-positive (M21) tumor on the left flank of the mouse. In contrast, no focal tracer accumulation is visible in the $\alpha_v\beta_3$-negative (M21-L) control tumor, bottom right image.[66]

2.5 Polymer therapeutics

In the '70s *Ringsdorf* described a model of a pharmacological active polymer:

> *To be pharmacologically active, the polymer must have a biostable and biodegradable backbone which is used as carrier for at least three different units. One area of the polymer is used to make the whole macromolecule soluble and non toxic, the second area is the region where the pharmacon is fixed; and the third area incorporates a transport system, the crucial property of which is represented by its ability to carry the whole polymer to the target cells. The separation of the different areas along the polymer chain may be accomplished by statistical polymerization or by block copolymerization.*[74] (Fig. 2.10)

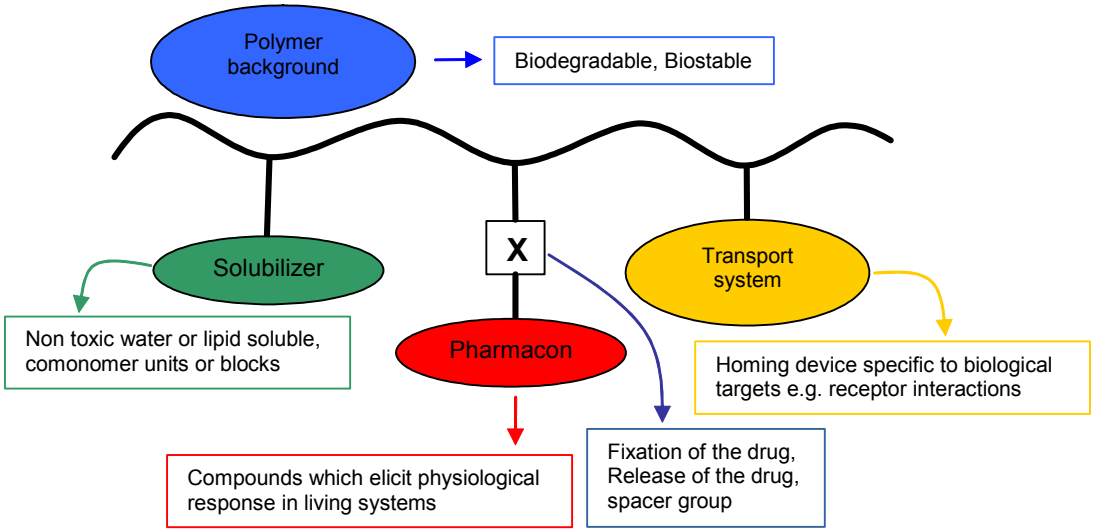

Fig. 2.10 *Ringsdorf*'s model for a pharmaceutically active polymer. Taken from [74].

Within the last 30 years this concept has been extended to what is called today 'polymer therapeutics', (Fig. 2.11) this term includes polymeric drugs, polymer-drug conjugates, polymer-protein conjugates, polymeric micelles, to which a drug is covalently bound, and multicomponent polyplexes, that are being developed as non-viral vectors.[6]

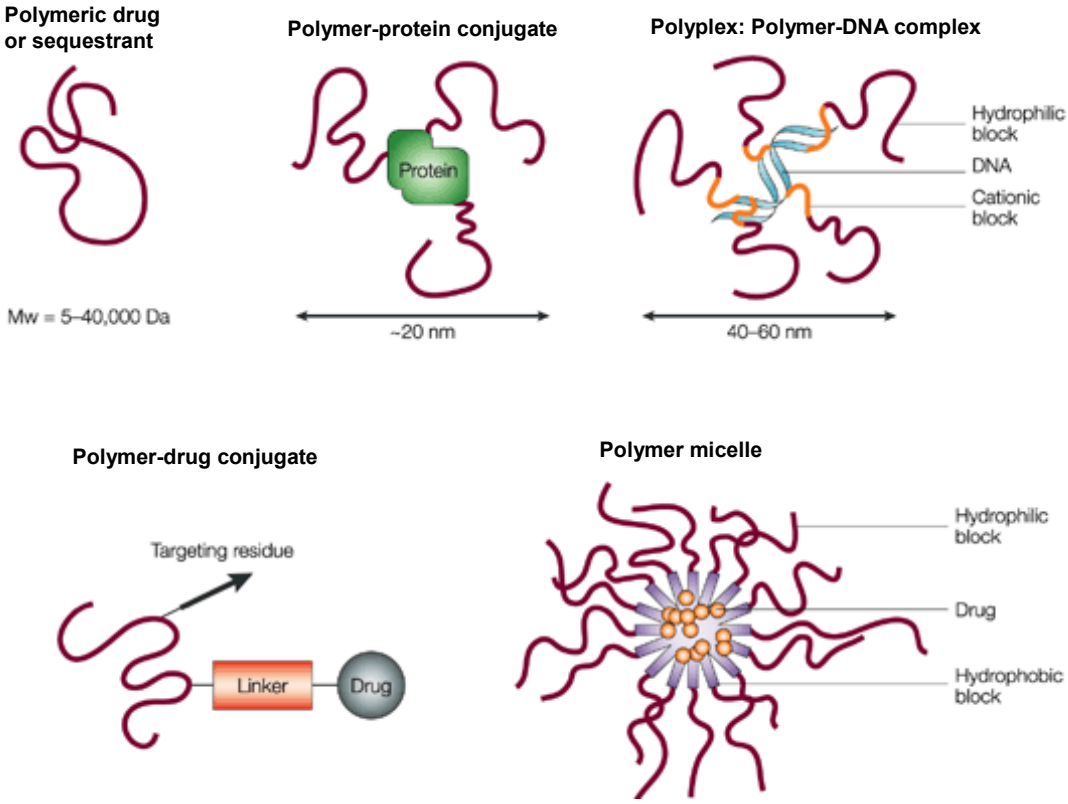

Fig. 2.11 Polymer therapeutics. Taken from *Duncan et al.* [6].

The "polymer pioneer" in medicinal chemistry was polyethylenglycol (PEG).[1] In the '70s it was discovered that PEG improved the pharmacokinetic[4] and pharmacodynamic[5] properties of polypeptide drugs by increasing solubility, reducing renal clearance and reducing toxicity. It is not degradable in the body and it is eliminated by kidneys (for PEGs < 30 kDa) or in the feaces (for PEGs > 20 kDa).[75]

[4] Pharmacokinetics: the movement of drugs throughout the body including their absorption, distribution, metabolism and excretion, and the mathematical models that describes these actions.
[5] Pharmacodynamics: changes in measurable clinical parameters related to a drug, such as increase in antitumor activity, decrease in nausea or decrease in viral loaded.

PEG has taken 20 years to emerge as a viable pharmaceutical tool. Nowadays, it can be found in combination with chemotherapy for different kind of leukaemia (as Oncaspar®),[76] as once-a-week treatment for hepatitis C (as PegIntron®)[77] and as hydrogel used in the lungs following removal of lung tumors or other chest surgeries (as FocaSeal®).[78] This hydrogel naturally degrades and dissolve. Spraygel® [79] is also a biodegradable hydrogel that prevents post-operative adhesion formation.[1]

R. Duncan's research group developed a system based on N-(2-hydroxypropyl)methacrylamide) (HPMA) as polymer carrier and doxorubicin as drug. (Fig. 2.11) It is commonly used in the treatment of carcinoma of the breast, lung, thyroid, ovary and soft tissue sarcomas.[6,80-82]

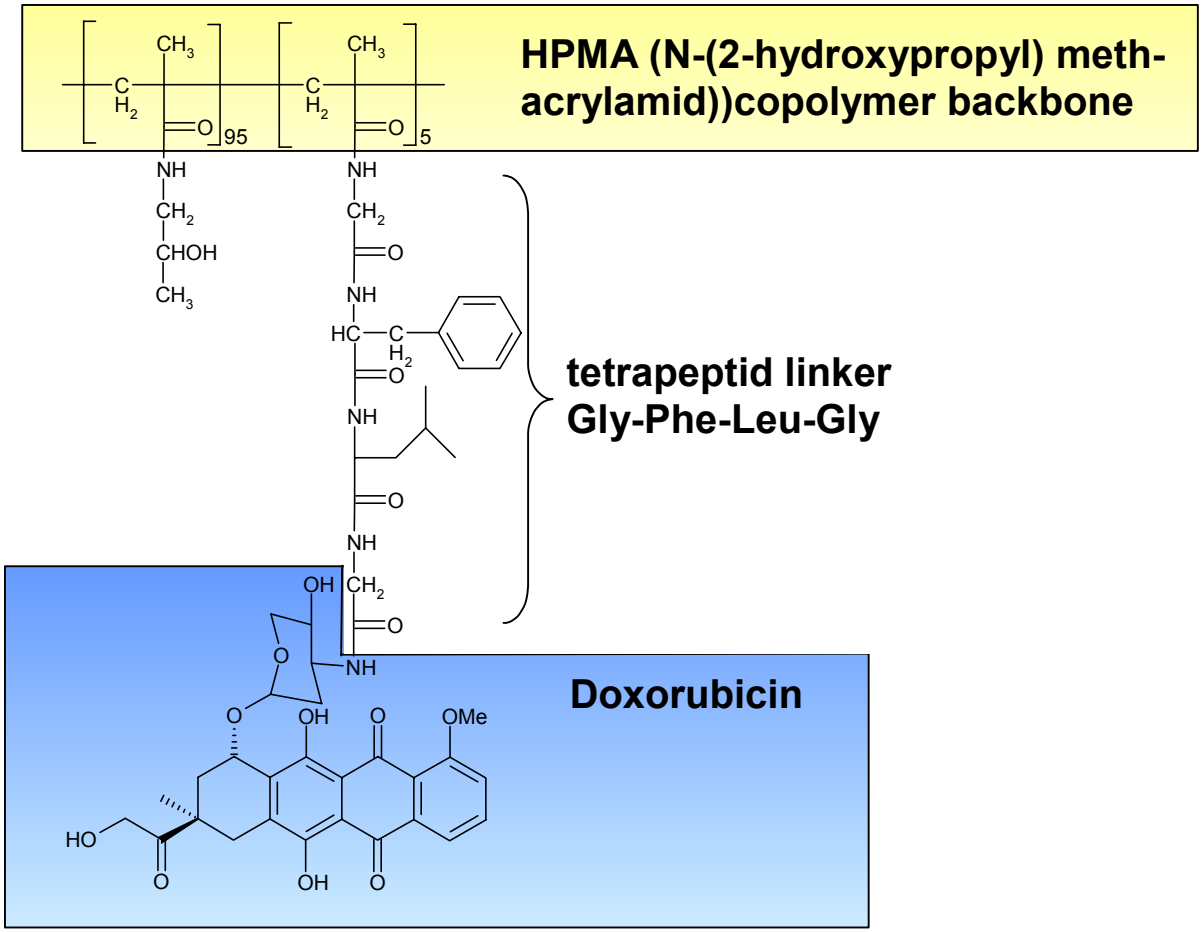

Fig. 2.12 Chemical structure of the system studied by *R. Duncan et al.* based on HMPA (N-(2-hydropropyl)methacrylamide) as polymeric carrier and doxorubicin as pharmacon connected by a linker. Taken from [6].

The mechanism behind the successful application of macromolecules as carriers is the EPR effect (EPR = enhanced permeability and retention).[6] The EPR effect was first

observed by *Maeda et al.* who tested the pharmacokinetic of the polymer-protein conjugate styrene maleic anhydride (SMA) – neocarzinostatin (NCS) called SMANCS.[83-86] This effect was afterwards confirmed for long-circulating macromolecules in general. Long-circulating macromolecules passively accumulate in tumor tissues by the EPR effect and intravenously administered drug-delivery systems can increase the tumor concentration of antitumor drugs up to 70-fold. The EPR effect was attributed by *Maeda* to two factors: the disorganized pathology of angiogenic tumor vasculature with its discontinuous endothelium leading to hyperpermeability to circulating macromolecules and the lack of effective tumor lymphatic drainage, which lead to subsequent macromolecular accumulation.[87]

Polymer chemistry offers a various number of structures, such as branched polymers,[88] graft polymers,[89,90] dendrimers,[4,91,92] block copolymers,[93] peptide derivatives,[94] which means many possibilities to build new structures.[6,95]

Even if the first results encourage the application of polymers in medical field, there are still many problems to be solved for polymer therapeutics. They are very well tolerated in humans but most of them are not biodegradable in the main chain. In the body, polymers are mainly eliminated through the kidneys if their molecular weight is below the renal threshold (~ 40 kDa). This represents a limitation for ensuring maximal tissue/tumor targeting.[1,96]

In this work, among all the polymers, the attention will be focused on poly(2-oxazoline).

2.6 Polymer background

Living polymerization

2-Oxazoline polymerization belongs to the class of the living polymerization as defined by *Szwarc*.[96] The mechanism of the living polymerization is given by the following bimolecular reactions, where I is the initiator, M is the monomer, $A^{\pm}$ is the active species and $P_n^{\pm}$ is the growing chain.

$$I + M \xrightarrow{k_i} A^{\pm} \qquad (2.1)$$

$$A^{\pm} + M \longrightarrow P_1^{\pm} \qquad (2.2)$$

$$P_n^{\pm} + M \xrightarrow{k_p} P_{n+1}^{\pm} \qquad (2.3)$$

The reaction governing the kinetics is the propagation ($k_i >> k_p$) hence k_p determines the reaction rate.

In absence of impurities, it can be assumed that during the propagation no other reactions, such as chain transfer reaction or termination by combination, are considered to happen and the concentration of the growing chain remains constant throughout the propagation reaction. The chain ends are stable and can only react with the monomers.

Referring to the reactions given above (2.1), (2.2), (2.3) the rate of the polymer propagation is:

$$r_p = - \frac{d[M]}{dt} = k_p [M] [P_n^{\pm}] \qquad (2.4)$$

Where $[P_n^{\pm}]$ is the concentration of the growing chain and [M] is the concentration of the monomer. Integration of equation (2.4) results in:

$$\ln \frac{[M]_0}{[M]_t} = k_p [P_n^{\pm}] t \qquad (2.5)$$

Where $[M]_0$ is the initial concentration of the monomer and $[M]_t$ is the monomer concentration at a certain time in terms of conversion (ξ) equation (2.5) yields:

$$- \ln (1 - \xi) = k_p [P_n^{\pm}] t$$

Plotting ln (1-ξ) vs. t, k_p can be directly obtained from the slope of the curve.

Considering that every monomer can react with every growing chain and the mixture is ideal, it can be followed that the average chain length is the same for all the

polymers. As a consequence, the molecular weight distribution is only depending on the probability that a given monomer reacts with one of the present active chain ends.
Advantages of living polymerizations are linear chains, direct control of the chain length by the initial monomer to initiator ratio ($[M]_0/[I]$) and narrow distribution of the molecular weight, low polydispersity index (PDI = M_w/M_n). Well-definded polymer architectures e.g. block copolymers can be synthesized and selective end-group functionalization of the polymer by means of initiation and/or termination steps can be performed.

2-Oxazoline and poly(n-acetylamine)s

2-Oxazoline monomers are cyclic iminoethers typically substituted in the second position (Fig. 2.13). They polymerize by a ring-opening, cationic mechanism, they show all typical features of a "living polymerization".
Starting at temperatures above 40 °C, the propagation progresses via ionic or covalent active species, the pathway strongly depends on the solvent and on the nature of the counter-ion. The more nucleophilic counter-ion leads to ionic mechanism. The propagation follows a S_N2 mechanism by nucleophilic attack of the nitrogen atom of the 2-oxazoline monomer onto the carbon atom in 5-position of the propagating 2-oxazolinium ion through ring-opening. As side reactions, chain transfer can take place. It proceeds via proton abstraction at the propagating end by a monomer and an enamine group.[98-100]
Typical initiator reagents are Lewis acids as well as their stable salts (such as BF_3, $Et_3O^+BF_4^-$), protonic acids, sulfonate esters and sulfonic anhydrides ($(CH_3)_2SO_4$, p-$CH_3C_6{\cdot}H_4SO_3CH_3$, $CF_3SO_3CH_3$), alkyl halides (i.e. CH_3I, $C_6H_5CH_2Br$), electron acceptors and oxazolinium salts.[98,99]
Nucleophilic agents terminate the polymerization. Termination reaction can occur in 2- and in 5-position, giving the kinetic and the thermodynamic products, respectively. Secondary cyclic amines (e.g. piperidine) terminate selectively in the 5-position, hence they are the most commonly used.[101]

Initiation

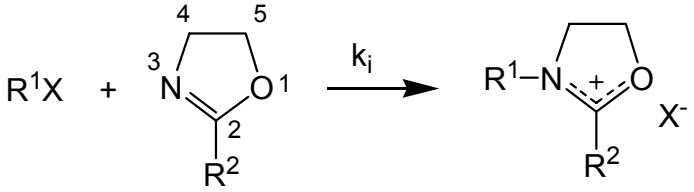

Propagation

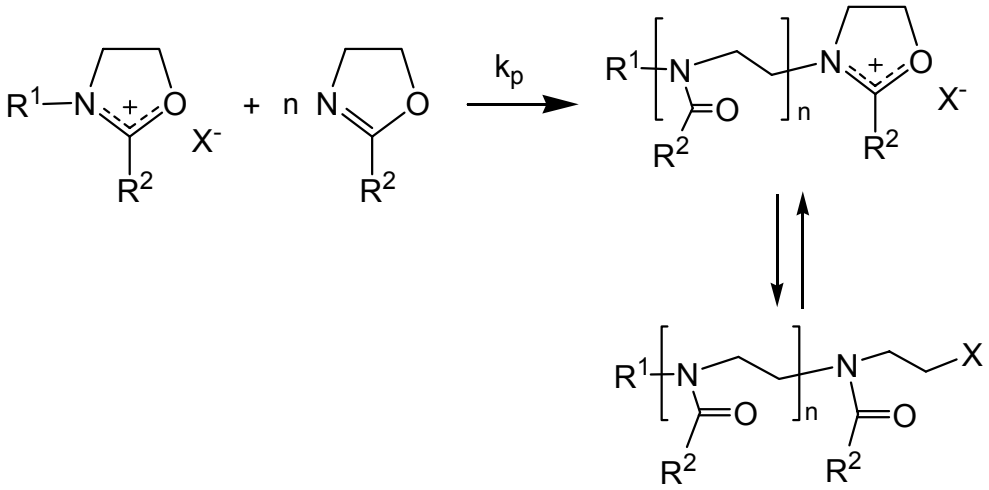

Termination

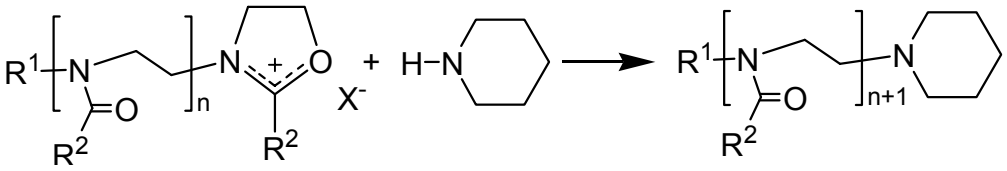

Fig. 2.13 Polymerization mechanism of 2-oxazoline.

For the monomer synthesis, a large variety of reactions are available such as dehydrohalogenation of haloamides, dehydratation of hydroxylamides, isomerization of N-acylazirines, reaction of nitriles with 2-aminoethyl alcohols, cyclization hydroxyalkyl isocyanide, reaction of nitriles with epoxides, cyclization of halo- or hydroxyalkyl imino ethers.[98,99]

3 Motivation

The purpose of this work was to create a new system based on poly(2-oxazoline)s as carrier for pharmacologically active polymers. In the light of the initial model proposed by *Ringsdorf* in 1975,[74] the concept can be specified as follows:

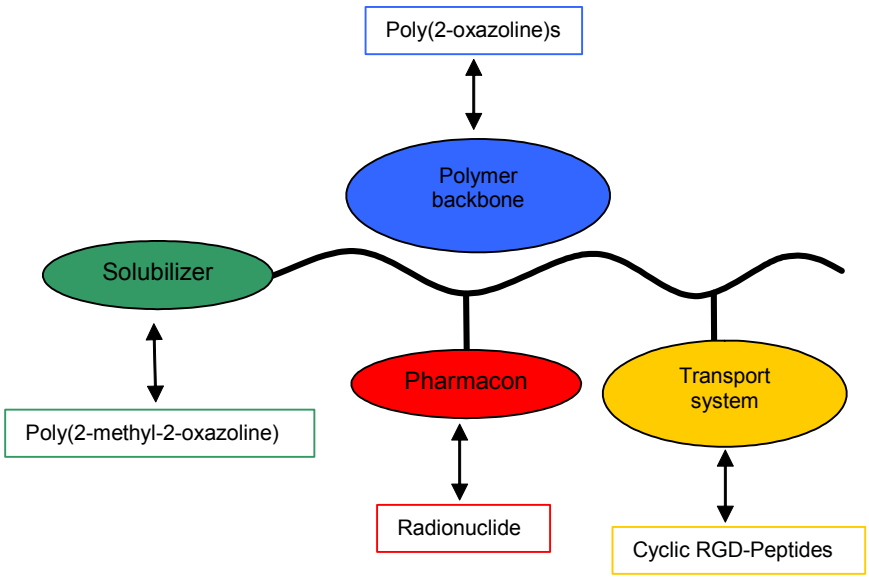

Fig. 3.1 *Ringsdorf*'s model for pharmacologically active polymers applied to our system.

As presented in Fig 3.1, three units should be linked together to form a functional macromolecule to be used as a polymeric therapeutic:

- First unit should guarantee the **water solubility of the molecule**, in case of poly(2-oxazoline) this feature can be satisfied by copolymerization with 2-methyl-2-oxazoline to give the water soluble **poly(2-methyl-2-oxazoline)**
- Second unit should be the **transport system**, the 'homing device' specific to the biological targets e.g. cell receptor: in this project the homing device will be the **cyclic RGD peptide**, (see 2.2), which interacts selectively with the cell receptor $\alpha_v\beta_3$-integrin involved in tumor angiogenesis, (see 2.3).
- Third unit is the **pharmacon**, the compound which elicit physiological response in living system: the therapeutically active moiety (described as the

'pharmacon') is in this case of radiotherapy and diagnosis a complexed or bound **radioactive nuclide**.

The biocompatibility[102,103] and the living character of poly(2-oxazoline)s motivated the use of these polymers as transport system. The results recently obtained developing polymeric systems for medical applications (see 2.5) encouraged the introduction of a new polymer in this field. The positive results, obtained in the studies of the cyclic RGD peptide as $\alpha_v\beta_3$-integrin antagonist in the development of antiangiogenic strategies (see 2.2 and 2.3) and its applications in the radio diagnosis (see 2.4), supported the possibility to apply the system described in Fig. 3.1 in radio diagnosis of tumors.

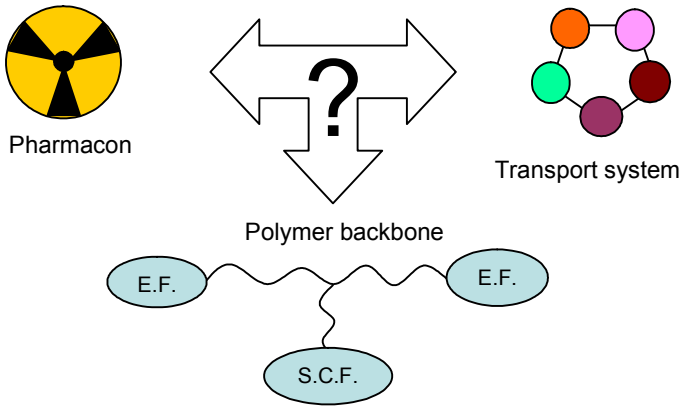

Fig. 3.2 Scheme of the motivation: how can be the three units chemically bound together?

The first point to deal with is, however, how the three units previously described, can be chemically bound together. An experimental answer to this question will put the bases for further applications. As first, the chemical coupling between the polymer and the target unit, cyclic RGD peptide will be considered.

4 Results and discussion

This project was performed in cooperation with Prof. H. Kessler's research group (TU München) and Dr. R. Haubner (Klinikum Rechts der Isar, München).
Dr. U. Hersel, Dr. C. Dahmen, J. Auernheimer and Dr. R. Haubner have synthesized the cyclic RGD peptides.

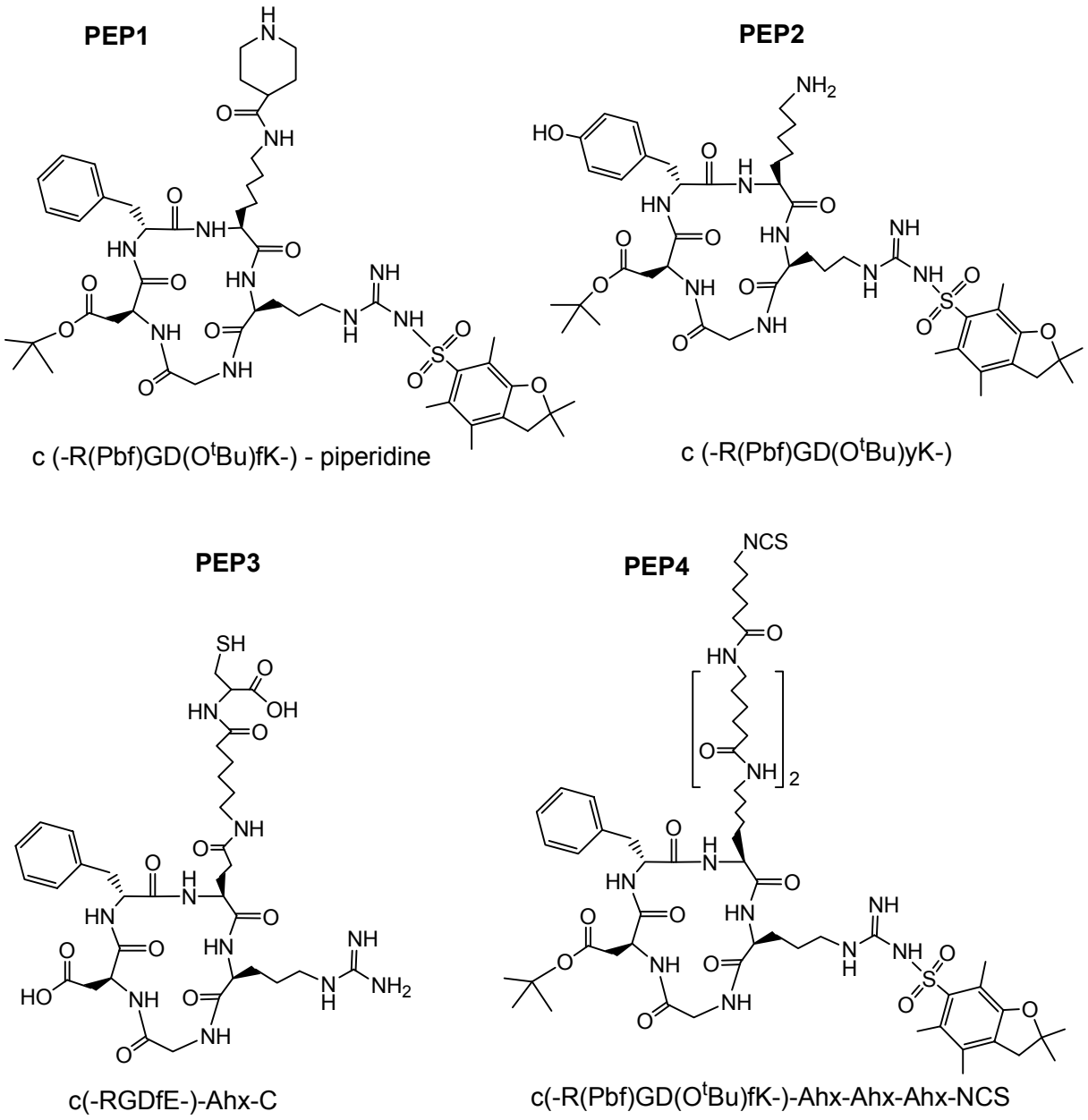

Fig. 4.1 Structure of the cyclic RGD peptides used in this work.

4.1 Polymer functionalization

The introduction of functional groups in the polymer can be obtained following three different strategies: the synthesis of the initiator, R^1X, the synthesis of the monomer, Mmer-R^2, and/or synthesis of the terminating agent, Nu-R^3.

The group R^1 as counter ion of the initiator covalently binds to the nitrogen of the first monomer unit. The group R^3 is covalently bound to the nucleophilic terminating agent. In both cases, an end functionalization (E.F.) can be obtained. The Mmer-R^2 bears a functional unit in 2-position introduced through the monomer synthesis, this gives rise to a side chain functionalization (S.C.F.) (Fig. 4.2).

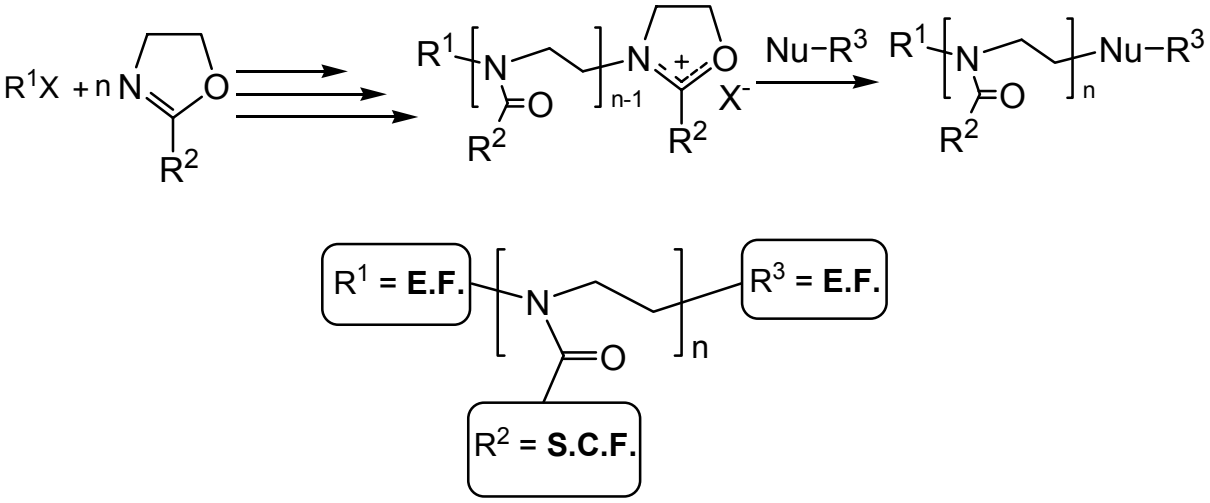

Fig. 4.2 Functionalization possibilities in poly(2-oxazoline)s (E.F. = end functionalization, S.C.F. = side chain functionalization).

4.1.1 Functionalization through initiation step

The introduction of functional moieties into the polymer via the initiation method has been reported by *Kobayashi et al.*, where the group prepared a series of n-alkyl tosylates and n-perfluoro alkyl tosylates to obtain non ionic polymeric surfactants.[101] In the mean time, several other research groups have extended this method to incorporate other functionalities into poly(2-oxazoline)s. The introduction of a

functionality into the starting "end" of the growing polymer chain is allowed by multi- and monofunctional, alkyl chloroformates,[104,105] dialkylsulfates,[106] alkyl toluenesulfonates,[107-109] allyl-[111,112] benzyl-[112-114] and propargylhalides.[115] These initiators constitute slow initiating systems, due to their relatively low electrophilicity, which can lead to broader molecular weight distributions. In contrast, esters of trifluoromethane sulfonic acid have a fast initiation behavior which results in a higher control of the polymerization reaction and lower polydispersity index.[116,117] Examples of initiators which contain triflate units as initiating system of poly(2-oxazoline)s have been developed in the last years and are listed in Fig. 4.3.

The equimolar reaction between the initiator and the monomer gives rise to the initiator salt, which is a particular initiating system. This method has been successfully used to introduce chromophores into amphiphilic block copolymers.[119]

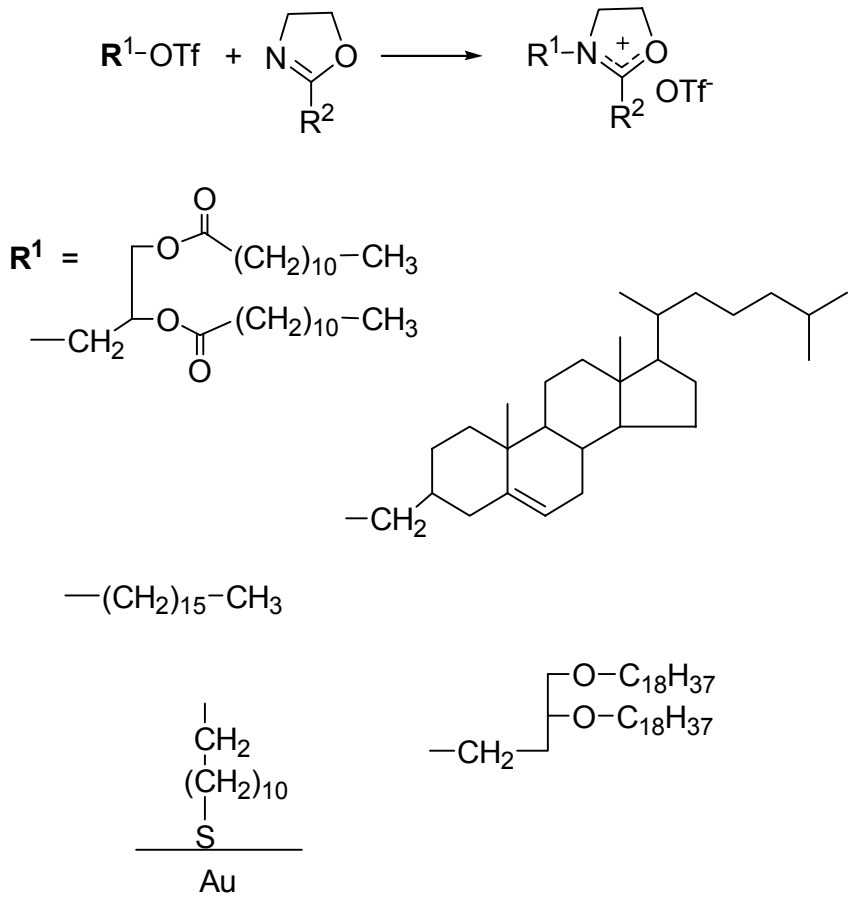

Fig. 4.3 Examples of initiators with a triflate as the counter ion.[116-118]

4.1.2 Functionalization through the side chains

The introduction of the functionalities in the side chains was developed in the past years, to increase the concentration of functional groups in the polymer. The most important feature a monomer should have is that the functional unit must not interfere with the cationic polymerization mechanism.

Mesogene[120] and siloxane[121] groups, for example, have been introduced in poly(2-oxazoline) monomers and, in particular, *Nuyken's* research group put much effort in the development of functional 2-oxazoline monomers used for micellar catalytic systems applied to other various reactions. Examples of functionalized 2-oxazoline monomers have been synthesized containing bipyridine ligands for atom transfer radical polymerization (ATRP) application[122] or N-heterocyclic carbene unit for the Heck reaction.[123] If the ligand or catalyst interferes with the polymerization mechanism a polymer analog must be synthesized. A poly(iodoaryl-modified-2-oxazoline) polymer was synthesized as precursor polymer to bind triphenylphosphine ligands, which were not inert under the necessary conditions for the ring-opening polymerization.[124,125] 2-oxazoline monomer with ester functionalities can be used to generate versatile COOH groups in the polymer, which can be used for various applications (Fig. 4.4).[126]

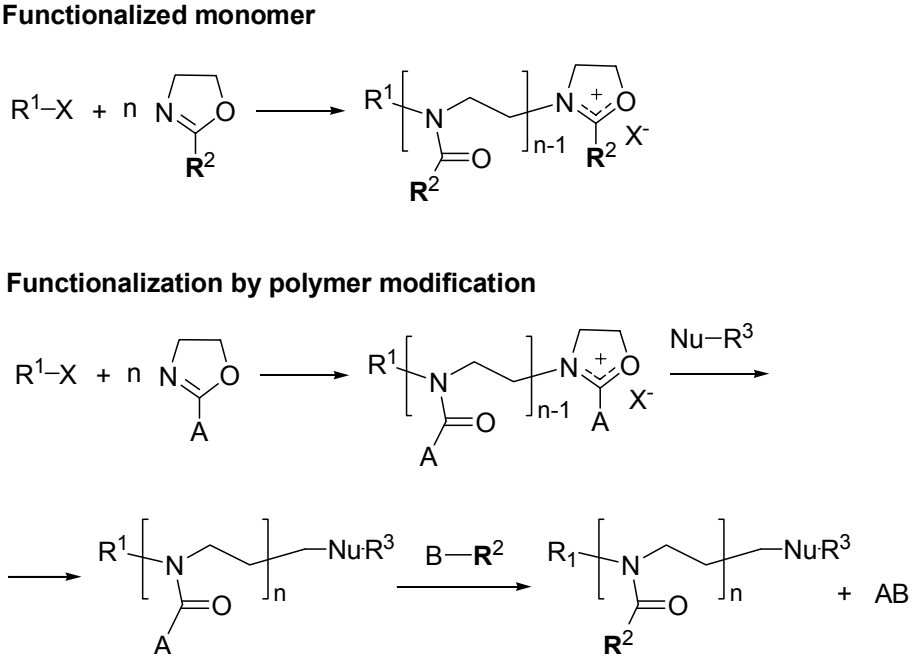

Fig. 4.4 Reaction scheme for the side chain functionalization.

4.1.3 Functionalization through the termination step

Poly(2-oxazoline)s were functionalized by means of a terminating reagent by *Kobayashi et al.* to obtain polymer surfactants and macroinitators for radical polymerization[101] and by *Jordan et al.* to introduce silane functional groups[117] and fluorescence dyes.[127]

The termination reaction of poly(2-oxazoline)s proceeds via ring-opening of the oxazolinium cation by a nucleophile.[101,113,128-141] The nucleophile can attack the 2-oxazoline ring of the living chain in 2- and 5-position. The addition in the 5-position gives rise to the stable acrylamide with the nucleophile covalently bound in β-position. The reversible addition in 2-position is kinetically controlled and produces the instable 3-methyl-oxazolidine-derivative. Water traces can hydrolyze 3-methyl-oxazolidine derivative to esteramine (Fig. 4.5) and separate the nucleophile from the polymer.[124,143] For a quantitative functionalization via termination route, the reaction conditions should be chosen in order to avoid the 2-position termination. Common terminating agents are secondary cyclic amines because they terminate selectively in 5-position, as *Nuyken et al.* have demonstrated.[143]

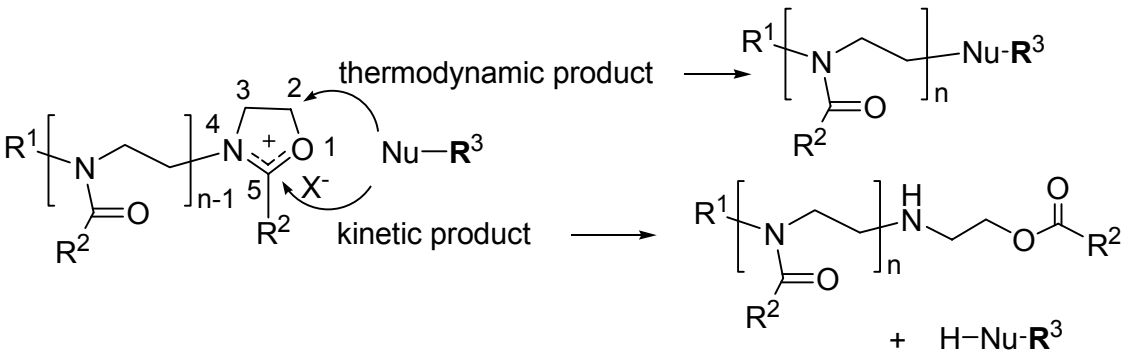

Fig. 4.5 Possible termination reactions.[124,142]

4.2 Functionalization by polymer modification

The concept of introducing functional groups by polymer modification, briefly introduced for the side chain functionalization (see 4.1.2), can also be extended to the end functionalization. Specific reactive groups or anchor groups can be introduced in

the polymer and afterwards be coupled with the peptides containing a complementary reactive group.

4.2.1 Amide coupling and chemoselective ligation

In peptide chemistry, binding of long chain molecules has been a research subject in the last years and different strategies have been developed. The most common procedure to bind peptides, or long chain molecules in general, is via a stable covalent amide bond: the nucleophilic *N*-terminus of the peptide reacts with a carboxylic group using a peptide coupling reagent, e.g. *N*-ethyl-*N,N'*-(dimethylaminopropyl)-carbodiimide (EDCI), dicyclohexylcarbodiimide (DCC) or *N,N*-carbonyldiimidazol (CDI) under mild reaction conditions.[144] Coupling of primary amines can proceed also with other functional groups, which can be preactivated.[145-152] (Fig. 4.6) These reactions represent an alternative to the amide coupling.

Further alternative reactions belong to a more recent approach called chemoselective ligation. The chemoselective ligation uses unique mutually reactive functionalities, one type on each segment, to covalently assemble long-chain molecules. The selected pairs of functional groups introduced in the long chain molecules form stable bonds without the need of an activating agent and without interfering with other eventual functional groups present on the molecules, a usual disadvantage of the amide coupling.[144,153-156]

Examples of possible reactions in the chemoselective ligation are presented in Fig. 4.7 Long chain molecules can be ligated by nucleophilic reaction between the SH group and a bromoacetyl functionality.[157] The SH group can also be linked to the acrylic acid or acryl amide by Michael's addition[158-160] or, as alternative, to the double bond of maleimide undergoing an alkylation reaction forming stable thioether bonds.[159] Stable oxinimine bonds are obtained by reaction of aminooxy groups with carbonyl groups.[162-164] Isothiocyanate group is often used for coupling with amino groups of proteins to form thiourea derivatives.[164]

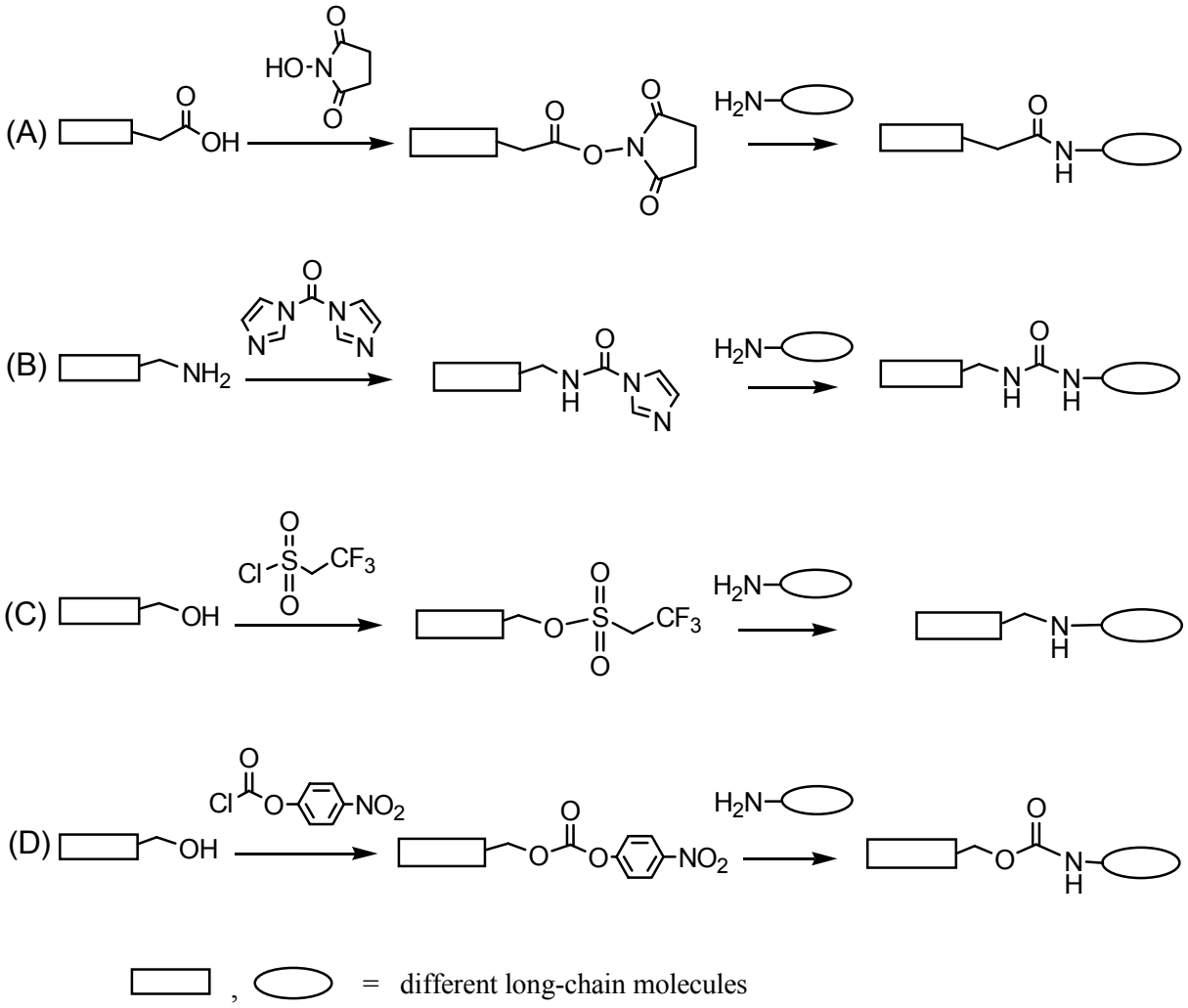

Fig. 4.6 Possible reactions with amine as functional group. (A) carboxylic acid group activated wit NHS-ester; (B) amine groups preactivated with CDI (carbonyldimidazol); (C) hydroxyl groups, activated as tresylate (2,2,2-trifluorosulfonate); (D) hydroxyl groups; preactivated with p-nitrophenyl-chloroformiate.[144]

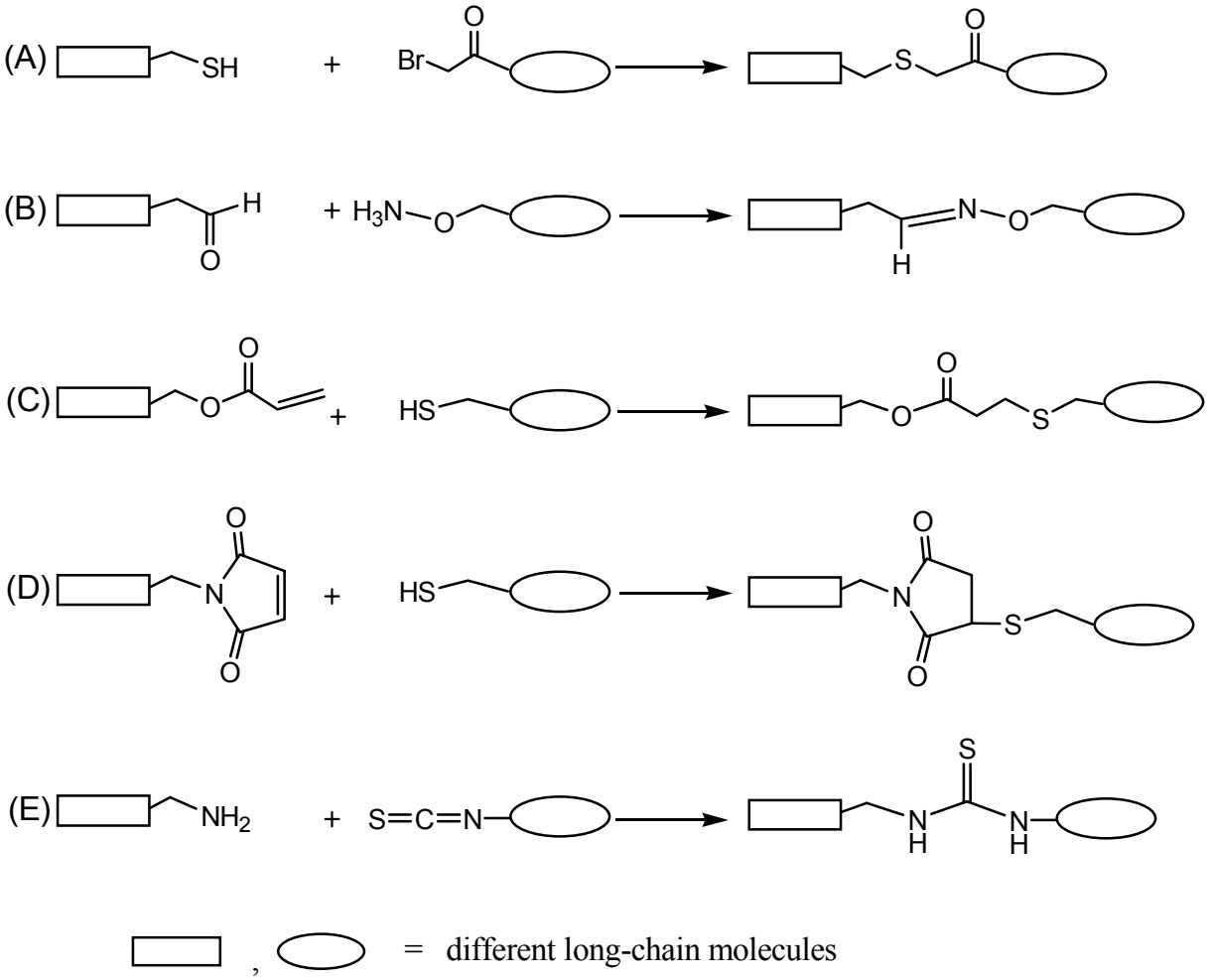

Fig. 4.7 Examples of chemoselective ligations. (A) Thiol and bromoacetyl functionalities; (B) Aldeyde and aminooxy functionalities; (E) amine and isothiocyanate functionalities.[144]

4.2.2 Functionalized peptides for the amide coupling and chemoselective ligation

The anchor groups can be introduced in the peptides through the fifth amino acid X, of the RGDfX sequence. As described in the introduction, the RGD sequence (arginine, glycine, aspartic acid) is the biological active one.[18,35,36] The hydrophobic phenylalanine increases the biological activity and its D-conformation gives rise to a βII-γ turn arrangement in the ring. The fifth amino acid has only a slide influence on the biological activity.[25,49] Therefore, it can be used to introduce the different anchor groups through its side chain. Fig. 4.8 shows the anchor groups introduced in the peptide, e.g. *Peptide*–SH, -O-NH_2, -NH_2 or -NCS.

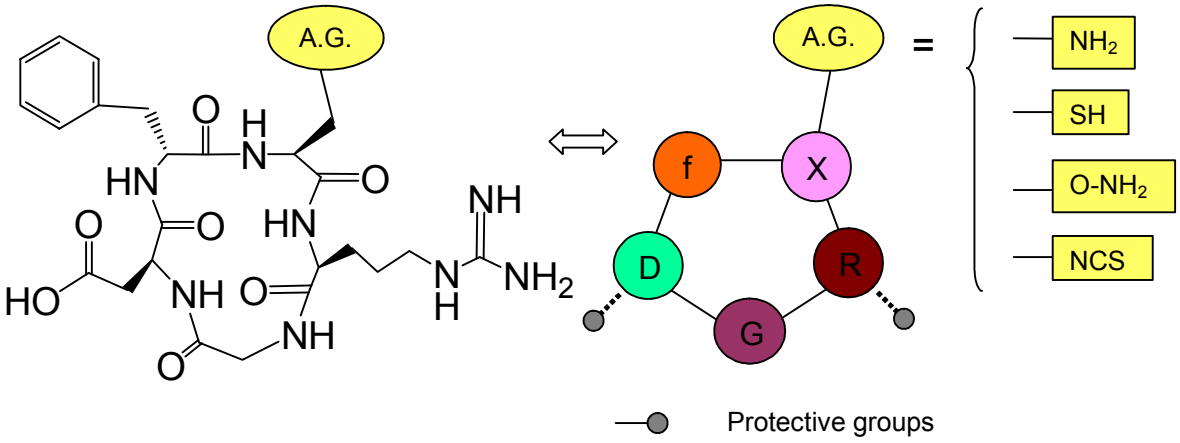

Fig. 4.8 Anchor groups (A.G.) introduced in the cyclic peptide.

4.3 End functionalization (E.F.) with RGD peptide

The direct functionalization of poly(2-oxazoline)s was attempted by terminating the living chain with **PEP1**. The piperidine unit, linked to the peptide through the side chain of the lysine (amino acid indicated with K), should guarantee the selective termination in 5-position. MeOTf initiated the polymerization of 2-methyl-2-oxazoline dissolved in ACN. The reaction proceeded at 80 °C for 15 h. The cyclic peptide was not soluble in ACN, as a consequence, most of the solvent was evaporated and substituted by MeOH.[165] The termination reaction proceeded in MeOH at room temperature for 13 h.

The direct termination of poly(2-methyl-2-oxazoline) with **PEP1** was not successful. As shown in the MALDI-TOF spectrum in Fig. 4.9, the peaks corresponding to the polymer distribution could be identified as well as those corresponding to the cyclic RGD peptide but no peaks corresponding to the poly(2-oxazoline) terminated with the cyclic peptide (m/z = 2525) could be found, concluding that the peptide did not terminate the poly(2-methyl2-oxazoline). The steric demand of the cyclic peptide probably influenced the reactivity of the terminating agent and no reaction took place. Methanol also probably competed with **PEP1** in the termination reaction.

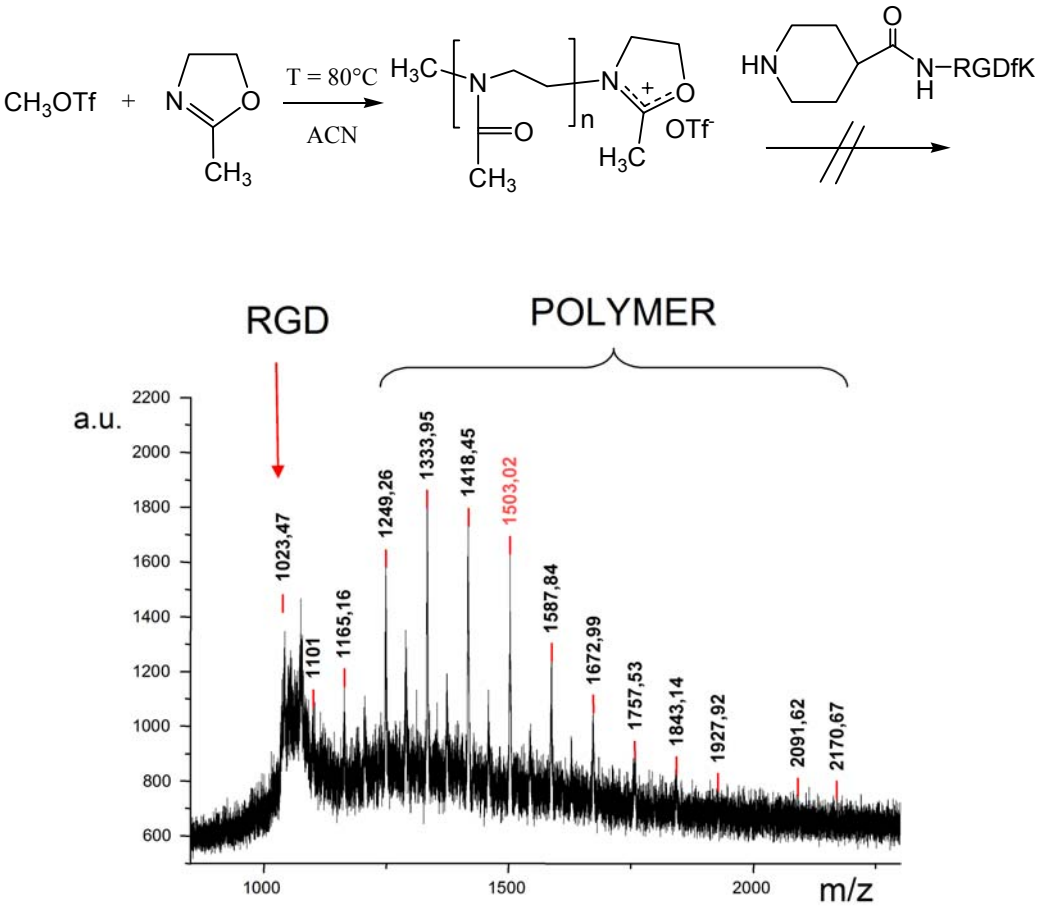

Fig. 4.9 Reaction mechanism and MALDI-TOF spectrum of the direct termination of poly(2-methyl-2-oxazoline) with **PEP1**.

4.4 Functionalization by polymer modification

Starting from available peptides already synthesized by the cooperating research groups, the functionalization by polymer modification represented a good alternative to the direct functionalization, as presented in 4.2. As described there, the chemical functionalities introduced in the peptides are: thiol, aminooxy, amine and isothiocyanate. To allow the coupling of these peptides with poly(2-oxazoline)s the corresponding anchor groups must be introduced in the polymer.

4.4.1 Standard procedure for the polymerization of poyl(2-oxazoline)s

As described in 4.1 poly(2-oxazoline)s can be functionalized through the initiation and/or termination step to realize an end functionalization and through the monomer to

obtain a side chain functionalization. In this work the end functionalization through the termination reaction and the side chain functionalization were considered.

2-Methyl-2-oxazoline was chosen as standard monomer to investigate the termination reaction. MeOTf was chosen as standard initiator in both functionalization moieties because of its fast initiation step, it guarantees a good control of the polymerization leading to a narrow molecular weight distribution.

A standard procedure to polymerize 2-oxazoline monomers is described as follows. The 2-oxazoline monomer and the initiator (MeOTf) were dissolved in ACN under dry nitrogen atmosphere. The solution was stirred at 80 °C for 15 h. After cooling to 0 °C the terminating agent was added. (The specific reaction conditions will be described in each of the following chapters concerning the functionalization) Once the termination of the living chains had occurred, the solvent was evaporated and the remaining solid was redissolved with DCM and dry K_2CO_3 was added. The suspension was stirred for another 15 h and K_2CO_3 removed by filtration. The solvent was evaporated and the residue was redissolved in chloroform and reprecipitated in diethyl ether at 0 °C. The polymer was dried in a vacuum oven for several hours to ensure that the solvent was evaporated.

4.5 End functionalization (E.F.) by polymer modification

4.5.1 Introduction of the carboxylic group during the termination step

The cyclic RGDfK peptide is amine functionalized through the side chain of the lysine (K). For further coupling between the peptide and the polymer via a stable amide bond (see 4.2.1), a carboxylic acid group was introduced in the polymer.

The carboxylic acid could be introduced as an end group through the commercially available 4-piperidine ethyl ester. The secondary amine guaranteed a quantitative efficient termination of the living chains[143] and by hydrolysis of the ester group the carboxylic acid function could be obtained. The ester protective group was needed because the carboxylic acid function could terminate the reaction itself.[133,168]

2-methyl-2-oxazoline was polymerized following the standard procedure, described in 4.4.1. The termination reaction was performed at room temperature and monitored by ^{1}H-NMR spectroscopy. After half an hour the polymerization was quantitatively terminated by 4-piperidine ethyl ester.

Fig. 4.10 shows the ^{1}H-NMR spectrum of the polymer before the terminating reaction. The four typical signals of the living chain, are indicated by numbers 1 to 4, and they are no more present in the spectrum represented in Fig. 4.11, which refers to the ^{1}H-NMR spectrum of the polymer recorded after 30 min of the termination. The signals corresponding to the ester group are indicated with the number 5 and 6. Poly(2-methyl-2-oxazoline) terminated ethyl ester (**P(MeOx)-Ter-EtEst**) was purified by reprecipitation in diethyl ether. The polymer was dissolved in a $NaOH_{aq}$ solution and stirred at room temperature for 15 h to cleave the ester protective group. Poly(2-methyl-2-oxazoline) terminated carboxylic acid (**P(MeOx)-Ter-CarAc**) could be obtained in good yields. Under these mild reaction conditions, chosen for the hydrolysis of the ester protective group, the polymer backbone remained unchanged. The hydrolysis of the ester protective group proceeded quantitatively. In ESI-MS spectra the peaks corresponding to the exact mass of the polymer chains of **P(MeOx)-Ter-CarAc** could be assigned and no peaks corresponding to the exact mass of the polymer chains of **P(MeOx)-Ter-EtEst** could be identified. In ^{1}H-NMR spectra the characteristic signals of the ethyl group disappeared and no changes were observed in the signals corresponding to the polymer backbone. GPC curve remained unchanged. All these results indicated that the reaction conditions were inert for the polymer backbone.

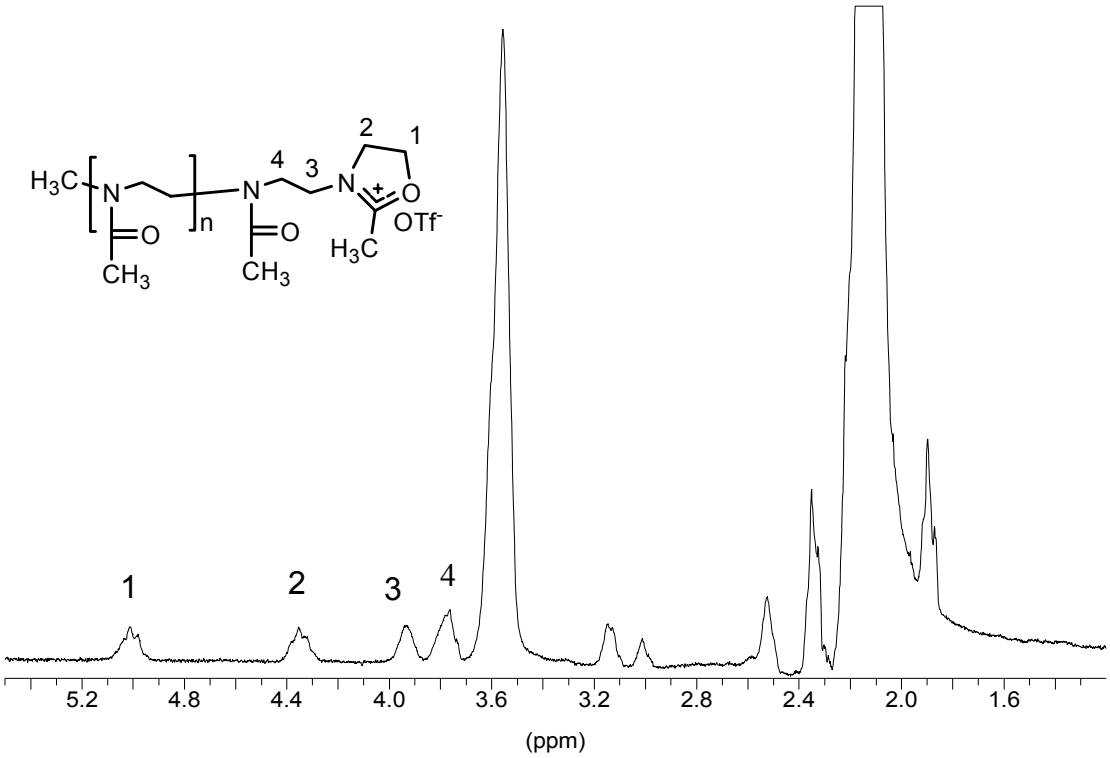

Fig. 4.10 [1]H-NMR spectrum of the living "polymer chain end".

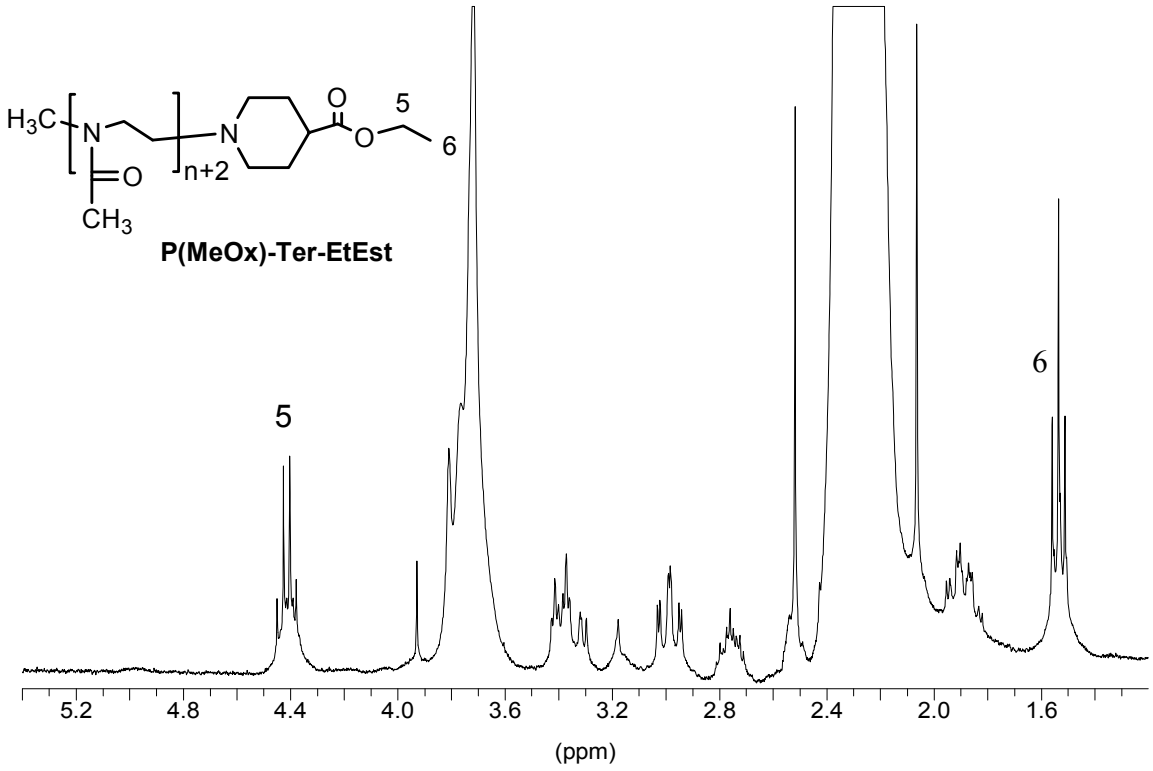

Fig. 4.11 [1]H-NMR spectrum of **P(MeOx)-Ter-EtEst**.

4.5.2 Introduction of activated double bonds as an anchor group

The introduction of the active double bond for a further ligation via Michael's addition with thiol groups can be performed by terminating the living polymer with acrylic acid and 3-maleimido propionic acid.[133,169,170] These compounds are commercially available and can be used without further purification. The living chain end of poly(2-methyl-2-oxazoline) were obtained following the standard procedure described in 4.4.1. The terminating agent was added to the polymer solution and reacted at 60 °C for 1 h before addition of triethylamine (TEA) as a proton trap. The reaction was allowed to complete within 15 h at 60 °C. Poly(2-methyl-2-oxazoline) terminated acrylic acid (**P(MeOx)-Ter-AcrAc**) and poly(2-methyl-2-oxazoline) terminated maleimide (**P(MeOx)-Ter-MalIm**) were obtained with high yield.

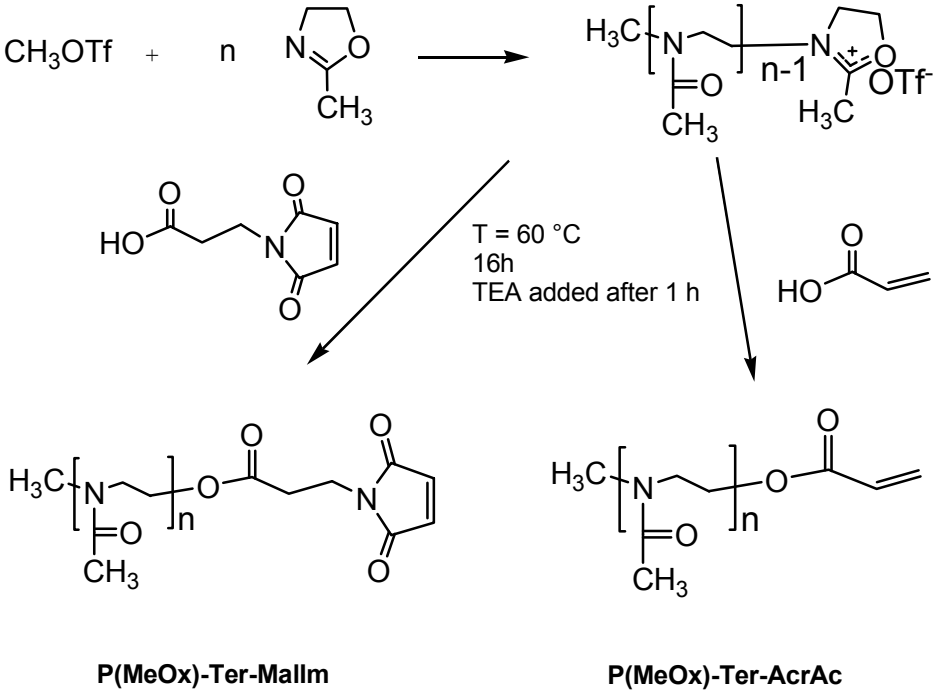

Fig. 4.12 Reaction scheme of the polymerization of 2-methyl-2-oxazoline and termination with acrylic acid to obtain **P(MeOx)-Ter-AcrAc** and 3-maleimido propionic acid to yield **P(MeOx)-Ter-MalIm**.

TEA used as proton acceptor, during the termination step, could terminate the living chain itself[133,168,169] and gave rise to poly(2-methyl-2-oxazoline) terminated with TEA as side product. As presented in Fig. 4.13, two polymer distributions were recognized in the ESI-MS spectrum. The peaks indicated with circles corresponds to the exact

mass of **P(MeOx)-Ter-MalIm**, whereas the peaks indicated by x corresponds to the distribution of the polymer terminated by TEA.

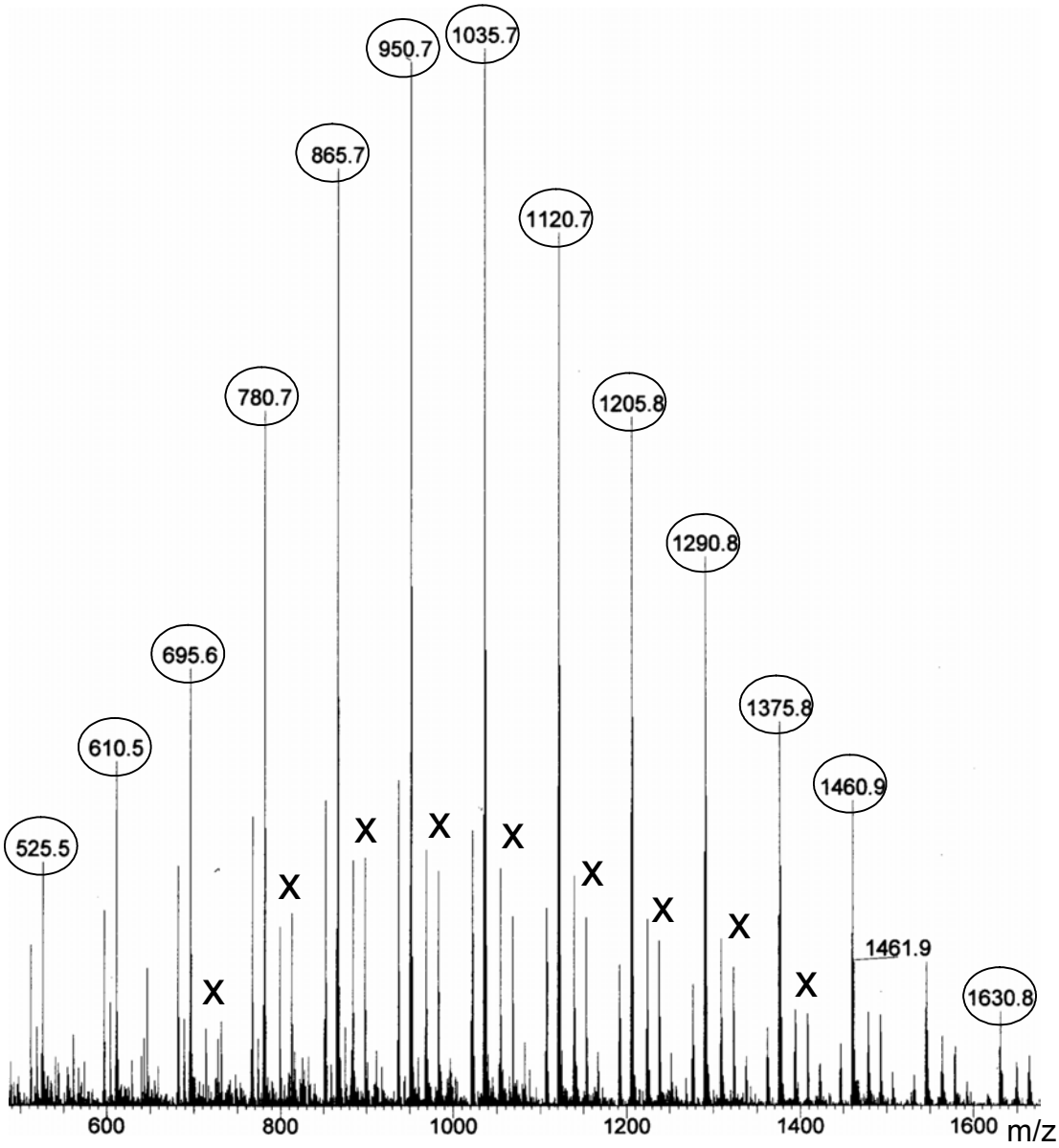

Fig. 4.13 ESI mass spectrum of **P(MeOx)-Ter-MalIm**. In circles is indicated the polymer distribution of **P(MeOx)-Ter-MalIm**, whereas with X is indicated the polymer distribution of poly(2-methyl-2-oxazoline) terminated with TEA, the side product.

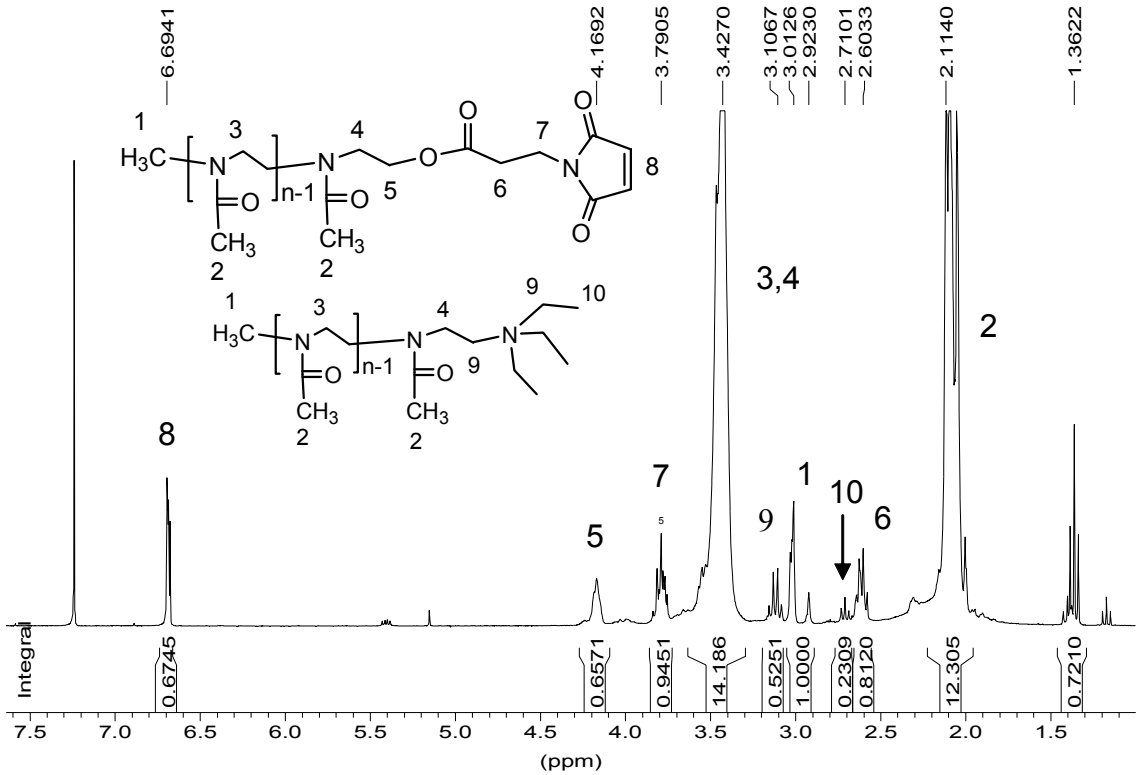

Fig. 4.14 ^{1}H-NMR spectrum of **P(MeOx)-Ter-MalIm**.

^{1}H-NMR spectroscopy allowed quantifying the degree of functionalization of the polymer. All the signals of the ^{1}H-NMR spectrum of **P(MeOx)-Ter-MalIm**, shown in Fig. 4.14, could be assigned to the protons of the polymer. The signals indicated from 1 to 8 belongs to **P(MeOx)-Ter-MalIm** and those indicated with 9 and 10 belongs to the end chain of the polymer terminated by TEA. The degree of functionalization was calculated by the ratio of the signal (1), which corresponds to the terminal CH_3-group coming from the initiator, and of the signal (5) corresponding to the signal of the terminal CH_2-O-. For **P(MeOx)-Ter-AcrAc** the degree of functionalization was 86 %, whereas for **P(MeOx)-Ter-MalIm** it was 81 %. The polymer terminated with TEA, however, is inert to the thiol addition on the activated double bond and it is supposed not to interfere with the consecutive coupling reaction.

4.5.3 Introduction of aldehyde and formaldehyde as anchor groups

Synthesis of the terminating agent

A suitable terminating agent was synthesized to introduce aldehyde groups in poly(2-oxazoline)s as end functionalization (Fig. 4.15). The terminating agent, 1-(2,2-diethoxy-ethyl)-piperazine (**Pip-Acetal**), contains the cyclic secondary amine, which guarantees a quantitative termination of the living chain end and the aldehyde function was introduced in its protected acetal form.

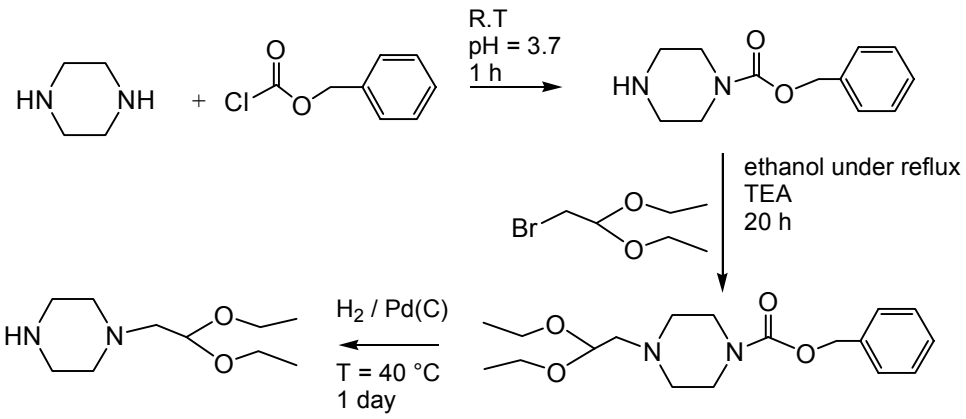

Fig. 4.15 Reaction scheme for the synthesis of 1-(2,2-diethoxy-ethyl)-piperazine (**Pip-Acetal**) terminating agent.

Piperazine was first protected with benzychloroformiate (Z-protection group),[170] it was dissolved in a mixture of water and MeOH and benzyl chloroformiate (Z-protective group) was added drop-wise at the same time to a $NaOH_{aq}$ solution in order to maintain a pH of 3.7, indicated by bromophenol blue which turned from blue to yellow. The double substituted piperazine could be separated from the monosubstituted product by extraction with toluene: the double substituted piperazine was extracted at pH = 3, whereas the monosubstituted one was extracted at pH = 13. ^{1}H- and ^{13}C-NMR spectroscopy verified the successful reaction and purity of the benzyl-1-piperazine carboxylate **(1)**.

1 (Fig. 4.15) reacted with the commercially available 2-bromo-1,1-diethoxyethane for 20 h under ethanol reflux.[171] The Z-protection group, which can be easily cleaved by hydrogenation as final step, ensures that **Pip-Acetal** used to terminate the living

polymer is monosubstituted. ^{1}H-NMR spectroscopy confirmed the purity of the obtained compound.

Polymerization and termination reactions

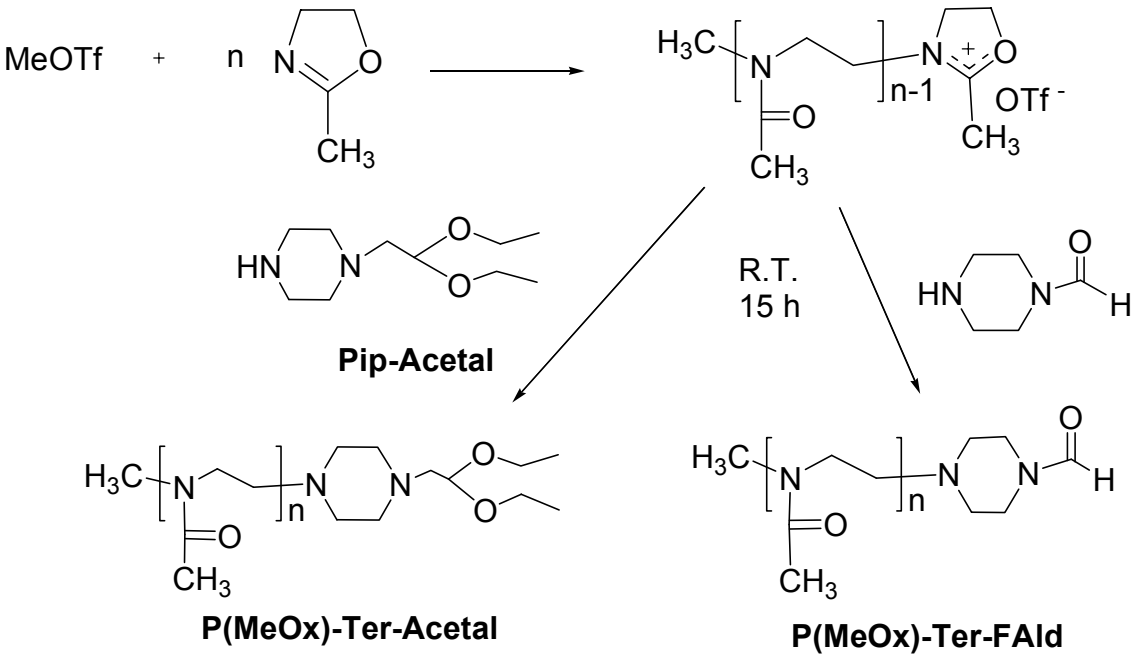

Fig. 4.16 Reaction scheme of the termination with a **Pip-Acetal** and N-formylpiperazine.

Following the standard procedure, described in 4.4.1, poly(2-methyl-2-oxazoline) was obtained and the living chain end were quantitatively terminated by **Pip-Acetal**, as confirmed by ^{1}H-NMR spectroscopy, ESI mass spectrometry and GPC. Different reaction conditions were tested to hydrolyze the acetal group of poly(2-methyl-2-oxazoline) terminated acetal (**P(MeOx)-Ter-Acetal**) but no aldehyde was obtained. As an alternative to this reaction, a formaldehyde group was introduced in the polymer terminating it with freshly distilled N-formyl-piperazine at room temperature. Poly(2-methyl-2-oxazoline) terminated formaldehyde (**P(MeOx)-Ter-FAld)** was obtained in high yield and the result was confirmed by ^{1}H-NMR spectroscopy and GPC.

4.5.4 Introduction of amine as anchor group

The termination of poly(2-oxazoline)s with piperazine and subsequent coupling with a isothiocyanate functionalized dye is possible.[127] Following the standard procedure (4.4.1), 2-methyl-2-oxazoline was polymerized and the living chains were terminated adding a saturated solution of piperazine in chloroform. Piperazine was used in large excess to prevent that the same piperazine molecule would terminate two living chain end. The successful reaction was monitored by ^{1}H-NMR spectroscopy and GPC.

4.6 Side chain functionalization (S.C.F.) by polymer modification

4.6.1 Introduction of carboxylic acid function as an anchor group

Monomer synthesis

Recently, an efficient way to introduce carboxylic acid groups within the polymer side chain of amphiphilic poly(2-oxazoline)s via ester protected monomers and subsequent hydrolysis was described by *Zarka et al.*[126]

The ester-functionalized 2-oxazoline monomer was synthesized according to a modified two-step procedure by Levy and Litt.[166] 2-Chloroethyl ammonium chloride was treated with methyl succinyl chloride to form **3**, as presented in Fig. 4.17. Triethylammonium chloride precipitated during the reaction and was separated by addition of water and decantation of the aqueous phase. The ring closing step was performed by carefully heating the solution of **3** with dry sodium carbonate. The monomer 2-(2-methoxycarbonylethyl)-2-oxazoline (**(MeEstOx)Mmer**) was obtained by distillation of the mixture in fine vacuum as a colorless liquid. The structure and the purity of the monomer were confirmed by ^{1}H and ^{13}C-NMR spectra.

By polymerization of **(MeEstOx)Mmer** or copolymerization with 2-methyl-2-oxazoline, three different structures were obtained: the homopolymer, the statistical copolymer and the block copolymer (Fig. 4.18).

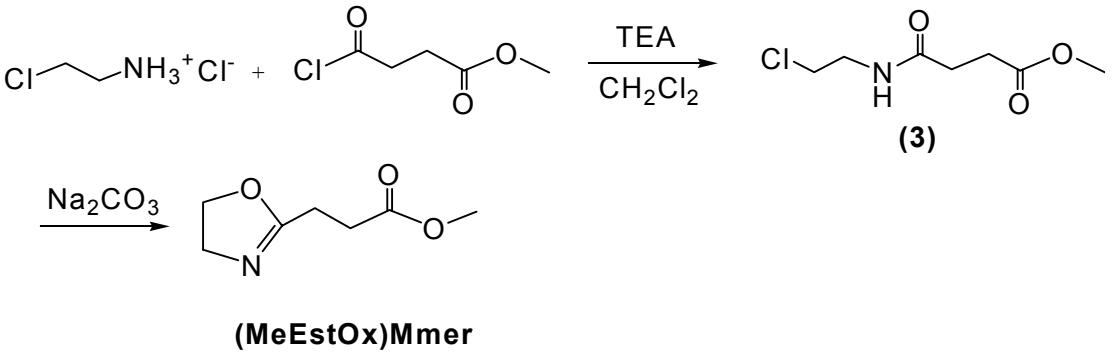

Fig. 4.17 Synthesis scheme of the monomer 2-(2-methoxycarbonylethyl)-2-oxazoline, **(MeEstOx)Mmer**.

Homopolymer

The polymerization of **(MeEstOx)Mmer** was performed with the same reaction conditions as described in 4.4.1. The polymerization was successful; however, due to incomplete precipitation of the poly(2-(2-methoxycarbonylethyl)-2-oxazoline) (**P(MeEstOx)**) in diethylether, the polymer yield was rather low (30%).

P(MeEstOx) was dissolved in $NaOH_{aq}$ for 15 h, to cleave the ester protective group. Under these reaction conditions the ester groups could not be hydrolyzed. The reaction time and the temperature (50 °C) were increased, however in ^{1}H-NMR spectra the signal corresponding to the methyl group did not disappear. The ester groups in the polymer could be too closed each other, therefore, the hydrolysis reaction resulted difficult. A statistical copolymer, where the ester groups are diluted by the 2-methyl-2-oxazoline monomer units, was synthesized to overcome this problem.

Statistical copolymer

The synthesis of the statistical copolymer proceeded as described in 4.4.1, both monomers and the initiator were dissolved in ACN and reacted for 15 h. poly[(2-methyl-2-oxazoline)-*stat*-(2-(2-methoxycarbonylethyl-2-oxazoline))] (**P[(MeOx)-*stat*-(MeEstOx)]**) was obtained in high yield. The polymer could be hydrolyzed with $NaOH_{aq}$ in 15 h at room temperature, as confirmed from ^{1}H-NMR spectra, giving the

carboxylic acid functionalized polymer, poly[(2-methyl-2-oxazoline)-*stat*-(2-(2-propionic acid ethyl-2-oxazoline) (**P[(MeOx)-*stat*-(CarAcOx)]**).

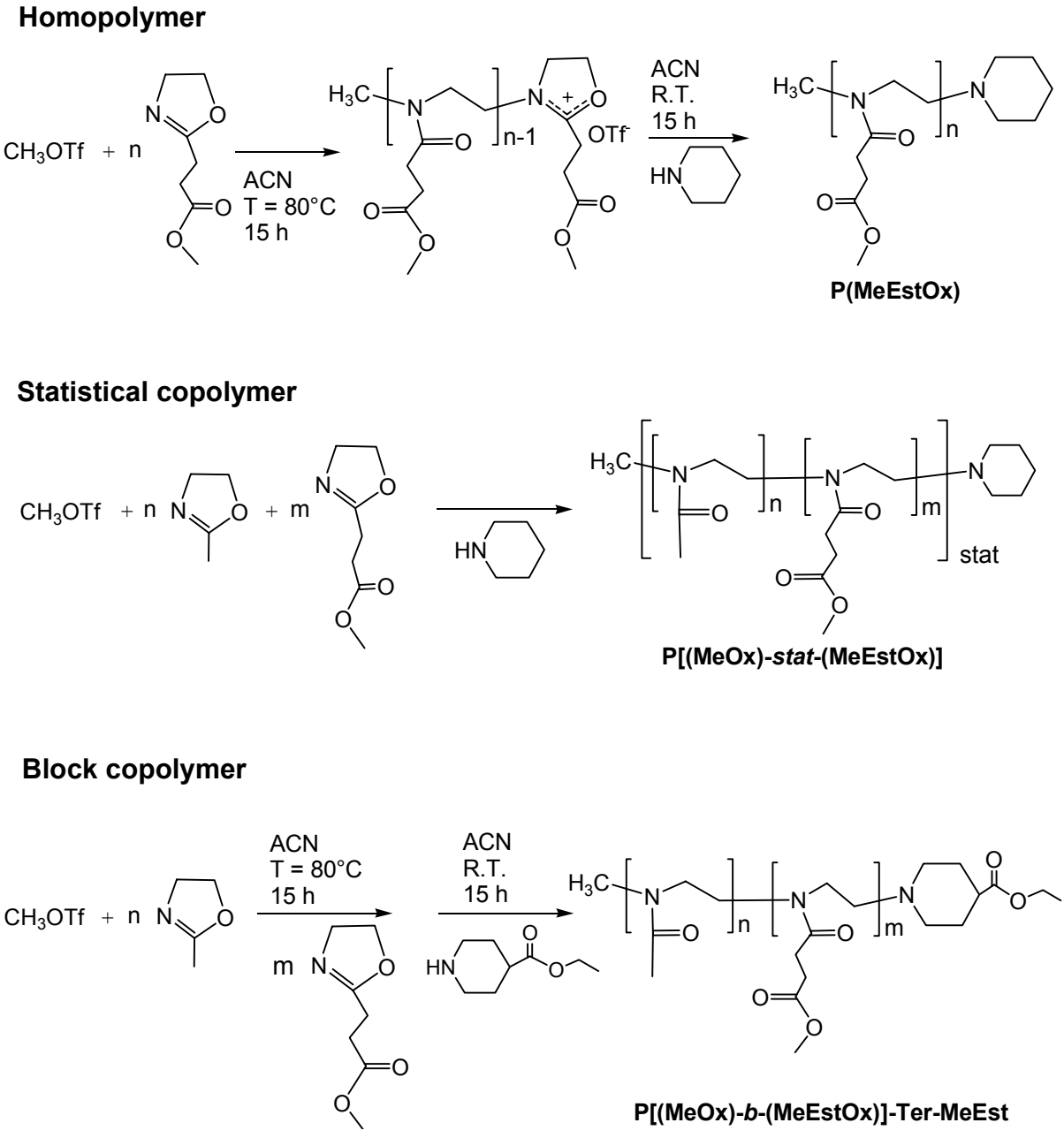

Fig. 4.18 Polymerization schema of **P[(MeOx)-*stat*-(MeEstOx)]** and **P[(MeOx)-*b*-(MeEstOx)]**.

Block copolymer

The synthesis of the block copolymer follows the standard procedure described in 4.4.1. First, 2-methyl-2-oxazoline was polymerized for 15 h and then **(MeEstOx)Mmer** was added to this solution and reacted for further 15 h. The polymerization was terminated by 4-piperidine-methylester yielding poly[(2-methyl-2-oxazoline)-*b*-(2-(2-methoxy-carbonylethyl-2-oxazoline))] (**P[(MeOx)-*b*-(MeEstOx)]-Ter-MeEst)**. GPC curves and ^{1}H-NMR spectra confirmed the results.
P[(MeOx)-*b*-(MeEstOx)]-Ter-MeEst was hydrolyzed with a $NaOH_{aq}$ at room temperature for 15 h. The ester protective group could be removed as confirmed from ^{1}H-NMR spectra and **P[(MeOx)-*b*-(CarAcOx)]-Ter-CarAc** was obtained in high yield.

4.6.2 Introduction of amine function as an anchor group

One possibility to introduce amines as anchor groups for further coupling with isothiocyanate functionalized peptides is by substitution of the methyl ester group of the polymers described in the previous paragraph (4.6.1) with diethyldiamine.

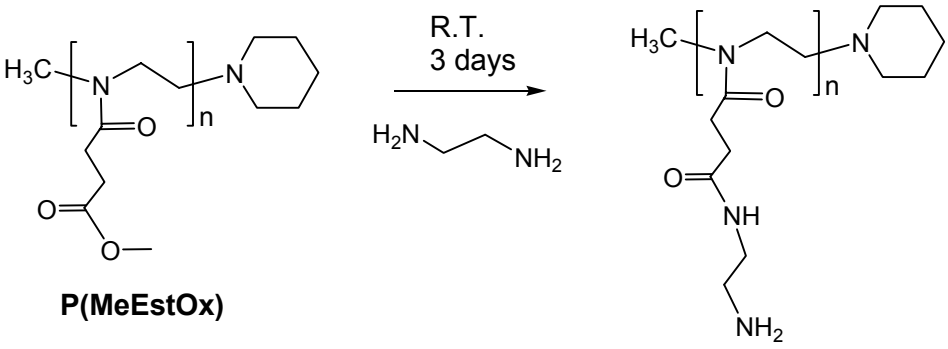

Fig. 4.19 Reaction scheme of the polymer modification of **P(MeEstOx)** with diethyldiamine.

P(MeEstOx) was dissolved in methanol and the solution was added to diethyldiamine. The reaction was monitored by ^{1}H-NMR spectroscopy recording one spectrum every

day. The signal corresponding to the methyl group of the ester decreased and the peak corresponding to the newly formed amide bond appeared.

The ^{1}H-NMR spectrum presented in Fig. 4.20 was recorded after 3 days the signal corresponding to the methyl ester group disappeared (signal indicated by the big arrow), whereas the signal corresponding to the amide group increased its intensity (signal indicated by the thin arrow). The substitution was very slow, the signal corresponding to the methyl group disappeared after 3 days, the advantage is that there was no cross-linking among the polymer chains. As demonstrated by the GPC curves, no shoulder corresponding to polymer fractions of higher molecular weights (lower retention time) was observed (Fig. 4.21).

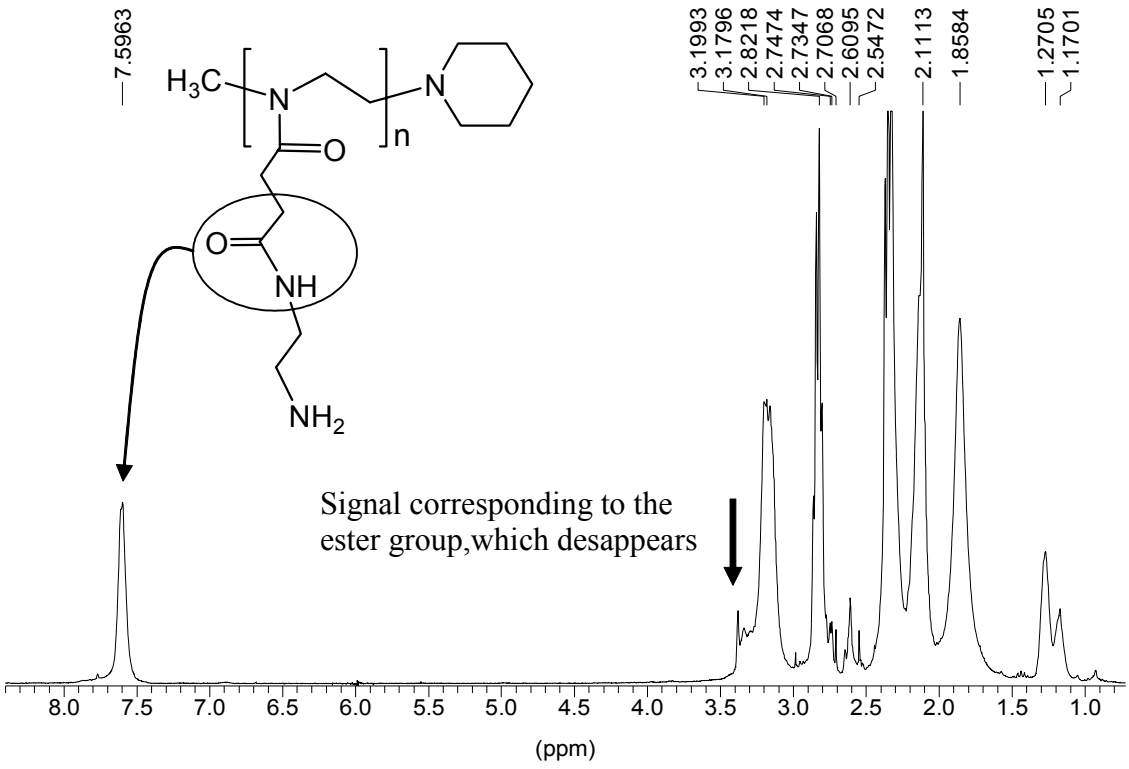

Fig. 4.20 ^{1}H-NMR spectrum of the modified **P(MeEstOx)** with diethylamine after three days.

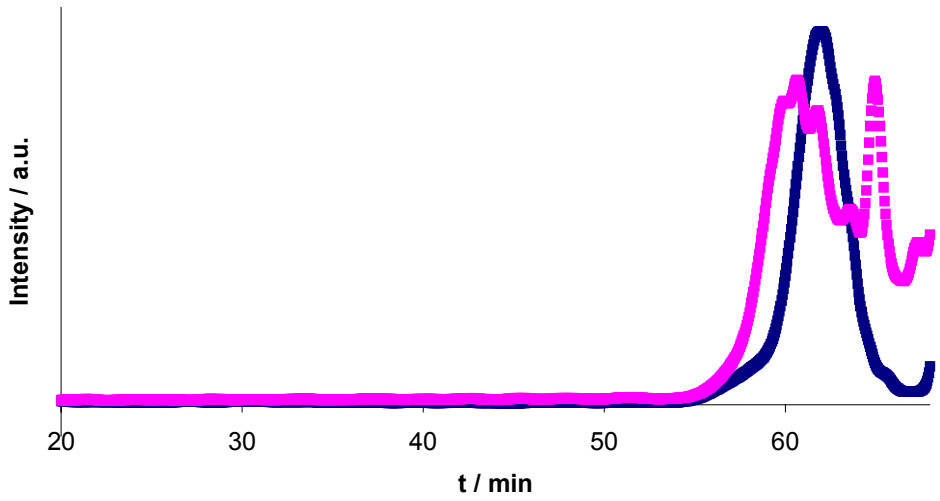

Fig. 4.21 GPC elugram of the polymer modification. The dark line corresponds to the **P(MeEstOx)** and the light line corresponds to **P(MeEstOx) mod. ethylendiamine**.

Monomer synthesis

The introduction of amines as a functional unit could also be performed by monomer synthesis, however, amines interfere in the polymerization mechanism, therefore, they were protected with *t*-butoxycarbonyl (BOC).

J. Auernheimer[6] has synthesized the intermediate [4-(2-chloro-ethylcarbamoyl)-pentyl]carbamic acid-*tert*-butyl ester **(5)**, shown in Fig. 4.22. 6-Amine hexanoic acid reacted with di-*tert*-butyldicarbonate resulting in *N*-BOC-6-aminohexanoic acid **(4)**, which was then coupled with 2-chloroethylammonium chloride salt using EDCI·HCl as coupling reagent and collidine as base.

For the ring closing step, the intermediate **(5)** was dissolved in dry THF and MeOH. This solution was added to a suspension of NaH in dry THF. The ring closing proceeded with an efficiency of ca. 50 % (based on ^{1}H-NMR spectroscopy). The *N*-BOC-5-amino pentyl-2-oxazoline (**(AmineOx)Mmer**) was separated from the side product by column chromatography. The obtained monomer was stored under nitrogen atmosphere. The monomer was characterized by ^{1}H-NMR spectroscopy and ESI-MS.

[6] Co-worker of Prof. Kessler's research group, TU München.

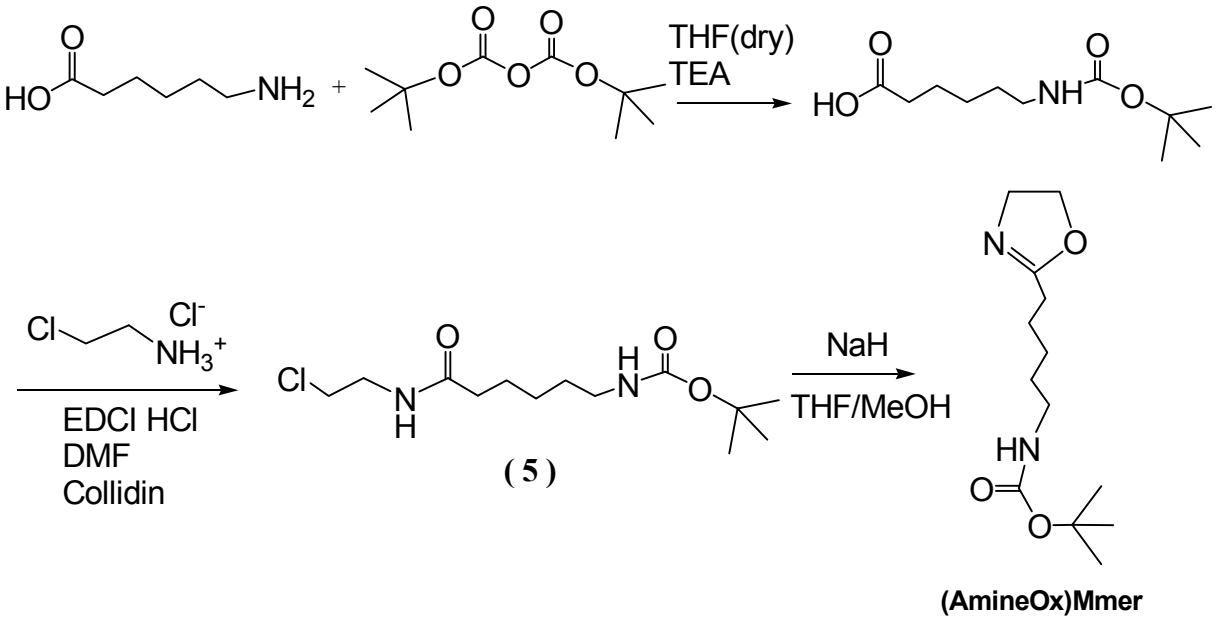

Fig. 4.22 Synthesis pathway of **(AmineOx)Mmer**.

Polymerization

(AmineOx)Mmer was dissolved in a mixture 1:1 of ACN and chlorobenzene. The polymerization was initiated by 2-methyl-oxazolinium triflate salt, since MeOTf would react with the carbamic protective group. The polymerization reaction proceeded for 20 h at 80 °C and it was terminated with piperdine yielding poly(N-Boc-5-amino pentyl-2-oxazoline) (**P(BocAmineOx)**). The polymer was characterized by ^{1}H-NMR spectroscopy and GPC and a narrow molecular weight distribution was obtained, with PDI of 1.15. The deprotection of the Boc-protective group was performed in 50 %-wg. TFA/dichloromethane at room temperature yielding poly(5-amino pentyl-2-oxazoline) (**P(AmineOx)**) and under these conditions the polymer backbone remained unchanged, as confirmed by ^{1}H-NMR spectroscopy.

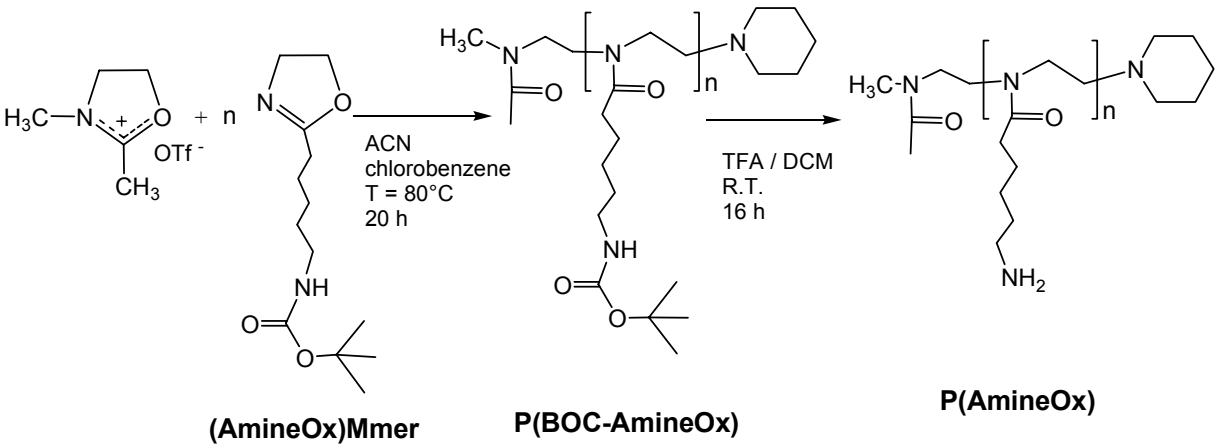

Fig. 4.23 Polymerization of **(AmineOx)Mmer** and cleavage of the protective group.

Tab 3.1 All the functionalized polymers divided by end functionalization (E.F.) and side chain functionalization (S.C.F.)

End Functionalization	
P(MeOx)-Ter-CarAc	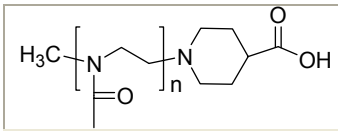
P(MeOx)-Ter-AcrAc	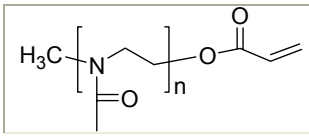
P(MeOx)-Ter-MalIm	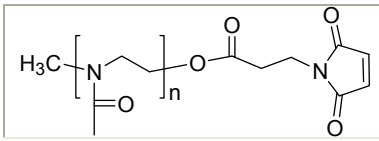
P(MeOx)-Ter-Acetal	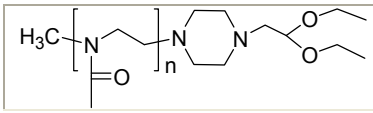
P(MeOx)-Ter-FAld	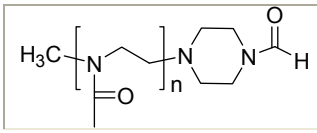
P(MeOx)-Ter-Pipaz	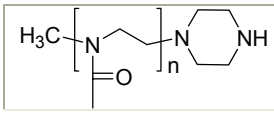
Side Chain functionalization	
P[(MeOx)-*b*-(CarAcOx)]-Ter-CarAc	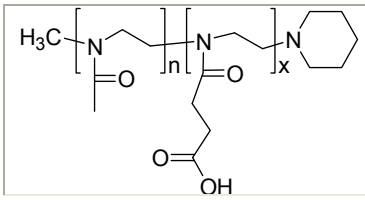
P[(MeOx)-*stat*-(CarAcOx)]-Ter-CarAc	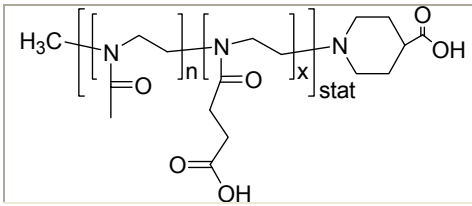
P(MeEstOx) mod. diethyldiamine	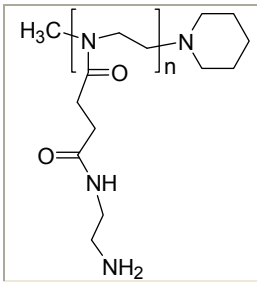
P(AmineOx)	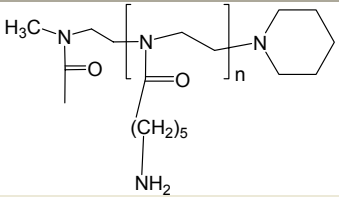

4.7 Coupling reaction

As presented in 4.2.1, the obtained polymers (listed in Tab 3.1) should be coupled with the available cyclic peptides.

A linear test peptide **PEP5** (Ac-FCGKF-NH_2) was synthesized by J. Auernheimer[7] to optimize the reaction conditions for the coupling reactions of the thiol addition and of the amide coupling. Different analytical methods are commonly used to characterize peptides and polymers. Cyclic RGD peptides are very expensive and in some cases the available amount used for the reactions, was not enough. Therefore, the molecules could not be detected with the common analytical methods used for polymers. The use of the test peptide allowed to determine if an analytical method would be appropriate to characterize the polymer-peptide conjugate newly formed (In detail explained in 4.8). The linear test peptide **PEP5** is composed of the following amino acids: phenylalanine (F), cysteine (C), glycine (G), lysine (K), phenylalanine (F), in the sequence FCGKF (Fig. 4.24). The two phenylalanine units put at each end of the linear peptide, mimic the sterical demand of the cyclic RGDfK peptide, cysteine and lysine with thiol and amine functionalities are representative to test the reaction conditions of the polymer-peptide coupling. In Fig. 4.24 the linear test peptide is depicted, along with the alternatively used protecting groups (circles).

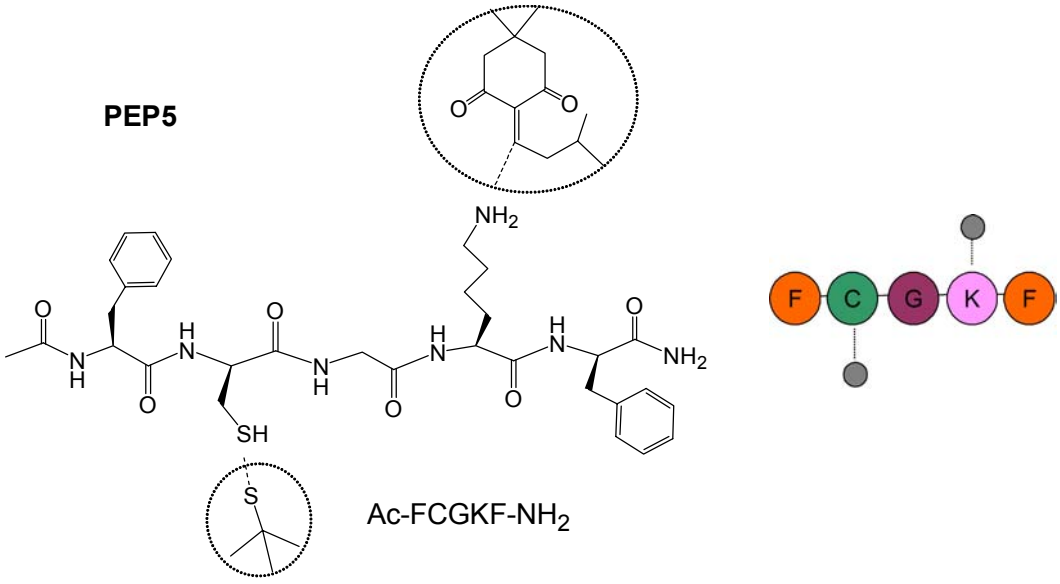

Fig. 4.24 Linear test peptide **PEP5**, Ac-FCGKF-NH_2, with the corresponding protective groups.

[7] Co-worker of Prof. Kessler's research group. TU München.

4.7.1 Michael's addition coupling

As presented in 4.2.1 a thiol group selectively adds to an activated double bond of acrylic acid or maleimide in a Michael's addition.

The reaction conditions were first tested with the linear test peptide **PEP5** protected on the lysine side chains, resulting in **PPC1** and **PPC3**. (Fig. 4.24). The same conditions were applied for the reaction with the cyclic c(-RGDfE-) peptide, **PEP3**.[158,160]

Coupling of **P(MeOx)-Ter-AcrAc** with **PEP3** peptide.

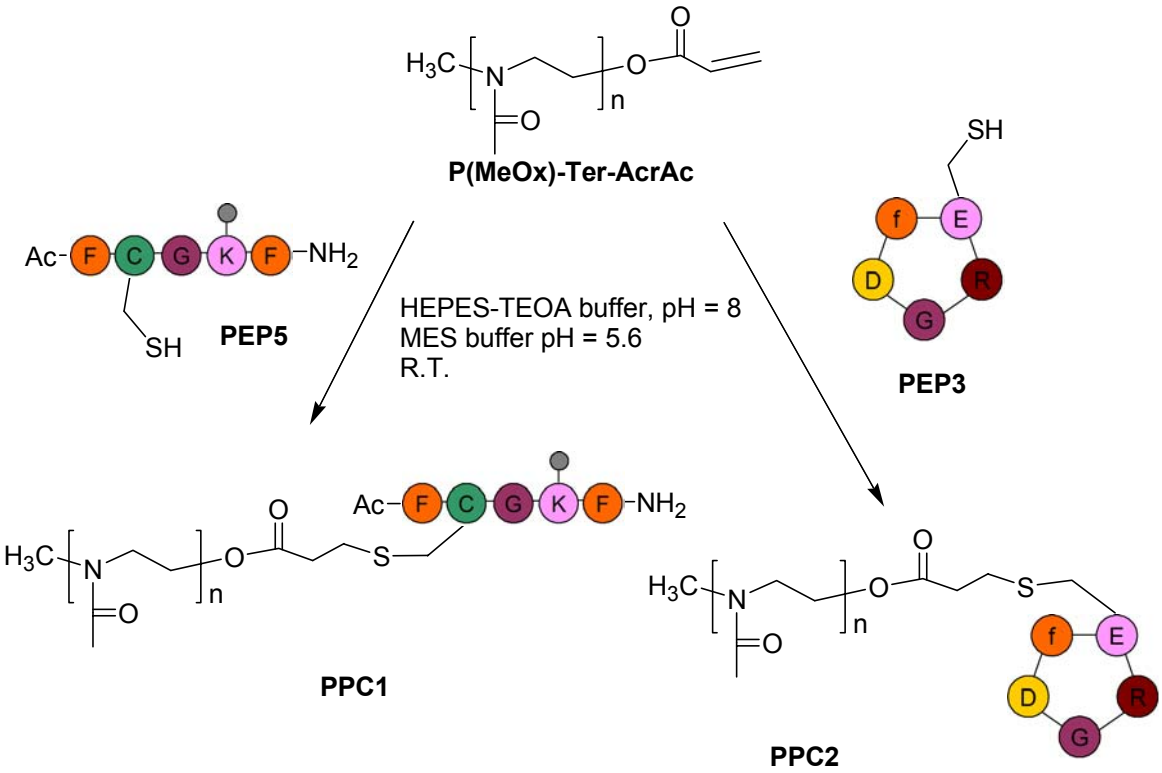

Fig. 4.25 Michael's addition of the thiol funtionalized cyclic peptide (**PEP3**) to **P(MeOx)-Ter-AcrAc**. HEPES = 2-[4-(2-hydroxyethyl)-1-piperazine]-ethane sulfonic acid, TEOA = triethanolamine, MES = 2-morpholine ethane sulfonic acid.

Following the literature,[158] **P(MeOx)-Ter-AcrAc** was dissolved in HEPES buffer at pH = 8 and added to the solution of **PEP3** in MES buffer at pH = 5.8. The mixture was stirred at room temperature for 1 day. After evaporation of the solvent and filtration of the salts, the remaining solid was purified via HPLC, a yellow powder was collected and characterized by ESI-MS and the ^{1}H-NMR spectroscopy. No peak corresponding

to the unreacted cyclic peptide could be found in ESI mass spectra, indicating that the reaction proceeded quantitatively. In Fig. 4.26 the ESI-MS spectrum of the polymer-peptide conjugate 2 (**PPC2**) is presented. The peaks with masses 879.7, 890.8 and 899.2 correspond to the mass of **PPC2** with chain length 10 detected as double charged ions respectively $(m + 2H^+)/2$, $(m + H^+ + Na^+)/2$ and $(m + H^+ + K^+)/2$ (indicated with the rectangles). The difference between two peaks corresponds to the half mass of the monomer unit (m(2-methyl-2-oxazoline) = 85; Δm = 42.5) and the homologous masses of **PPC2** + $2H^+$ are identified with circles. In ^{1}H-NMR spectrum most of the signals could be assigned, except for those that overlap with the solvent signal.

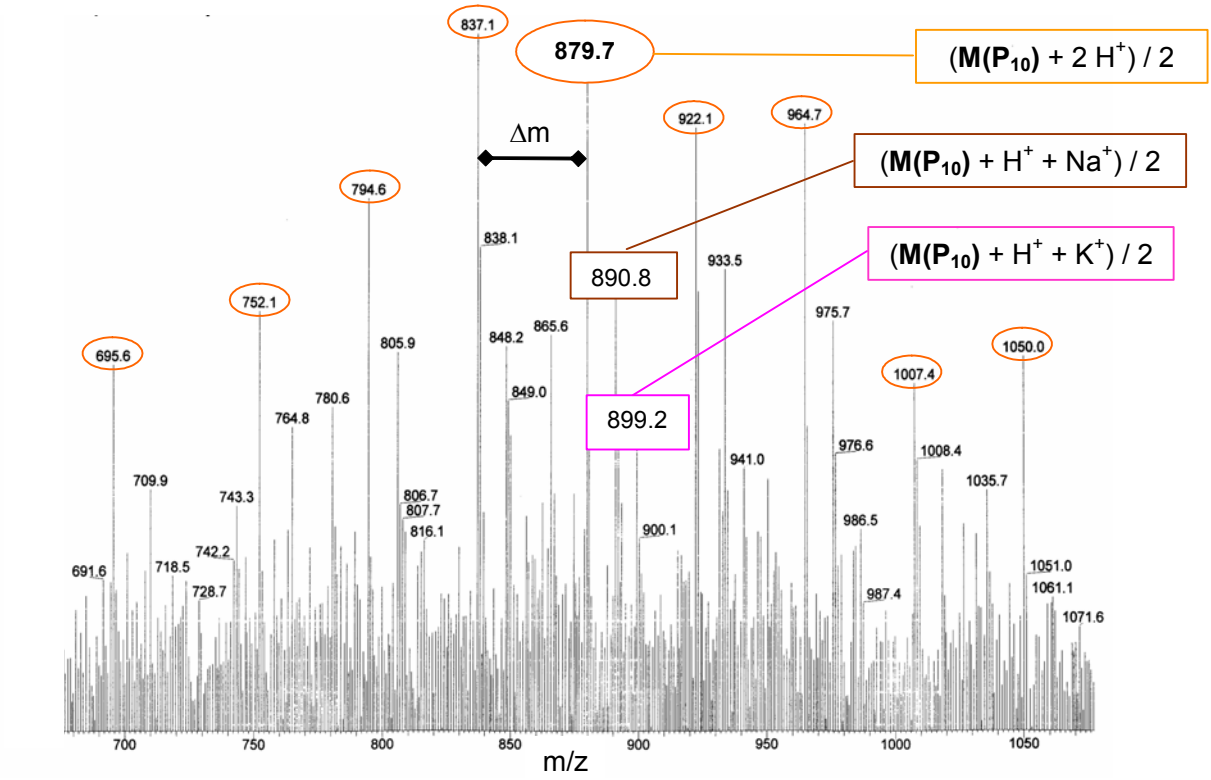

Fig. 4.26 ESI-MS of **PPC2**. M(P_{10}) indicates the exact mass of the polymer-peptide conjugate where the polymer has a degree of polymerization of 10. With the circles are indicated the exact masses corresponding to the distribution of the polymer-peptide conjugate. Δm indicated between two peaks, equal to 42.5, corresponds to the half mass of the monomer 2-methyl-2-oxazoline (m=85).

Coupling of **P(MeOx)-Ter-MalIm** with **PEP3** peptide

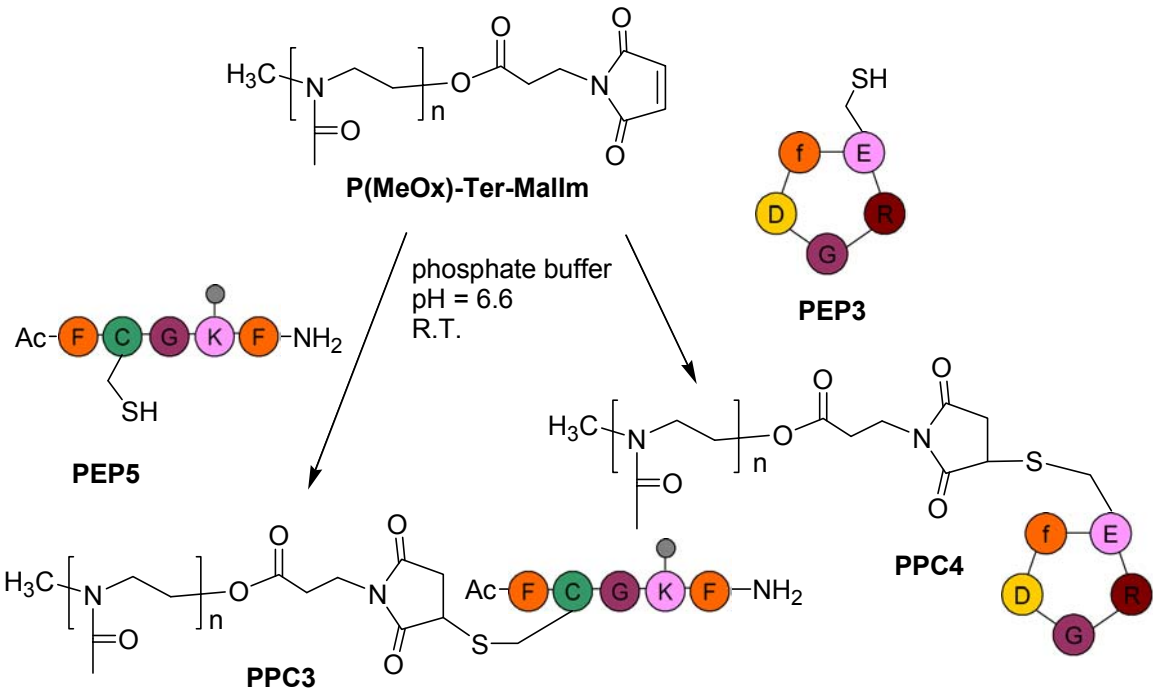

Fig. 4.27 Addition of the thiol group of the cyclic peptide (**PEP3**) to the maleimide functionalized polymer (**P(MeOx)-Ter-MalIm**).

The addition of the thiol group to the double bond of maleimide was also successful. First the reaction was tested with the linear test peptide **PEP5**, equipped with the amine protecting group in the lysine side chain (Fig. 4.24) at 4 °C as well as at room temperature. ESI mass spectra were measured in both cases and the peaks could be assigned to the exact masses of **PPC3**. **P(MeOx)-Ter-MalIm** and **PEP3** were dissolved in phosphate buffer at pH = 6.6 and the mixture reacted at room temperature for 15 h. After evaporation of the solvent the remaining solid was dissolved in MeOH, filtrated and after evaporation of the solvent purified by HPLC. The yellow powder was collected and characterized with ESI-MS and ^{1}H-NMR spectrometry. The peaks recorded by ESI-MS could be assigned to the exact masses of **PPC4**. No peaks corresponding to the cyclic peptide could be assigned and this allows to conclude that the reaction proceeded quantitatively. ^{1}H-NMR spectra revealed that the purification step, in this case, was not completely efficient. All the signals of **PPC4** could be assigned, however, the signal at 6.69 ppm, which corresponds to the double bond of

the not reacted maleimide functional group, did not completely disappear. This indicates that unreacted polymer was still present after purification. **P(MeOx)-Ter-MalIm** was added in excess because the degree of functionalization of the polymer was ca. 81 %, as explained in 4.5.2. It was found that with HPLC the different polymeric products could not be separated.

4.7.2 Isothiocyanate coupling

End functionalization

P(MeOx)-Ter-Pipaz and **PEP4** were dissolved in MeOH and the solution reacted for 3 days at room temperature (Fig. 4.28) and after evaporating the solvent, the remaining solid was separated by HPLC. Each fraction was analyzed by ESI-MS.

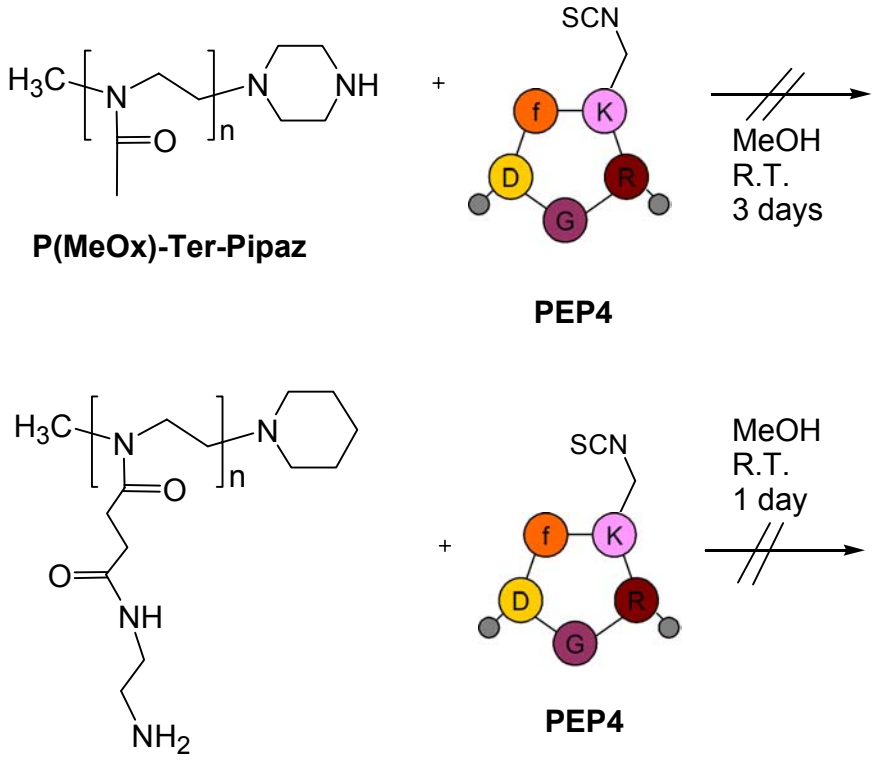

Fig. 4.28 Reaction schema of the isothiocyanate coupling.

In Fig. 4.29 the ESI-MS spectrum is shown. The peak with m/z = 1293.4 corresponds to the cyclic RGD peptide, **PEP4**. The difference between the exact masses of the two signals is 86, which corresponds to a piperazine unit. The peak with m/z = 1379.7 could be assigned to the peptide-piperazine adduct. As described in 4.5.4 a high excess of piperazine was necessary to guarantee a quantitative termination. A small amount of piperazine, remained as an impurity, reacted with the peptide much faster than the polymer would do, this led to the side product.

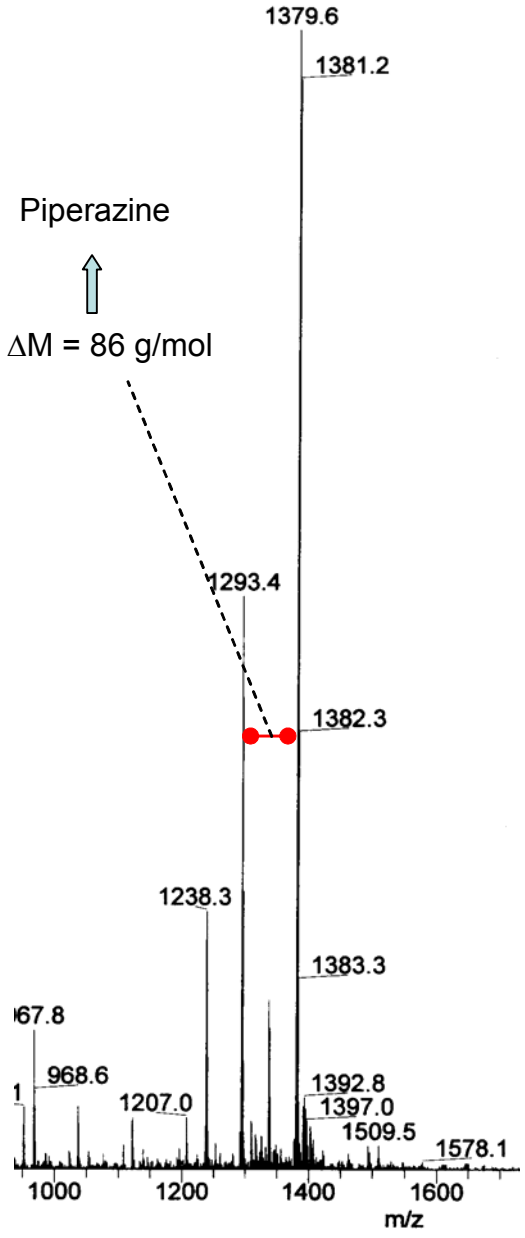

Fig. 4.29 ESI-MS of isothiocyanate RGD after the reaction. The main peak corresponds to the exact mass of the cyclic RGD functionalized with the isothiocyanate anchor group (**PEP4**) which reacted with the piperazine present as impurity. The lower peak corresponds to the exact mass of **PEP4**.

Side chain functionalization

P(MeEstOx) mod. diethyldiamine and **PEP4** were dissolved in MeOH and the solution reacted for 1 day (Fig. 4.28). After evaporating the solvent, the products were separated by HPLC. The resulting chromatogram is depicted in Fig. 4.30.

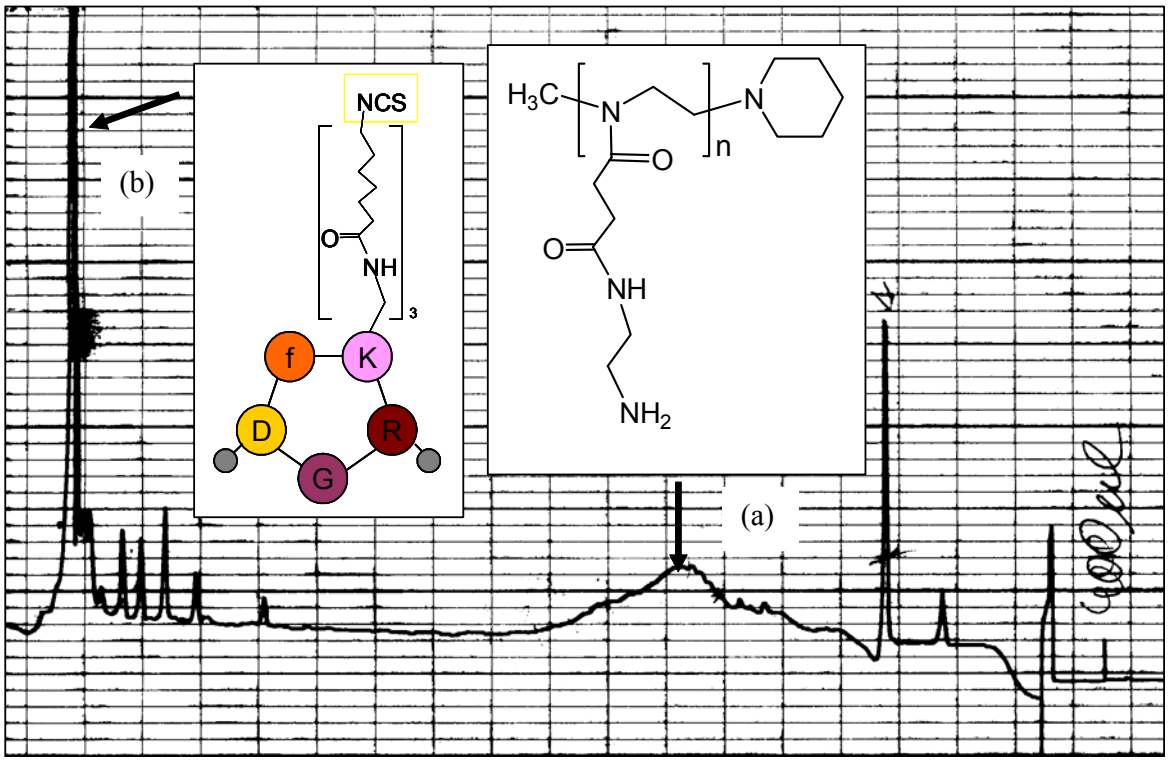

Fig. 4.30 HPLC-chromatogram after the reaction between the isothiocyanate and **P(MeEstOx) mod. diethylamine**.

Two main peaks could be recognized and each fraction was analyzed by ESI-MS. The mass spectrum obtained from the fraction (b) presented a main peak, which corresponded to the exact mass of the cyclic RGD peptide. In the mass spectrum of the peak indicated with (a) many peaks appeared but an assignment resulted very difficult. As explained in detail in 4.8, ESI-MS was not always an efficient way to characterize polymers. In this specific case, the distribution of the exact masses of **P(MeEstOx) mod. diethyldiamine** could not be assigned. A very high number of peaks were generated by the positively charged amines and by the many distributions, due to the statistical substitution of diethyldiamine in the polymer side chains of **P(MeEstOx)**. Even if the reaction would be successful, the characterization of this polymer-peptide

conjugate was not possible. ESI-MS resulted inefficient to characterize this kind of polymer-peptide conjugate. The available amount of peptide was not enough to be detected by GPC, therefore, it could not be observed if an increasing in the molecular weight occurred.

4.7.3 Oxime ligation

The formaldehyde group is of particular interest for poly(2-oxazoline)s because it can be introduced as an end functionalization through the termination of the living chain with N-formyl-piperazine (4.5.3) and, more over, polymerizing the unsubstituted oxazoline monomer, a side chain functionalization could be easily obtained. The coupling between aminooxy and formaldehyde was not found in the literature, therefore, the reaction between N-formyl piperazine and amino-oxy acetic acid was tested (Fig. 4.31).

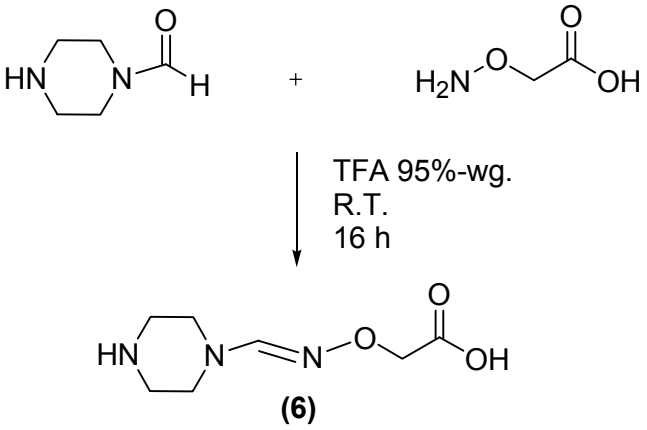

Fig. 4.31 Model reaction to verify the reactivity between the formaldehyde and aminooxy anchor groups.

N-formyl-piperazine and aminooxy hydrochloride acetic acid were dissolved in a 95 % wg. TFA/H_2O solution (TFA = trifluoroacetic acid) and stirred for 15 h. The coupling reaction was successful. In Fig. 4.32 the ^{1}H-NMR spectra of the reagent N-formyl-piperazine (upper spectrum) and of the obtained molecule, piperazine-1-ylmethylenaminooxy-acetic acid **(6)** (lower spectrum) are shown. The signal corresponding to the proton of the formaldehyde (1) at 7.87 ppm disappears, whereas

at 7.59 ppm appears the signal corresponding to the proton of the newly formed bond (6), in Fig. 4.32. The exact mass of the compound **(6)** was obtained by ESI-MS operating in negative mode.

As described in 4.5.3 N-formyl piperazine terminated quantitatively the living polymerization of poly(2-methyl-2-oxazoline)s and it resulted in **P(MeOx)-Ter-FAld**. Under the same reaction conditions used for the coupling between aminooxy hydrochloride acetic acid and N-formaldeyde, described above, **P(MeOx)-Ter-FAld** reacted with aminooxy hydrochloride acetic acid but the reaction was not successful. In ESI mass spectra the peaks could be assigned to the exact masses of the unreacted polymer and to the polymer with piperazine as terminal group. It is possible that the newly formed bond was also hydrolyzed. In ^{1}H-NMR spectra the signals could be assigned to the unreacted polymer. Alternative solutions were tested. Instead of TFA, HCl (1M) was used and the reaction was also performed in neutral conditions, however, no coupling was obtained.

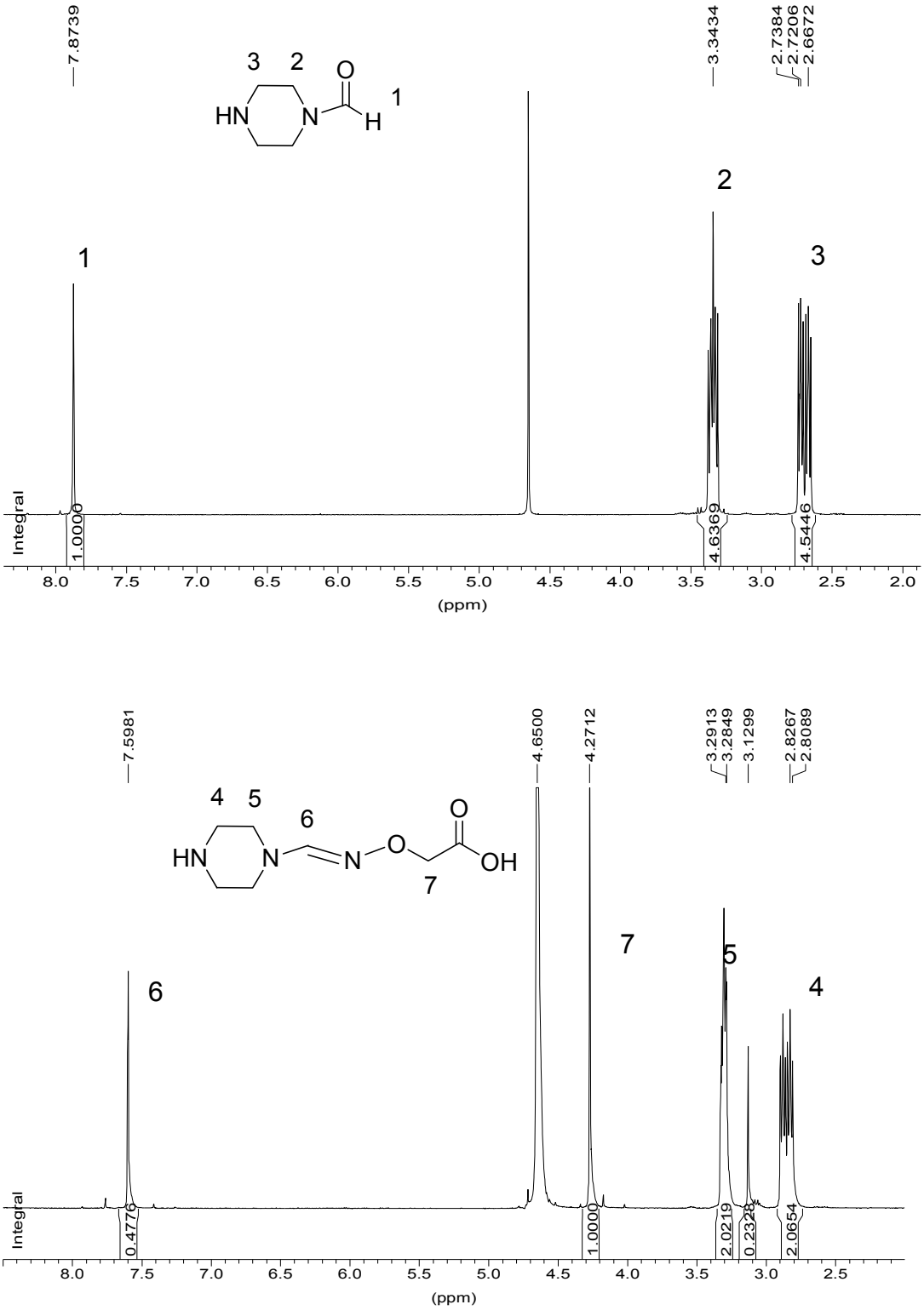

Fig. 4.32 [1]H-NMR spectrum of the model reaction.

4.7.4 Amide coupling

As explained in 4.2.1, the amide coupling is a standard method to covalently bind long chain molecules. This coupling was performed with the amino functionalized peptide and poly(2-oxazoline)s functionalized with carboxylic acid groups as an end functionalization (**P(MeOx)-Ter-CarAc**) and as a side chain functionalization (**P[(MeOx)-*b*-(CarAcOx)]** and **P[(MeOx)-*stat*-(CarAc)]**).

End functionalization

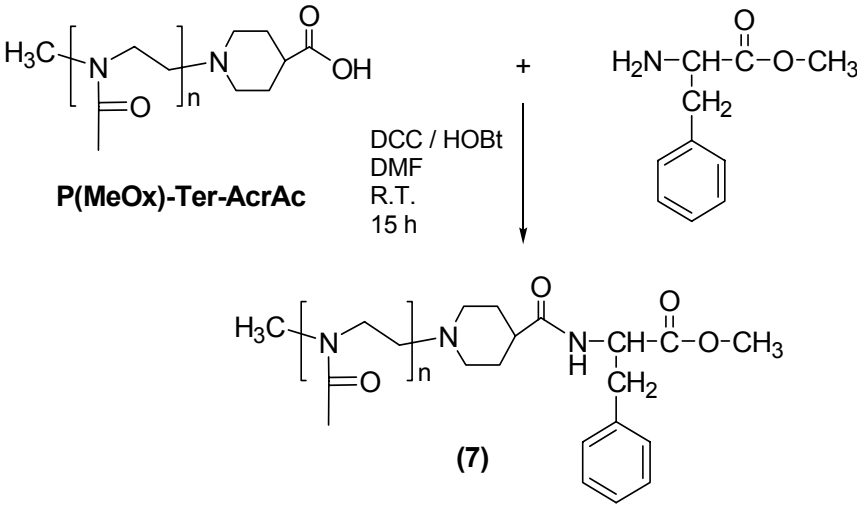

Fig. 4.33 Coupling between **P(MeOx)-Ter-CarAc** and phenylalanine methyl ester. (DMF = dimethylformamide, DCC = dicyclohexylcarbodiimide, HOBt = 1-hydroxy-benzotriazole).

The reaction conditions for the coupling of **P(MeOx)-Ter-CarAc** were optimized with phenylalanine methyl ester, as presented in Fig. 4.33. The polymer was dissolved in DMF and DCC/HOBt were added and DIPEA was used as base (DMF = dimethylformamide, DCC = dicyclohexylcarbodiimide, HOBt = 1-hydroxybenzotriazole, DIPEA = diisopropylethylamine). The coupling reaction proceeded at room temperature for 15 h and resulted in **(7)** as verified by ESI-MS and ^{1}H-NMR spectroscopy.

Under the same reaction conditions, the **PEP2** did not react with **P(MeOx)-Ter-CarAc**. ESI-MS spectra, the peaks could be assigned to the molecular mass distribution of **P(MeOx)-Ter-CarAc**. The reaction is probably significantly slower because of the sterical hindrance in the cyclic peptide, as compared to phenylalanine methyl ester. The carbon atom in α-position of the carboxylic acid is a tertiary carbon atom and it could also have an influence on the reactivity.

The block copolymer **P[(MeOx)-*b*-(CarAcOx)]** can be considered as an intermediate structure between an end functionalized polymer and a side chain functionalized polymer. The functional groups are accumulated on one end of the polymer and increasing the number of the reactive groups in one molecule, the efficiency of the coupling reaction may also be increased.

P[(MeOx)-*b*-(CarAcOx)] was coupled with the test peptide **PEP5** (Fig. 4.24) using PyBOP/HOBt and TEA as base resulting in **PPC5** (PyBOP = benzotriazole-1-yl-oxy-tris-pyrrolidino-phosphinium hexafluorophosphate). The increasing of the molecular weight observed by GPC analysis indicated the successful reaction.

Under the same reaction condition, the cyclic RGD peptide was coupled with **P[(MeOx)-*b*-(CarAcOx)]**. The reaction was monitored by GPC but the molecules could not be detected. The available amount of the cyclic RGD peptide used was much lower than the amount used in the test reaction. Unfortunately, the concentration of the product was not high enough to be detected by GPC.

Side chain functionalization

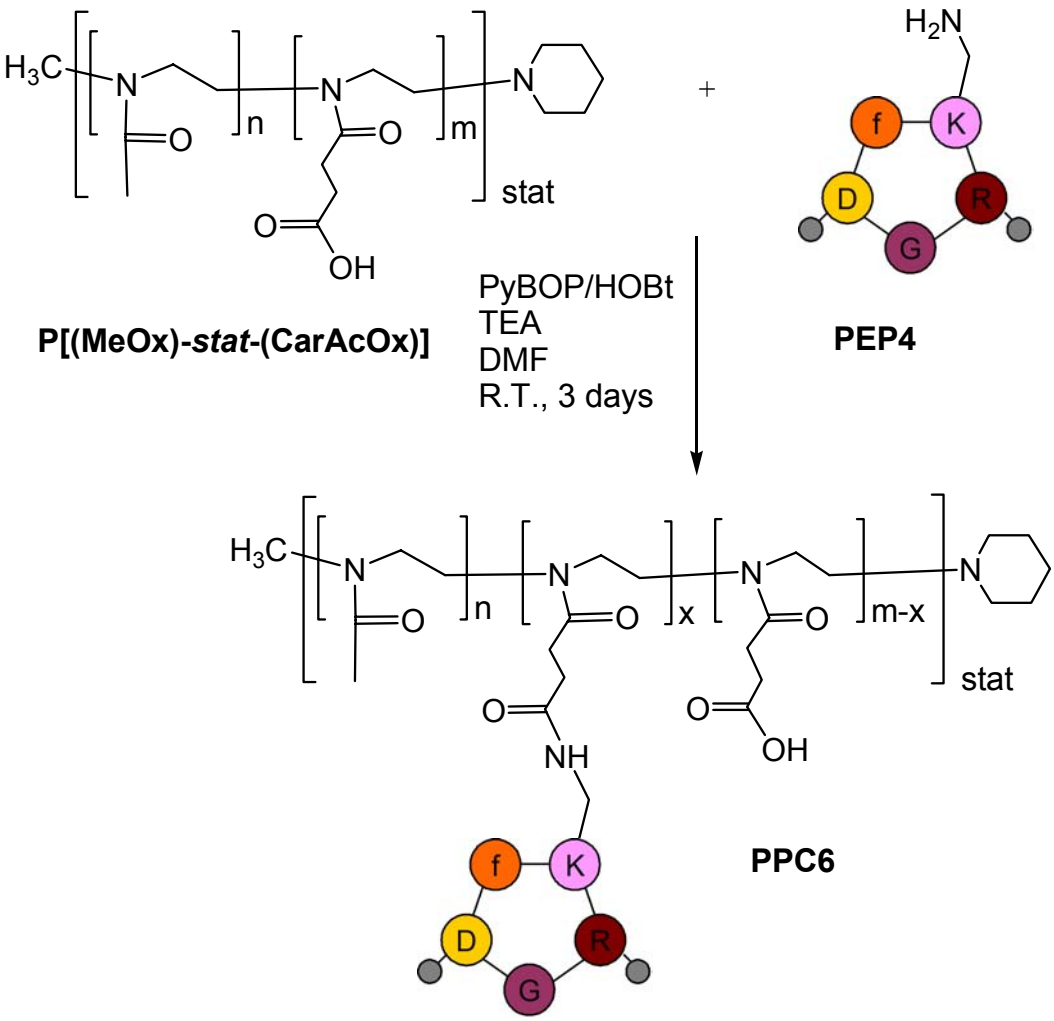

Fig. 4.34 Coupling reaction between the cyclic RGD peptide and **P[(MeOx)-*stat*-(CarAcOx)]**. (PyBOP = benzotriazole-1-yl-oxy-tris-pyrrolidino-phospinium hexafluorophosphate, HOBt = 1-hydroxybenzotriazole, DMF = dimethylformamide, TEA = triethylamine).

The homopolymer **P(MeEstOx)** and the statistical copolymer **P[(MeOx)-*stat*-(CarAcOx)]** were synthesized to perform a side chain functionalization via amide coupling. The side chain functionalization has the advantage that the concentration of functional units per molecule increases.

Dimer and tetramer peptides, where 2 and 4 cyclic RGD peptides are bound in one molecule, have been synthesized and it has been demonstrated that the biological activity of these molecules increases with the increasing number of cyclic peptides.[73,173]

This concept could be extended to the polymeric system. Through the side chain functionalization more functional units could be introduced in one molecule. In this specific case of living polymerization, the number of functional units introduced can be controlled through the monomer initiator ratio, therefore, a series of polymers could be synthesized varying the number of functional groups introduced in the polymer.

The simplest structure that could be synthesized would be a homopolymer containing only carboxylic acid in the side chains. **P(MeEstOx)** was synthesized with a degree of polymerization of 10 and 20. The number of cyclic RGD peptides, which should have been linked to the polymer, would have been controlled by the stoichiometry of the coupling reaction. However, as described in 4.6.1, hydrolysis of the ester protective group was not successful, as a consequence further coupling could not be performed.

As an alternative structure, a statistical copolymer (**P[(MeOx)$_n$-*stat*-(CarAcOx)$_m$]**) was synthesized. In this case a series of polymer with different numbers of functional reactive groups could be synthesized varying the monomer initiator ratio (n = 8, m =2; n = 16, m =4; n = 12, m = 8). For medical applications, it is important that the polymer is water soluble and the copolymerization of **(MeEstOx)Mmer**, bearing the functional unit, with 2-methyl-2oxazoline guarantees that the copolymer remains water soluble.

P[(MeOx)$_n$-*stat*-(CarAcOx)$_m$] with n = 16, m = 4 was coupled under the same reaction conditions used for **PPC5** (PyBOP/HOBt, TEA as base) resulting in **PPC6**, which was purified by HPLC after filtration of the salts. In the HPLC chromatogram, three peaks appeared. Two of them are overlapped, resulting in two main peaks. Each fraction collected was characterized by MALDI-TOF mass spectrometry. In MALDI-TOF spectra, to any of the two fractions, no peak corresponded to the exact mass of the cyclic peptide was detected and it can be concluded that the peptide reacted quantitatively. Fig. 4.35 displays the GPC elugram of the polymer before the coupling (dark line) and after the coupling (light line). As it can be observed, the molecular weight increases (the light line is shifted to lower retention time), which indicates the success of the coupling reaction.

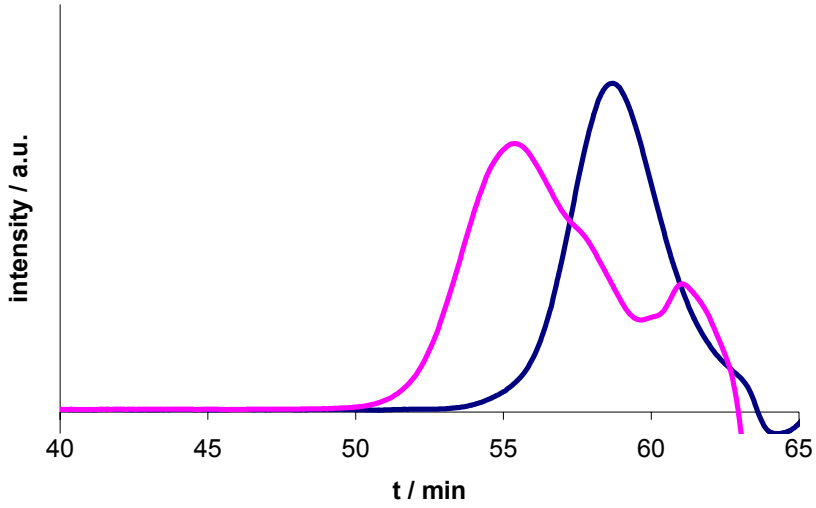

Fig. 4.35 GPC curves of **PPC6** (the light one) and of **P[(MeOx)-*stat*-(MeEstOx)]**.

^{1}H-NMR spectroscopy was also used to characterize **PPC6**, with the aim to establish the number of peptides linked to the polymer. However, it was difficult to find a suitable solvent for the compound. DMSO was used as solvent but poly(2-oxazoline)s form some aggregates and even if the signals could be assigned, the intensities did not correspond to the number of protons in the molecule, therefore, they could not be used to calculate the degree of functionalization peptide-polymer conjugate.

4.8 General consideration about the characterization of the molecules

The central point of this work was to combine the chemistry of synthetic polymers and of cyclic RGD peptides. Some limits had to be considered to study this new system, RGD peptides are much more expensive than poly(2-oxazoline)s and only a few milligrams were available for the coupling reactions, as a consequence the analytical methods usually used to characterize polymers could not always be applied for the characterization of polymer-peptide conjugates (PPC). The amount of substance was too small to be detected.

The standard degree of polymerization of poly(2-methyl-2-oxazoline)s used for the end functionalization was 10. ESI-MS is a standard analytical method used to characterize peptides, or molecules in general which contain nitrogen atoms. With this

technique, it is possible to measure the masses of molecules lower than 3000. As a consequence, the mass of the polymer-peptide conjugate after the coupling reaction should remain below this value. The cyclic RGD peptides used have molecular weights around 1000 g/mol, the masses of the molecular weight distribution of poly(2-methyl-2-oxazoline)s should remain between 1000 g/mol and 1500 g/mol. The molecular weight of a monomer unit is 85 g/mol, therefore, a degree of polymerization of 10 would verify the requirement $10 \leq DP_n \leq 15$.

ESI-MS was an efficient method to characterize the polymers used for the end functionalization and the corresponding polymer-peptide conjugates. As it concerns the polymers used for the side chain functionalization, the homopolymer and the block copolymer could still be characterized but in the mass spectra of the statistical copolymer too many peaks appeared and it was no more possible to assign them. The polymer-peptide conjugates obtained through the side chain functionalization reached molecular weights higher than 3000, therefore these molecules were characterized with MALDI-TOF instead of with ESI-MS.

MALDI-TOF, as characterization method, presents two difficulties: The first one is still related to the high number of signals due to the statistical distributions of the polymer itself and to the statistical ligation of the peptide with the polymer. The second one is related to the method itself. MALDI-TOF is the abbreviation for matrix assisted laser desorption / ionization - time of flight and the ionization energy is transmitted to the analyzed molecules through a matrix[8]; poly(2-oxazoline)s and peptide are usually detected using different matrices and it may be possible that none of the two is efficient for the polymer-peptide conjugate.

The methods used to characterize the molecules allowed in most cases to conclude if the coupling reaction occurred or not but the quantification remains another task.

[8] Matrix: is a small organic compound absorbing in the area of the UV wavelength of the laser used to excite the molecules. The matrix must have a good compatibility in solution and a good miscibility in the solid phase with the analyzed substance.

5 Summary and outlook

Inspired to *Ringsdorf*'s model for pharmacologically active polymers, the aim of this work was to create a new system, which uses poly(2-oxazoline)s as carrier, cyclic RGD peptides as targeting molecule and radioactive compounds as pharmacon. Cyclic RGD peptides were chosen as biological target because they selectively interact with $\alpha_v\beta_3$-integrins, which are cell receptors over-expressed in epithelial cells activated by growth factors produced by tumor cells. Radiolabeled cyclic RGD peptides could image tumors in mice.

The main point of this work was to combine these three units together, or in other words: to develop the chemistry which allows to combine peptides with synthetic polymers.

The peptide chosen was a cyclic RGD composed of five amino acids c(RGDfX) (R, arginine, G, glycine, D, aspartic acid, f, D-phenylalanine, X indicates a variable amino acid). The primary sequence, RGD, is the biologically active sequence, the D-phenylalanine stabilizes the ring in a βII-γ turn, X is a variable amino acid usually used to introduce the functional reactive group through its side chain.

Cyclic RGD peptides were available with the following functional groups: amine, thiol, isothiocyanate and aminooxy. The coupling of these peptides would be possible if the corresponding functional groups could be introduced in the polymer.

Poly(2-oxazoline)s can be functionalized by means of end functionalization, through the initiation and/or termination step, and of side chain functionalization through the monomer synthesis following three different strategies: in the initiation step, R^1X, in the termination step.

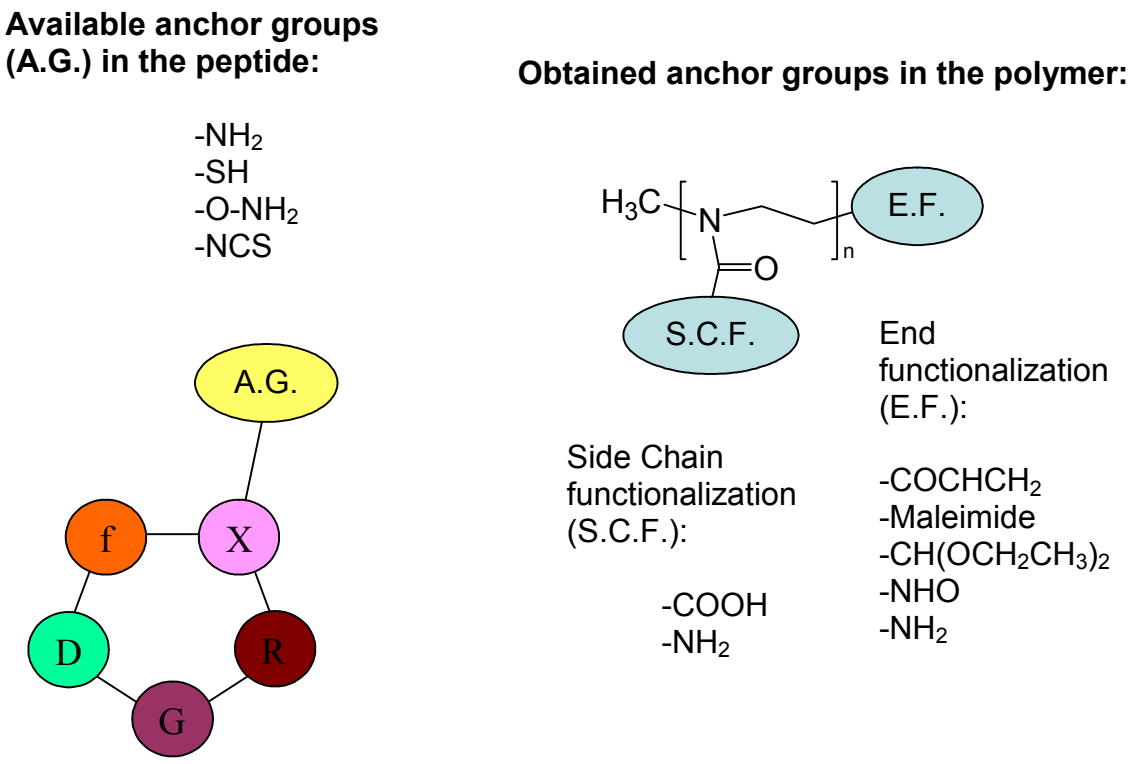

Fig. 5.1 Functional groups introduced in the cyclic RGD peptide and in poly(2-oxazoline)s.

Fig. 5.1 presents the functional groups of the available peptides, on the left hand side, and those introduced in the polymer in this work on the right hand side. Terminating the living polymerization of poly(2-methyl-2-oxazoline) with acrylic acid and following the same procedure with 3-maleimide propionic acid, an activated double bond could be introduced as an end functionalization. Aldehyde groups could be introduced in its protected form, synthesizing a terminating agent, or as formaldehyde, terminating the living polymer with N-piperazino-formaldehyde. Secondary amines can be easily introduced by terminating the living polymer with piperazine. Carboxylic acid functions could be introduced as an end functionalization, as well as as side chain functionalization. A new synthetic pathway resulted in the introduction of amine functionalities in the side chains.

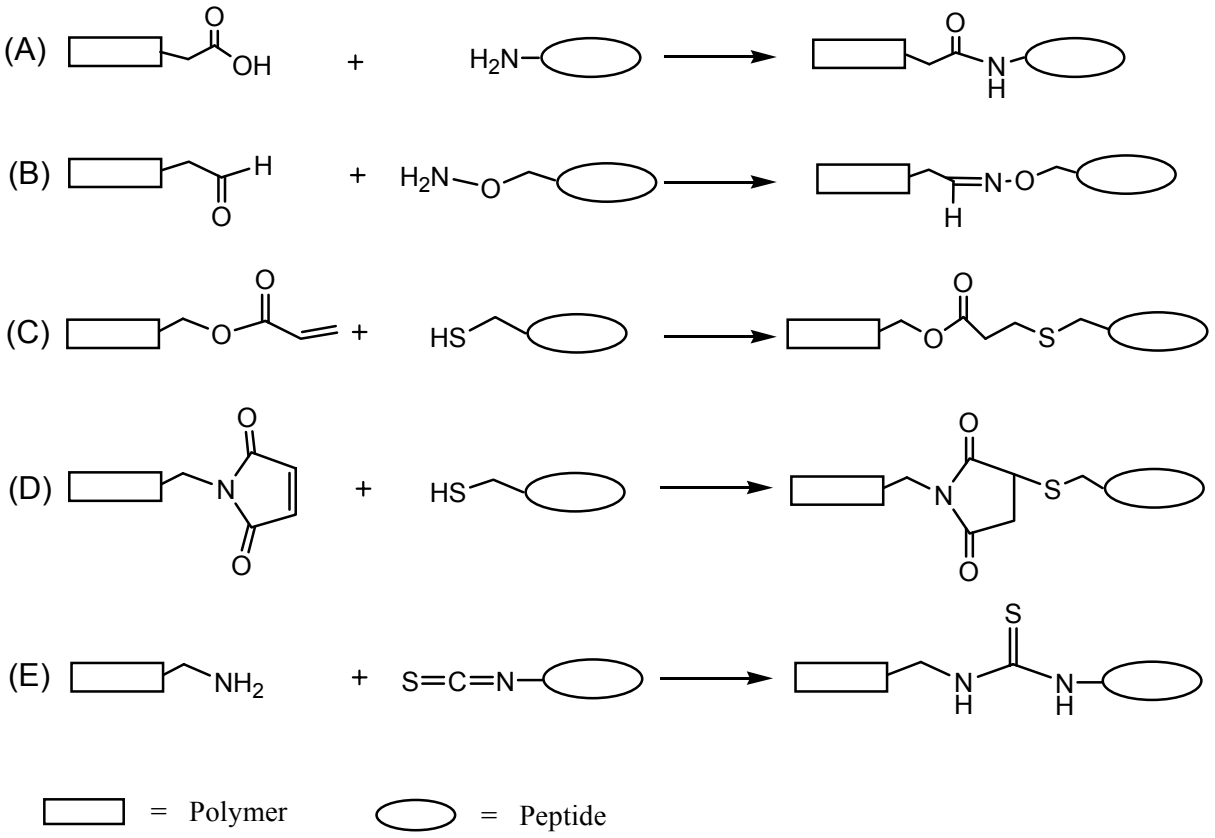

Fig. 5.2 Coupling reaction chosen in this work. (A) carboxylic acid on the polymer and amine on the peptide; (B) aldehyde on the polymer and aminooxy on the peptide; (C) acrylate on the polymer and thiol on the peptide; (D) maleimide on the polymer and thiol on the peptide; (E) amine on the polymer and isothiocyanate on the peptide.

The coupling reactions chosen in this work for the combination of the cyclic RGD peptides and polymers were the amide coupling, the addition of the thiol group to activated double bonds, given by acrylic acid and maleimide, the oxime ligation, obtained by the reaction between aminooxy and aldehyde or formaldehyde and the formation of thiourea derivatives obtained by the reaction of isothiocyanate with amines (Fig. 5.2).

The addition of thiol groups to the activated double bonds (acrylic acid and maleimide) allowed the end functionalization of poly(2-oxazoline)s with cyclic RGD peptides. Only small molecules, such as phenylalanine, could be bound via the amide coupling to the polymer with carboxylic acid as the end functionalization, whereas the carboxylic group in the side chains of the statistical copolymer poly(2-methyl-2-oxazoline)-*stat*-(2-propionic acid-2-oxazoline)s could be successfully ligated with the amino functionalized peptide. In Fig. 5.3 are summarized all the possible

functionalities, which could be successfully introduced in the polymer and the coupling reactions.

Functionalized polymers		Coupling with peptide	
		FCGKF	c(RGDfX)
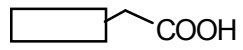	**P(MeOx)-Ter-CarAc** **P[(MeOx)-*b*-(CarAcOx)]-Ter-CarAc** **P[(MeOx)-*stat*-(CarAcOx)]**	**PPC5**	**PPC6**
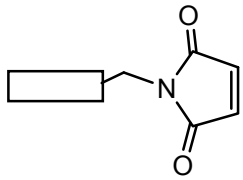	**P(MeOx)-Ter-MalIm**	**PPC3**	**PPC4**
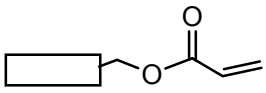	**P(MeOx)-Ter-AcrAc**	**PPC1**	**PPC2**
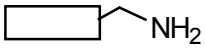	**P(MeOx)-Ter-Pipaz** **P(MeEstOx) mod. diethylamine** **P(AmineOx)**	?	?
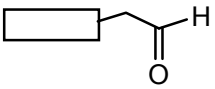	**P(MeOx)-Ter-Acetal** **P(MeOx)-Ter-Fald**	?	?

Fig. 5.3 Summary of the functionalities introduced into poly(2-ocazoline)s and coupling reactions with the test peptide and with the cyclic RGDfX peptide.

6 Experimental part

6.1 Material and methods

All polymerization reactions were performed under inert nitrogen atmosphere to prevent a hydrolysis reaction or reaction with oxygen. Nitrogen was passed over BTS-Catalyst from BASF and dry molecular sieve (4Å). Before using the solvents, they were distilled and dried according to the literature and stored, over molecular sieve (4Å) under inert nitrogen atmosphere.
Michael's addition of the thiol group to the activated double bond was performed in oxygen free buffer to prevent oxidation of the thiol groups. Chemicals were obtained from *Fluka-Aldrich* and used as received. 2-Methyl-2-oxazoline was distilled under nitrogen atmosphere and stored over molecular sieve (4Å).

NMR spectroscopy:

NMR data were recorded using *Bruker* ARX 300 equipment at 300.13 MHz (^{1}H-NMR) and 75.47 MHz (^{13}C-NMR) in the indicated solvents.

The numeration of the molecules used to indicate the NMR shifts do not correspond to the IUPAC rules.

Gelpermeation chromatography (GPC):

GPC measurements in $CHCl_3$ using UV/RI detector were carried out using PLgel 5 µm MIXED-C columns (PLgel 5 µm Guard, 50 x 7.5 mm, PLgel 5 µm MIXED-C, 300 x 7.5 mm, PLgel 5 µm MIXED-C, 600 x 7.5 mm) using a *Waters* 410 differential refractometer detector, *Waters* 484 UV-detector (λ = 254 nm) and a Water 510 as pump. The flow rate was 1.0 mL/min. The GPC columns were calibrated *vs* polystyrene standards (Polymer Standard Service (PSS), molecular weights 580 to 1.57×10^{6} g/mol).

GPC measurements in DMAc (N,Ndimethylacetamide) were carried out using PLgel 5 μm MIXED-C and PLgel 5 μm MIXED-E columns (PLgel 5 μm MIXED-C, 300 x 7.5 mm MIXED-C, 300 x 7.5 mm, PLgel 5 μm MIXED-E, 300 x 7.5 mm) using a 410 differential refractometer detector for measurements (from *Waters*) and a *Waters* 510 pump. The flow rate was 0.5 mL/min. CPG colums were calibrated *vs* poly(methylmethacrylate) standards (Polymer Standards Service (PSS), molecular weights 960 to 1.64 x 10^6 g/mol)

MALDI-TOF

MALDI-TOF experiments were carried out on a *Bruker* Biflex III using a N_2 laser (λ = 337 nm). 1,8,9-anthracentriol was used as matrix to characterize poly(2-oxazolines) and α-cyano-4-hydroxycinnamic acid was used as matrix to characterize peptides.

Analytical, semi- and preparative HPLC: were performed with the equipments from *Beckman*, *Amersham Pharmacia Biotech* and columns from *YMC Europe GmbH*.

Equipment (A) *Beckman*: System gold, consisting of programmable solvent module 125, programmable detector module 166 and the following column materials were used: (1) *YMC*-ODS-A 120 5-C_{18} (5 μm, 250 mm x 20 mm) semipreparative; (2) *YMC*-ODS-A 120 10-C_{18} (10 μm, 250 mm x 20 mm) semipreparative.

Equipment (B) *Pharmacia* Basic 10 F, contained a pump system P-900, an autosampler A 900, software from: Unicorn, version 3.00 and the following column materials were used: *YMC*-ODS-A 120 5-C_{18} (5 μm, 250 mm x 4.6 mm) analytic.

Equipment (C) *Pharmacia* Basic 100 F, consisting of a pump system P-900 detection system UV-900 and software: Unicorn, version 3.00 and the following

column materials were used: (1) *YMC*-ODS-A 120 10-C_{18} (10 µm, 250 mm x 20 mm) semipreparative; (2) *YMC*-ODS-A 120 11-C_{18} (11 µm, 250 mm x 30 mm) preparative.

As eluent, a mixture of water (bidest. + 0.1 % TFA) and ACN (+ 0.1 % TFA) were used with linear gradient. In case of equipment (C) water (bidest. + 0.1 % TFA) and ACN/water (90 % ACN / 10 % bidest. water + 0.1 % TFA) were applied as eluents instead of pure ACN (+ 0.1 % TFA). The flow rates were 1 mL/min (analytic), 8 mL/min (semipreparative) and 25 mL/min (preparative). The detection was performed at wavelength of 220 and 254 nm.

HPLC-ESI-MS:

A *Finnigan* instrument, type LCQ ggf. was used in combination with HPLC system Hewlett Packard HP 1100 (column material: *YMC* ODS-A 120-3C_{18} (3 µm, 125 mm x 2 mm), flow rate 0.2 mL/min) for HPLC-ESI-MS measurements. Water (bidest. + 0.1 % formic acid) and ACN (+ 0.1 % formic acid) with a linear gradient (15 min) were applied as eluent.

The mass was determined as follows: X $[m(n=Y) + Z]^+$, X is the detected value, Y represent the degree of polymerization of the detected polymer chain, Z indicates the cation, which charged the molecule for the detection. The peak with the maximum intensity was indicated by bold characters.

6.2 Amide coupling

6.2.1 Synthesis of P(MeOx)-Ter-EtEst

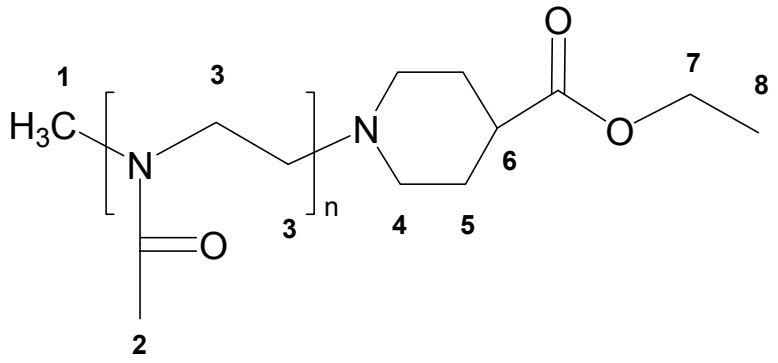

2-methyl-2-oxazoline (1.062 g, 0.0125 mol) was dissolved in ACN (25 mL) and MeOTf (0.205 g, 0.00125 mol) was added under nitrogen atmosphere. The mixture was stirred at 80 °C for 15 h. After cooling the solution to 0 °C, 4-piperidine ethyl ester (0.588 g, 0.00375 mol) was added under nitrogen atmosphere. The solution was stirred for further 12 h at room temperature. The solvent was evaporated in vacuo, the residue was redissolved in 10 mL dichloromethane and dry K_2CO_3 was added. The suspension was stirred for 12 h. K_2CO_3 was removed by filtration and the solvent was evaporated. The yellow residue was dissolved in 5 mL chloroform and precipitated in 100 mL diethylether. A solid colorless powder was collected by filtration and dried in vacuo at 50 °C. Yield = 0.975 g (77%).

^{1}H-NMR ($CDCl_3$): δ in ppm = 1.2 (3H, H^8); 1.8 – 2.2 (4H, H^5; 3H, H^2; 4H, H^4); 2.4 (1H, H^6); 2.9 (3H, H^1); 3.4 – 3.6 (4H, H^3); 4.1 (2H, H^7).

n = 7; M_n = 766.94 g/mol.

HPLC (0 – 50 %, 30 min): R_t = 9.96.

ESI-MS: m/z 597.6 [m(n=5) + H^+]; 682.4 [m(n=6) + H^+]; 767.5 [m(n=7) + H^+]; 852.5 [m(n=8) + H^+]; 937.6 [m(n=9) + H^+]; **1022.6 [m(n=10) + H^+]**; 1107.6 [m(n=11) + H^+];

1192.7 [m(n=12) + H^+]; 1277.7 [m(n=13) + H^+]; 1362,7 [m(n=14) + H^+]; 1447.8 [m(n=15) + H^+]; 1532.8[m(n=16) + H^+]; 1617.9 [m(n=17) + H^+]; 1703.6 [m(n=18) + H^+].

GPC ($CDCl_3$): M_n = 1133 g/mol; M_w = 1276 g/mol; MP = 1498 g/mol; PDI = 1.13.

6.2.2 Hydrolysis of the ester protective group (P(MeOx)-Ter-CarAc)

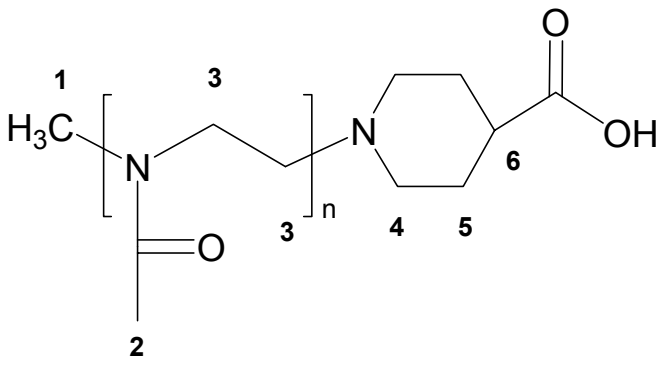

0.210 g of **P(MeOx)-Ter-EtEst** were dissolved in 0.824 mL of 1 N $NaOH_{aq}$ solution and stirred for 15 h. The solution was neutralized with a 1 N HCl_{aq}. Water was evaporated and the solid residue was redissolved in methanol. After filtration of the salts, the solution was concentrated and the remaining solid residue was lyophilized. Yield = 0.190 g, (90 %).

^{1}H-NMR ($CDCl_3$): δ in ppm = 1.8 – 2.2 (4H, H^5; 3H, H^2; 4H, H^4); 2.4 (1H, H^6); 2.9 (3H, H^1); 3.4 – 3.6 (4H, H^3).

ESI-MS: m/z 655.6 [m(n=6) + H^+]; 739.5 [m(n=7) + H^+]; 824.5 [m(n=8) + H^+]; 909.5 [m(n=9) + H^+]; **994.6 [m(n=10) + H^+]**; 1079.7 [m(n=11) + H^+]; 1164.6 [m(n=12) + H^+]; 1249.6 [m(n=13) + H^+]; 1334.6 [m(n=14) + H^+]

6.2.3 Coupling with Phenylalanin-C-methylester (7)

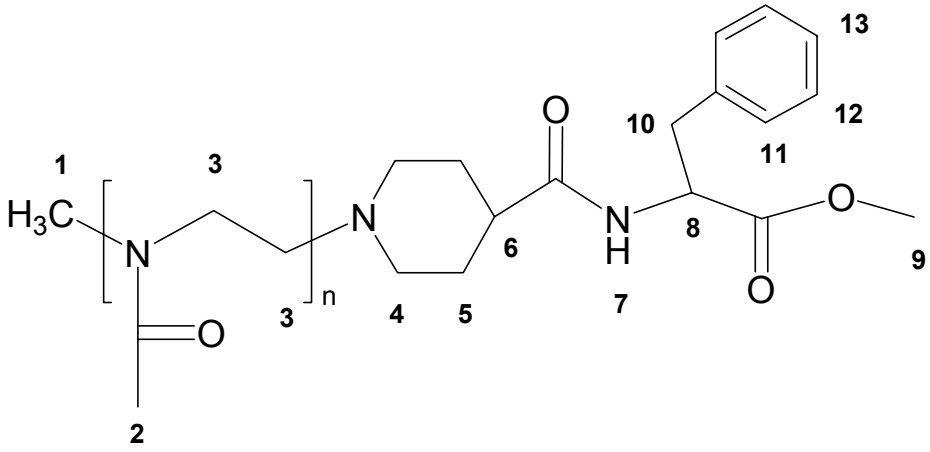

P(MeOx)-Ter-CarAc (11.8 mg, 0.01188 mmol) was dissolved in dry DMF and HOBt (1.8 mg, 0.0123 mmol), DCC (2.6 mg, 0.0123 mmol), phenylalanine methylester (3.2 mg, 0.0178 mmol) and 5 eq. of DIPEA relative to the amount of peptide were added. After stirring the solution for 15 h at room temperature, the solvent was evaporated and the residue was dissolved in dichloromethane and filtrated. The solution was concentrated and precipitated in diethylether. A colorless powder was collected. Yield = 9 mg (66 %).

^{1}H-NMR (DMSO) δ in ppm = 2.1 – 2.2 (3H, H^3; 4H, H^4; 4H, H^5); 2.9-3.0 (3H, H^1; 2H, H^{10}); 3.4 – 3.6 (4H, H^3); 3.6 (3H, H^9); 4.1 (1H, H^8); 7.2 – 7.3 (5H, $H^{11,12,13}$); 7.9 (1H, H^7(NH)).

HPLC (10 – 90 %, 30 min): R_t = 7.83 – 8.07

ESI-MS: m/z 815.5 [m(n=6) + H^+]; 900.6 [m(n=7) + H^+]; 985.6 [m(n=8) + H^+]; 1070.6 [m(n=9) + H^+]; **1155.6 [m(n=10) + H^+]**; 1240.7 [m(n=11) + H^+]; 1325.7 [m(n=12) + H^+]; 1410.8 [m(n=13) + H^+]; 1495.8 [m(n=14) + H^+]; 1580.8 [m(n=15) + H^+]; 1665.9 [m(n=16) + H^+]; 1751.9 [m(n=17) + H^+].

GPC ($CHCl_3$): M_n = 806 g/mol; M_w = 890 g/mol; MP = 1030 g/mol; PDI = 1.10

6.2.4 Synthesis of N-(2-chloroethyl)-3-methoxycarbonylpropanamide (3)

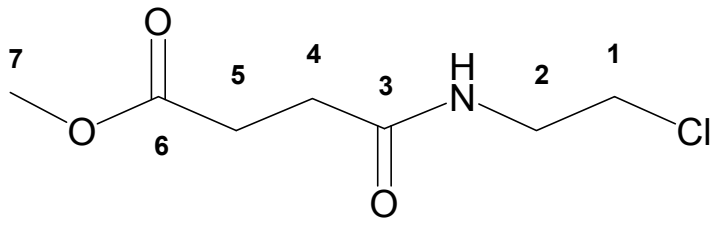

Methyl succinyl chloride (10 g, 0.065 mol) and 2-chloroethylammonium chloride salt (7.75 g, 0.065 mol) were suspended in 100 mL dichloromethane and TEA (15 g, 0.148 mol) was added dropwise at 0 °C. The suspension was stirred for 18 h at room temperature and then 30 mL water were added to the mixture. The organic phase was washed twice with a saturated aqueous NaCl solution and the aqueous phase was extracted twice with 20 mL dichloromethane. The organic phase was dried over anhydrous Na_2SO_4 and the solvent was evaporated. The yellow oil was collected. Yield = 7.07 g (56%)

^{1}H-NMR ($CDCl_3$): δ in ppm = 2.52 (2H, H^5); 2.69 (2H, H^4); 3.62 (4H, $H^{1,2}$); 3.7 (3H, H^7)

^{13}C-NMR ($CDCl_3$): δ in ppm = 29.3 (C^5), 30.9 (C^4); 41.3 (C^2); 43.9 (C^1); 51.9 (C^7); 171.7 (C^6); 173.4 (C^3)

6.2.5 Synthesis of 2-(2-methoxycarbonylethyl)-2-oxazoline ((MeEstOx)Mmer)

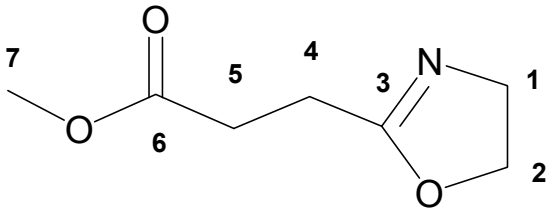

Dry Na_2CO_3 (2 g, 0.018 mol) was added to 7.07 g (0.0365 mol) of N-(2-chloroethylcarbonylpropanamide. The mixture was heated to 40 °C in vacuo until gases were produced. After the evacuation of the gas, the temperature was increased to 160 °C. At 80 °C a colorless fluid was distilled. Yield = 3.55 g (62%)

^{1}H-NMR ($CDCl_3$): δ in ppm = 2.58 (2H, H^4); 2.68 (2H, H^5); 3.7 (3H, H^7); 3.82 (2H, H^1); 4.24 (2H, H^2)

^{13}C-NMR ($CDCl_3$): δ in ppm = 23.1 (C^4); 30.1 (C^5); 51.8 (C^7); 54.4 (C^1); 67.5 (C^2); 167.0 (C^3); 172.8 (C^6)

6.2.6 Synthesis of P[(MeOx)-b-(MeEstOx)]-Ter-MeEst block copolymer

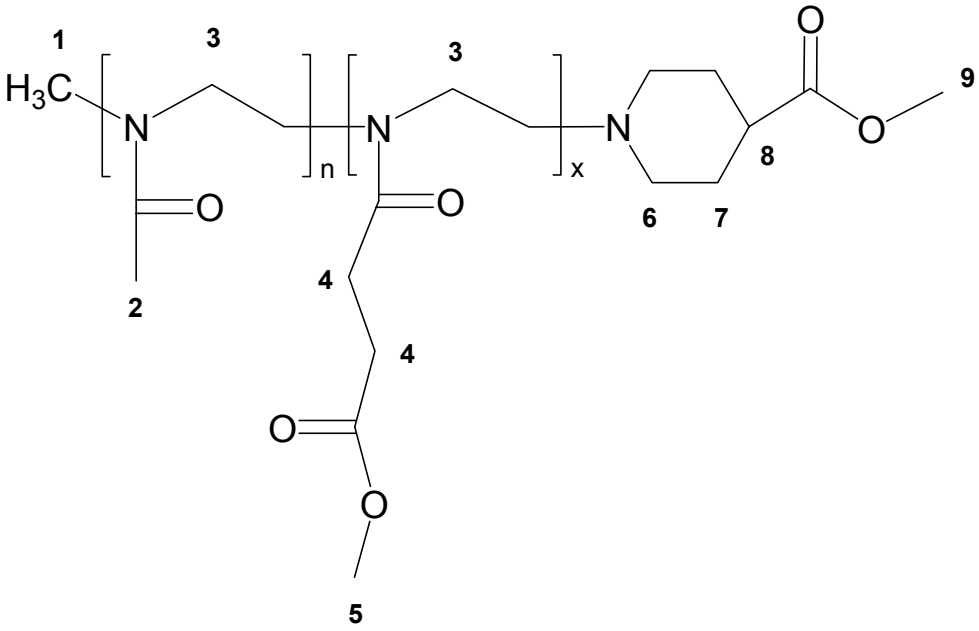

2-methyl-2-oxazoline (0.295 g, 0.003474 mol) was dissolved in ACN and MeOTf (0.056 g, 0.0003474 mol) was added under nitrogen atmosphere. The mixture was stirred for 15 h at 80 °C. After cooling the mixture to 0 °C, 2-(2-methoxycarbonylethyl)-2-oxazoline (0.273 g, 0.00173 mol) was added and stirred for additional 15 h at 80 °C. 4-piperidine methyl ester (0.163 g, 0.00104 mol) was added

at 0 °C and allowed to react for 12 h at room temperature. The solvent was removed in vacuo and the residue was dissolved in 10 mL dichloromethane before dry K_2CO_3 was added. The suspension was stirred for 15 h. After filtration the solvent was removed. The residue was dissolved in chloroform and precipitated in diethylether. The polymer was collected by filtration and dried in vacuo. Yield = 0.39 g (78%).

^{1}H-NMR (D_2O): δ in ppm = 2.0 – 2.1 (3H, H^2); 2.3 (4H, H^6); 2.6 (4H, H^4); 2.9 – 3.0 (3H, H^1); 3.4 – 3.6 (4H, H^3); 3.65 (3H, H^5; 3H, H^9)

n + x = 15; n = 12; x = 3; M_n = 1734.78 g/mol

GPC ($CDCl_3$) M_n = 1279 g/mol; M_w = 1614 g/mol; MP = 1953 g/mol; PDI = 1.26

ESI-MS: m/z 2147.2 m[(n=11,x=4) + H^+]; 1989.5 m[(n=11,x=3) + H^+]; 1833.4 m[(n=11,x=2) + H^+]; 1675.9 [m(n=11,x=1) + H^+]; 1519 m[(n=11,x=0) + H^+]; 2219.3 m[(n=10,x=5) + H^+]; 2061.7 [m(n=10,x=4) + H^+]; 1905.4 m[(n=10,x=3) + H^+]; 1747.6 m[(n=10,x=2) + H^+]; 1590.5 m[(n=10,x=1) + H^+]; 1433.7 m[(n=10,x=0) + H^+]; 2134.2 m[(n=9,x=5) + H^+]; 1977.6 m[(n=9,x=4) + H^+]; 1819.4 [m(n=9,x=3) + H^+]; 1663.3 m[(n=9,x=2) + H^+]; 1506.6 m[(n=9,x=1) + H^+]; 1348.6 [m(n=9,x=0) + H^+]; 2206.1 m[(n=8,x=6) + H^+]; 2049.2 m[(n=8,x=5) + H^+]; 1892.3 m[(n=8,x=4) + H^+]; 1734.4 m[(n=8,x=3) + H^+]; 1577.5 m[(n=8,x=2) + H^+]; 1420.6 m[(n=8,x=1) + H^+], 1264.4 m[(n=8,x=0) + H^+]; 1964.4 m[(n=7,x=5) + H^+]; 1806.6 m[(n=7,x=4) + H^+]; 1649.7 m[(n=7,x=3) + H^+]; 1492.2 m[(n=7,x=2) + H^+]; 1335.5 m[(n=7,x=1) + H^+]; 1178.6 m[(n=7,x=0) + H^+]; 2193.6 m[(n=6,x=7) + H^+]; 2035.6 m[(n=6,x=6) + H^+]; 1879.0 m[(n=6,x=5) + H^+]; 1721.2 m[(n=6,x=4) + H^+];1564.5 m[(n=6,x=3) + H^+]; **1407.7 m[(n=6,x=2) + H^+]**; 1250.5 m[(n=6,x=1) + H^+]; 1093.9 m[(n=6,x=0) + H^+]; 2264.8 m[(n=5,x=8) + H^+]; 2107.4 m[(n=5,x=7) + H^+]; 1951.3 m[(n=5,x=6) + H^+]; 1794.3 [m(n=5,x=5) + H^+]; 1637.3 m[(n=5,x=4) + H^+]; 1480.1 m[(n=5,x=3) + H^+]; 1323.4 m[(n=5,x=2) +H^+]; 1165.6 m[(n=5,x=1) + H^+]; 2023.2 m[(n=4,x=7) + H^+]; 1865.1 m[(n=4,x=6) + H^+]; 1708.5 m[(n=4,x=5) + H^+]; 1551.8 m[(n=4,x=4) + H^+], 1394.5 [(n=4,x=3) + H^+]; 1237.4 m[(n=4,x=2) + H^+]; 1080.0 m[(n=4,x=1) + H^+]; 1623.6

m[(n=3,x=5) + H^+]; 1466.8 m[(n=3,x=4) + H^+]; 1152.8 m[(n=3,x=2) + H^+]; 995.9 m[(n=3,x=1) + H^+]

6.2.7 Hydrolysis of the methylester protective group of P[(MeOx)-b-(EtEstOx)]-Ter-EtEst (P[(MeOx)-b-(CarAc)]-Ter-CarAc)

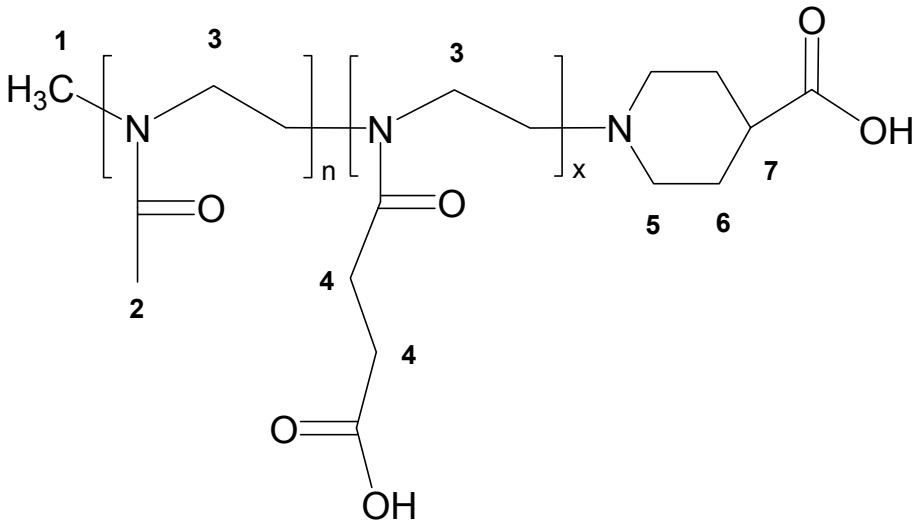

The methyl ester protecting group was hydrolyzed by dissolving 0.2 g of P[(MeOx)-*b*-(MeEstOx)]-Ter-MeEst in 0.556 mL of 1 N $NaOH_{aq}$ solution. After stirring the solution for 15 h, 1 N HCl_{aq} was added before the solvent was evaporated. The solid residue was dissolved in methanol and separated from the salts by filtration. The solution was concentrated and the remaining colorless powder was lyophilized. Yield = 0.17 g (90%)

^{1}H-NMR (D_2O): δ in ppm = 2.1 – 2.3 (3H, H^2; 4H, H^6; 4H, H^4); 2.9 – 3.0 (3H, H^1); 3.4 – 3.6 (4H, H^3)

GPC (DMAc) M_n = 2336 g/mol; M_w = 2548 g/mol; MP = 2176 g/mol; PDI = 1.09

ESI-MS m/z All the corresponding peaks to the masses of P[(MeOx)-*b*-(CarAcOx)]-Ter-CarAc can be assigned as in the case of P[(MeOx)-*b*-(MeEstOx)]-Ter-MeEst.

6.2.8 Coupling between test peptide FCGKF and P[(MeOx)-b-(CarAcOx)]-Ter-CarAc

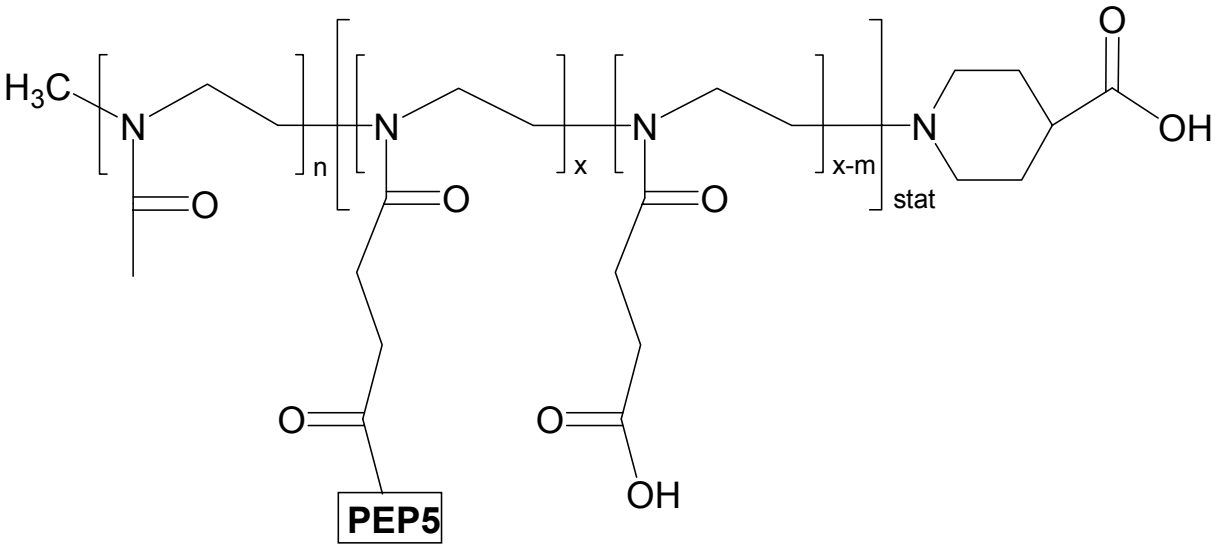

P[(MeOx)-*b*-(CarAcOx)]-Ter-CarAc (5.7 mg, 0.00456 mmol) was dissolved in 0.1 mL dry DMF. Test peptide **PEP5** (10 mg, 0.0137 mmol) was added together with 7.84 mg (0.01507 mmol) of the coupling reagent, PyBOP, 2.03 mg (0.01507 mmol) HOBt and 0.015 mL TEA. The mixture was stirred for 2 days at room temperature. The solvent was evaporated and the residue was dissolved in methanol, filtrated and the solution was concentrated and finally purified via HPLC. Yield = 6.5 mg (35%).

GPC (DMAc) M_n = 3215 g/mol; M_w = 4191 g/mol; MP = 2086 g/mol; PDI = 1.3

6.2.9 Synthesis of the homopolymer P(MeEstOx)

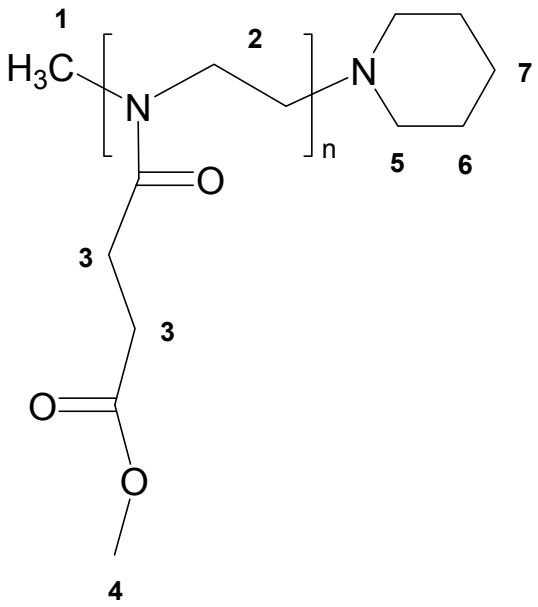

Methyl 2-(2-methoxycarbonylethyl)-2-oxazoline (0.94 g, 0.006 mol) was dissolved in 24 mL ACN under a dry nitrogen atmosphere and MeOTF (0.0984 g, 0.0006 mol) was added. The mixture was stirred for 16 h at 80 °C and then cooled down to 0 °C, before piperidine (0.1512 g, 0.0018 mol) was added. The solution was stirred for further 13 h at room temperature. The solvent was evaporated, the solid residue was dissolved in 10 mL dichloromethane before dry K_2CO_3 was added. The suspension was stirred for 16 h, K_2CO_3 was removed by filtration and the solvent evaporated. The remaining solid was dissolved in chloroform and precipitated in diethylether (-20 °C). The solid was filtrated and dried in vacuo at 50 °C. Yield = 0.3 g (30%).

^{1}H-NMR ($CDCl_3$): δ in ppm = 1.5 (4H, H^6; 2H, H^7); 2.4 (4H, H^5); 2.5 – 2.6 (4H, H^3); 2.9 – 3.0 (3H, H^1); 3.4 – 3.5 (4H, H^2); 3.6 (3H, H^4)

n = 6; M_n = 1042.19 g/mol

GPC ($CHCl_3$): M_n = 1017 g/mol; M_w = 1167 g/mol; MP = 1223 g/mol; PDI = 1.15

ESI-MS: m/z 885 [m(n=5) + H^+]; 1042.6 [m(n=6) + H^+]; 1199.7 [m(n=7) + H^+]; **1356.7 [m(n=8) + H^+]**; 1513.7 [m(n=9) + H^+]; 1670.7 [m(n=10) + H^+]; 1827.8 [m(n=11) + H^+]; 1895.7 [m(n=12) + H^+]

6.2.10 Synthesis of the statistical copolymer P[(MeOx)-stat-(MeEstOx)]

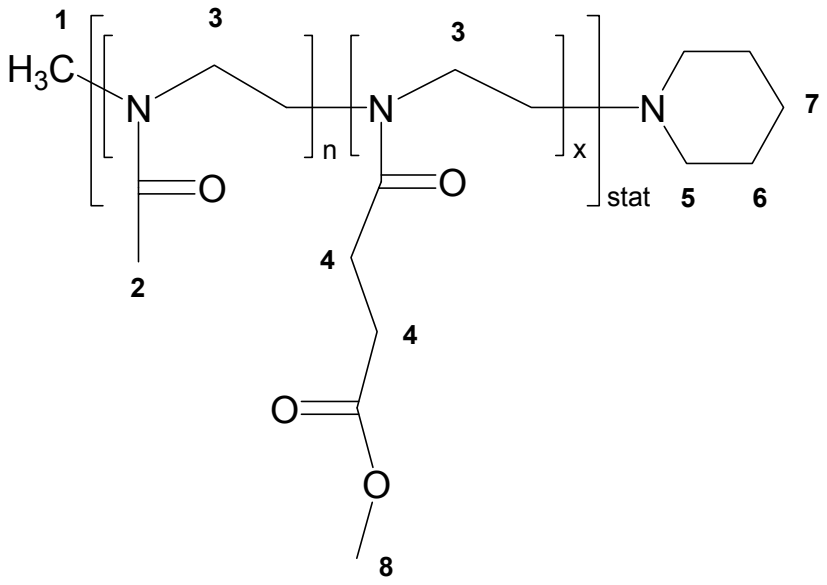

A mixture of 2-methyl-2-oxazoline (0.975 g, 0.01147 mol) and methyl 3-(oxazol-2-yl)propionate (0.451 g, 0.00287 mol) was dissolved in 28 mL ACN under a dry nitrogen atmosphere and MeOTf (0.117 g, 0.000717 mol) was added under stirring. The mixture was heated to 80 °C for 18 h. After cooling the solution to 0 °C, piperidine (0.180 g, 0.00215 mol) was added and the mixture was stirred at room temperature for further 12 h. The solvent was evaporated and the remaining solid was dissolved in dichloromethane before dry K_2CO_3 was added. The suspension was stirred for 14 h, K_2CO_3 was removed by filtration and the solvent was evaporated. The remaining solid was dissolved in chloroform and precipitated in diethylether, cooled in an ice bath. The solid part was collected by filtration and dried in a vacuum oven at 50 °C. Yield = 0.83 g (83%)

^{1}H-NMR (CD_3OH): δ in ppm = 1.5 (4H, H^6; 2H, H^7); 2.0 – 2.2 (3H, H^2); 2.5 – 2.6 (4H, H^4); 3.06 (3H, H^1); 3.4 – 3.6 (4H, H^3); 3.6 (3H, H^8)

n + m = 19; n = 14; m = 5; M_n = 2075.2 g/mol

GPC (DMAc): M_n = 2772 g/mol; M_w = 3040 g/mol; MP = 3019 g/mol; PDI = 1.1

6.2.11 Hydrolysis of the methyl ester protective group of P[(MeOx)-stat-(MeEstOx)] (P[(MeOx)-stat-(CarAcOx)])

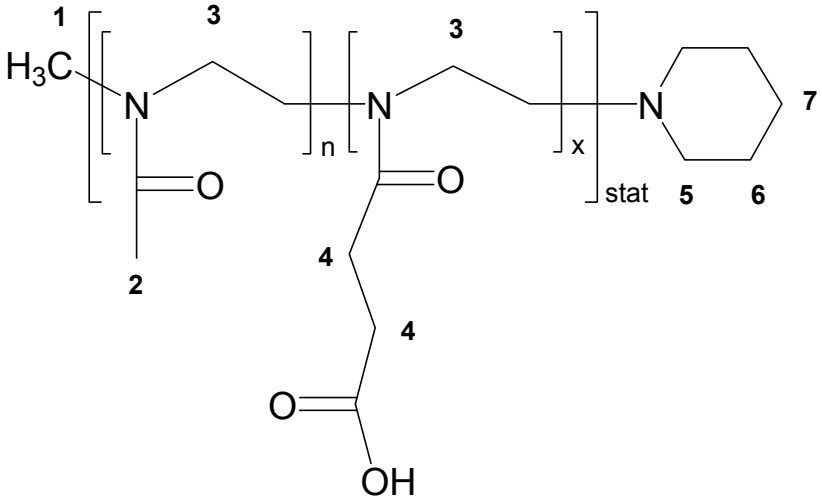

P[(MeOx)-*stat*-(MeEstOx)] (0.7 g) were dissolved in 3.35 mL of a 1 N $NaOH_{aq}$ solution. The solution was stirred for 12 h at room temperature and 1.5 h at 60 °C. The solvent was evaporated and the remaining solid was lyophilized. Yield = 0.644 g (92%)

^{1}H-NMR (CD_3OH): δ in ppm = 1.5 (4H, H^6; 2H, H^7); 2.0 – 2.2 (3H, H^2); 2.5 – 2.6 (4H, H^4); 3.06 (3H, H^1); 3.4 – 3.6 (4H, H^3)

6.2.12 Coupling between P[(MeOx)-stat-(CarAcOx)] and PEP2 (PPC6)

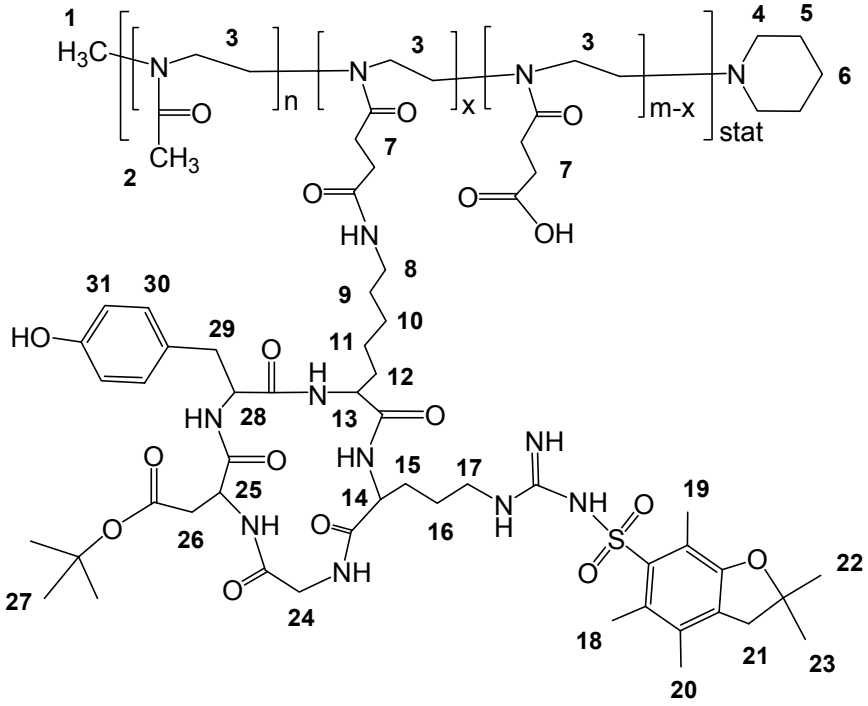

P[(MeOx)-*stat*-(CarAcOx)] (10.33 mg, 0.00508 mmol) was dissolved in 0.150 mL dry DMF. 10 mg of **PEP2** (0.01016 mmol) were added together with PyBOP (5.8 mg, 0.0118 mmol), HOBt (1.59 mg, 0.0118 mmol) and 0.015 mL TEA. The mixture was stirred for 3 days. The solvent was evaporated and the remaining residue was dissolved in methanol and filtrated. The remaining solution was evaporated and the solid residue was purified via HPLC. Yield = 6 mg (30%).

^{1}H-NMR (DMSO) δ in ppm = 1.3 – 1.5 (4H, H^5; 2H, H^6; 2H, H^9; 2H, H^{10}; 2H, H^{11}; 2H, H^{16}, 2H, H^{22}; 2H, H^{23}; 9H, H^{27}); 1.6 (2H, H^{12}; 2H, H^{15}); 2.08 – 2.3 (3H, H^2; 4H, H^7; 3H, H^{18}; 3H, H^{19}; 3H, H^{20}); 2.6 (4H, H^4; 2H, H^{17}; 2H, H^{26}); 2.9 – 3.0 (3H, H^1; 2H, H^{21}; 2H, H^{29}); 7.5 (2H, H^{31}); 7.7 (2H, H^{30})

Signal corresponding to the protons H^8, H^3, H^{25}, H^{28} have been overlapped by the solvent signals.

Signals H^{13}, H^{14}, H^{24} could have a too low intensity and can be confused with the noise of the background line.

GPC (DMAc): M_n = 3948 g/mol; M_w = 5140 g/mol; MP = 5826 g/mol; PDI = 1.3

6.3 Thiol addition

6.3.1 Synthesis of P(MeOx)-Ter-AcrAc

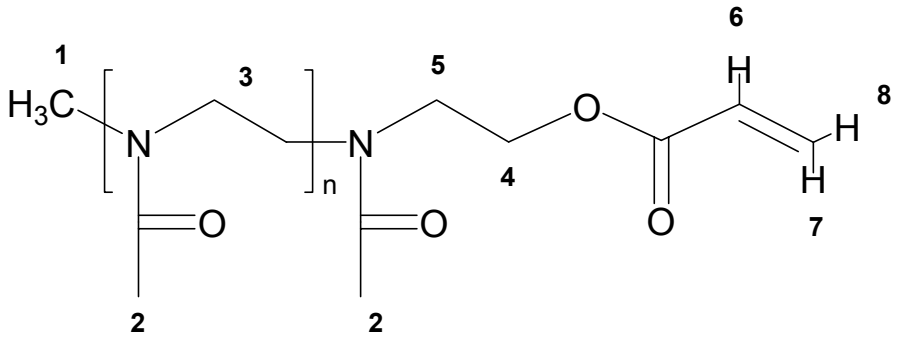

2-Methyl-2-oxazoline (0.908 g, 0.01068 mol) was dissolved in 21 mL ACN and MeOTf (0.175 g, 0.001068 mol) was added under stirring and under a dry nitrogen atmosphere. The solution was stirred for 15 h at 80 °C. After cooling the solution at 0 °C, acrylic acid was added (0.385 g, 0.00534 mol). The solution was stirred for 1 h at 60 °C before the vessel was cooled again and 0.431 g (0.0043 mol) of TEA were added. The mixture was heated to 60 °C for another 15 h. The solvent was evaporated and the solid residue was dissolved in dichloromethane before dry K_2CO_3 was added. The suspension was stirred for 14 h at room temperature. K_2CO_3 was removed by filtration and the solvent was evaporated. The solid was dissolved in chloroform and precipitated in diethylether. The remaining solid was collected by filtration and lyophilized. Yield = 0.8 g (80%)

^{1}H-NMR ($CDCl_3$): δ in ppm = 2.1 (3H, H^2); 2.9-3.1 (3H, H^1); 3.3-3.4 (4H, H^3); 3.5 (2H, H^5); 4.2 (2H, H^4); 5.8 (1H, H^7); 6.1 (1H, H^6); 6.3 (1H, H^8)

n = 10; M_n = 936.99 g/mol

ESI-MS: m/z 512 [m(n=5) + H^+]; 597 [m(n=6) + H^+]; 628.5 [m(n=7) + H^+]; 767.6 [m(n=8) + H^+]; 852 [m(n=9) + H^+]; **937,6 [m(n=10) + H^+]**; 1022 [m=(n=11) + H^+]; 1107,6 [m(n=12) + H^+]; 1192,6 [m(n=13) + H^+]; 1277.7 [m(n=14) + H^+]; 1362.7 [m(n=15) + H^+]; 1447 [m(n=16) + H^+]

GPC ($CHCl_3$): M_n = 969 g/mol; M_w = 1044 g/mol; MP = 1217 g/mol; PDI = 1.08

6.3.2 Coupling between P(MeOx)-Ter-AcrAc and the test peptide PEP5 (PPC1)

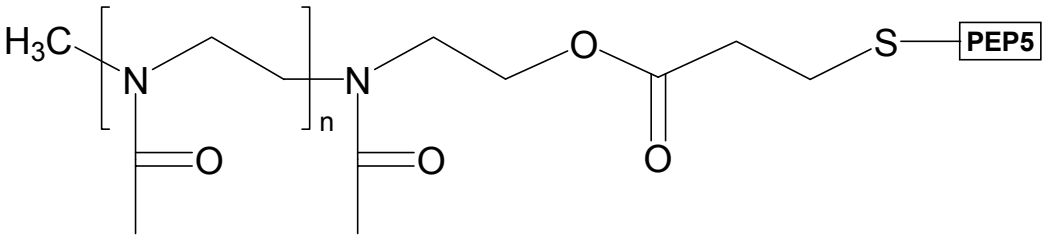

P(MeOx)-Ter-AcrAc (10 mg, 0.0105 mmol) was dissolved in 0.250 mL of HEPES buffer (0.12 g HEPES, 0.85 g TEOA in 50 mL, pH = 8), whereas, 7.12 mg (0.0084 mmol) of test peptide **PEP5** were suspended in 0.040 mL MES buffer (1 mM, 195.2 mg/L, pH = 5.8) and the solutions were combined. The mixture was stirred at room temperature for one day. The solvent was evaporated and the solid residue was dissolved in methanol and filtrated. The solution was concentrated and a solid white powder was obtained. Yield = 5.4 mg (36%)

HPLC (20-80%, 30 min) R_t = 10.35-10.89

ESI-MS: m/z 1381.6 [m(n=5) + Na^+]; 1466.7 [m(n=6) + Na^+]; 1551.7 [m(n=7) + Na^+]; 1636.7 [m(n=8) + Na^+]; 1721.8 [m(n=9) + Na^+]; 1807 [m(n=10) + Na^+]; 1892.9 [m(n=11) + Na^+]; 1977.8 [m(n=12) + Na^+]; 1529.7 [m(n=7) + H^+]; 1614.7 [m(n=8) + H^+]; 1699.8 [m(n=9) + H^+]; 1784.6 [m(n=10) + H^+].

6.3.3 Coupling between P(MeOx)-Ter-AcrAc and PEP3 (PPC2)

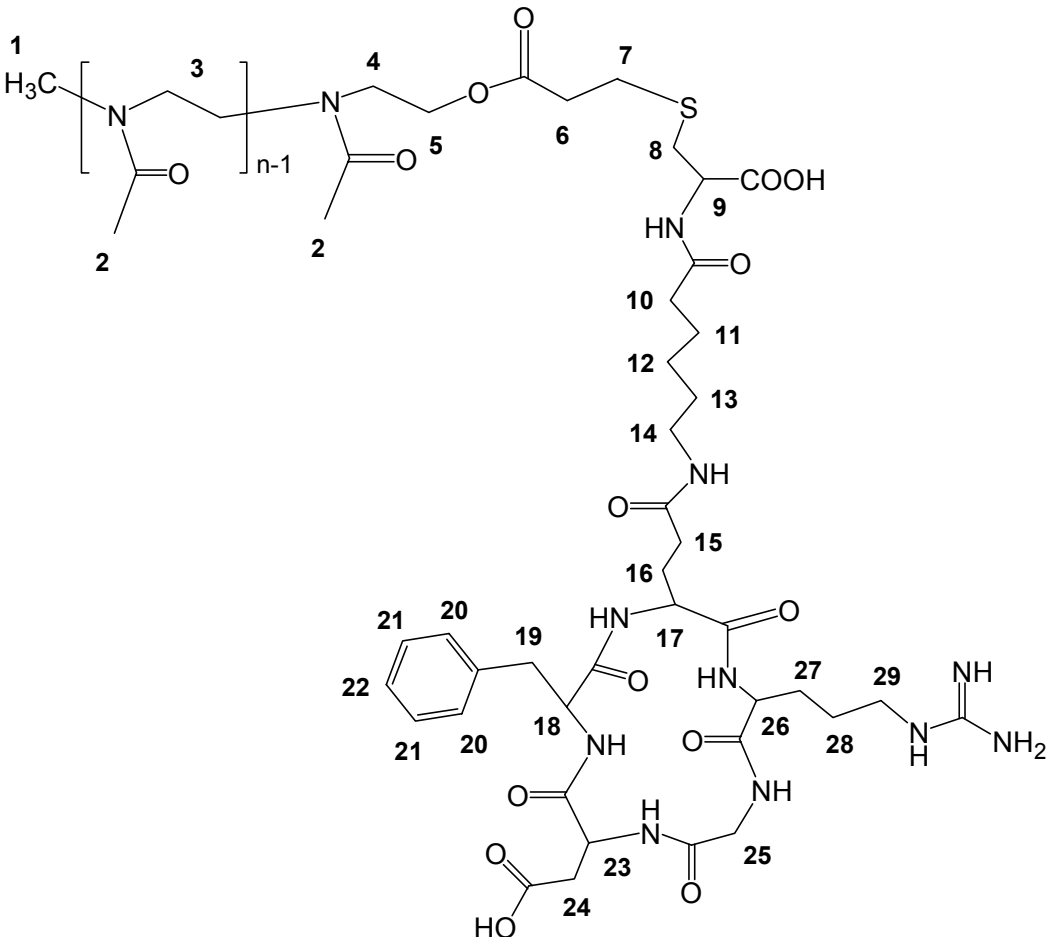

P(MeOx)-Ter-AcrAc (7 mg, 0.0076 mmol) was dissolved in 0.160 mL of HEPES buffer (0.12 g HEPES, 0.85 g TEOA in 50 mL, pH=8), whereas 5 mg (0.0061 mmol) of **PEP2** were dissolved in 0.024 mL MES buffer (1 mM, 195.2 mg/L). The solutions were combined. The mixture was stirred at room temperature for 1 day. The solvent was evaporated and the solid residue was dissolved in methanol and filtrated. The solution was concentrated and the remaining solid was purified by HPLC. Yield = 4 mg (33%)

^{1}H-NMR (CD_3OH): δ in ppm = 1.09 – 1.2 (2H, H^{11}; 2H, H^{12}; 2H, H^{13}; 2H, H^{28}); 1.6 (2H, H^{27}); 1.8 – 2.2 (2H, H^{16}; 2H, H^{15}; 2H, H^{10}; 3H, H^{2}); 2.5 – 2.6 (2H, H^{29}; 2H, H^{6});

2.7 (2H, H^{24}; 2H, H^{7}); 2.9 (2H, H^{8}; 3H, H^{1}); 3.1 – 3.4 (2H, H^{19}; 4H, H^{4}; 2H, H^{14}); 4.1 (2H, H^{25}); 4.3 (2H, H^{5}); 4.5 (1H, H^{17}; 1H, H^{26}); 7.0 (2H, H^{21}); 7.3 (2H, H^{23}; 1H, H^{24})
The signals corresponding to the protons H^{23}, H^{18}, H^{9} overlap with the signal of the solvent.

HPLC (10-90%, 30 min): R_t = 6.58-6.79.

ESI-MS: 794.6 [(m(n=8) + $2H^+$)/2]; 837.3 [(m(n=9) + $2H^+$)/2]; 879.4 [(m(n=10) + $2H^+$)/2]; 922.2 [(m(n=11) + $2H^+$)/2]; 964.2 [(m(n=12) + $2H^+$)/2]; 1007.5 [(m(n=13) + $2H^+$)/2]; 1049.4 [(m(n=14) + $2H^+$)/2]; 1092.3 [(m(n=15) + $2H^+$)/2]; 807.2 [(m(n=8) + H^+ + Na^+)/2]; 848.8 [(m(n=9) + H^+ + Na^+)/2]; 890.7 [(m(n=10) + H^+ + Na^+)/2]$^+$;932.8 [(m(n=11) + H^+ + Na^+)/2]; 975.6 [(m(n=12) + H^+ + Na^+)/2]; 1019.4 [(m(n=13) + H^+ + Na^+)/2].

6.3.4 Synthesis of P(MeOx)-Ter-MalIm

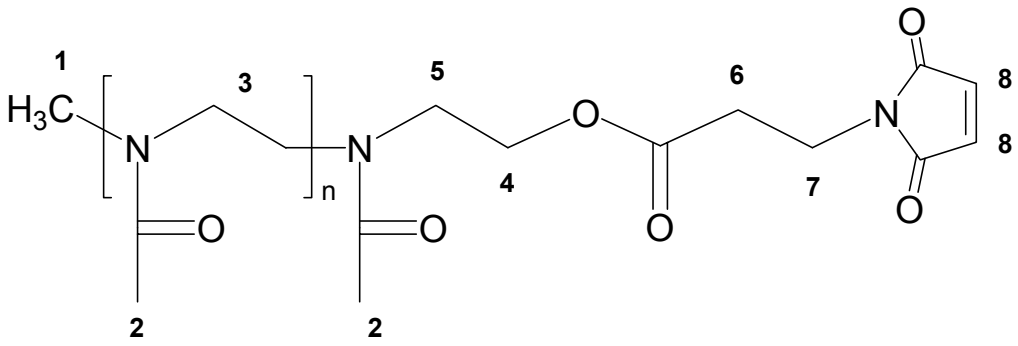

2-Methyl-2-oxazoline (0.668 g, 0.00786 mol) was dissolved in 10 mL ACN and MeOTf (0.129 g, 0.000786 mol) was added under stirring and under a dry nitrogen atmosphere. The solution was heated to 80 °C for 15 h. 3-maleimide propionic acid was added (0.665 g, 0.0393 mol) at 0 °C and then the mixture was stirred for 1 h at 60 °C. The vessel was cooled again and 0.278 g (0.03144 mol) of TEA were added. The mixture was heated again to 60 °C for another 15 h. The solvent was evaporated and the solid residue was dissolved in dichloromethane before dry K_2CO_3 was added. The suspension was stirred for 14 h. K_2CO_3 was removed by filtration and the solvent

was evaporated. The remaining solid was dissolved in chloroform and precipitated in diethylether. The solid part was collected by filtration and lyophilized. Yield = 0.639 g (79 %).

^{1}H-NMR ($CDCl_3$): δ in ppm = 2.1 (3H, H^2); 2.6 (2H, H^6); 2.9 (3H, H^1); 3.4-3.6 (4H, H^3; 2H, H^5); 3.7 (2H, H^7); 4.1 (2H, H^4); 6.7 (2H, H^8).

n = 11; M_n = 1118.21 g/mol

ESI-MS: m/z 524.5 [m(n=4) + H^+]; 609.5 [m(n=5) + H^+]; 694.6 [m(n=6) + H^+]; 779.7 [m(n=7) + H^+]; 864.7 [m(n=8) + H^+]; 949.7 [m(n=9) + H^+]; 1034.7 [m(n=10) + H^+]; 1204.8 [m(n=12) + H^+]; 1289.8 [m(n=13) + H^+]; 1374.8 [m(n=14) + H^+]; 1459.9 [m(n=15) + H^+].

GPC ($CHCl_3$): M_n = 1285 g/mol; M_w = 1427 g/mol; MP = 1516 g/mol; PDI = 1.11

6.3.5 Coupling between P(MeOx)-Ter-MalIm and test peptide PEP5 (PPC3)

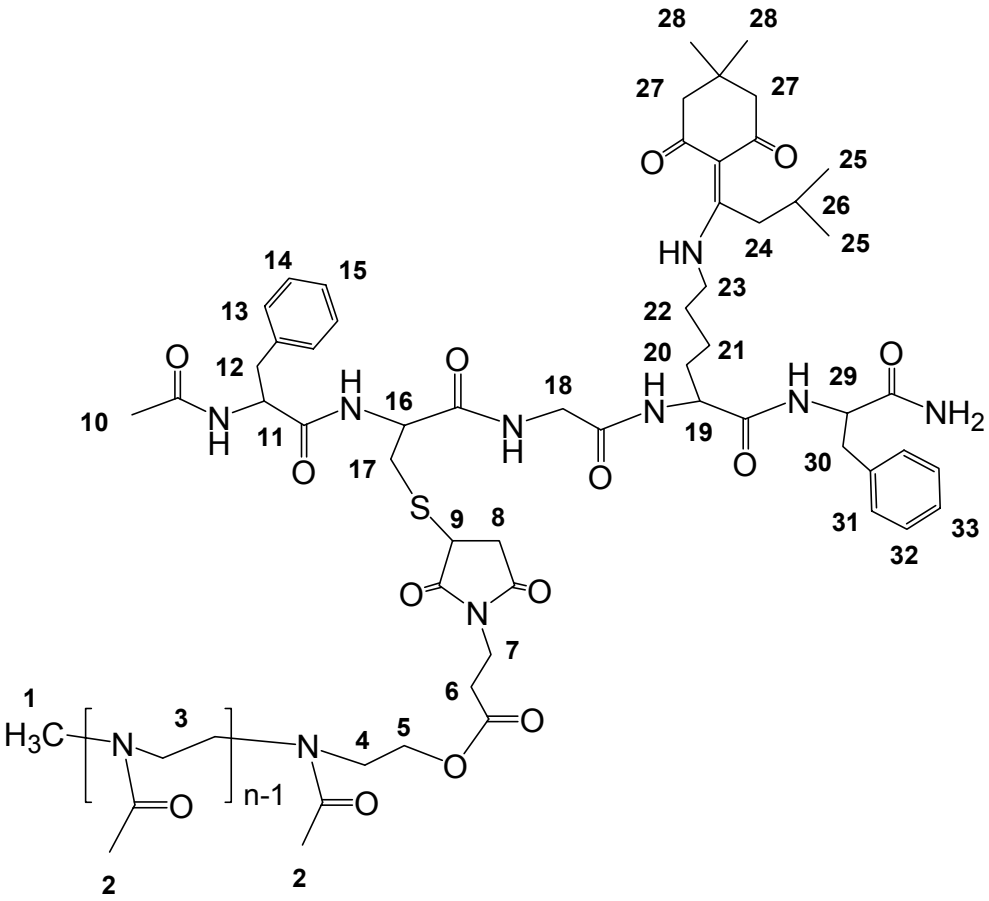

The test peptide **PEP5** (7 mg, 0.0079 mmol) was dissolved in 22 mL phosphate buffer (0.1 M, pH = 6.6) and 10 mg (0.0099 mmol) of **P(MeOx)-Ter-MalIm** were added. The suspension was stirred for one day. The reaction was tested at room temperature as well as at 4 °C. In both cases the reaction was successful. The solvent was evaporated and the remaining solid was dissolved in methanol and filtrated. The solution was concentrated and the remaining solid was purified by HPLC. Yield = 5 mg (35%).

^{1}H-NMR (CD_3OH): δ in ppm = 0.9 – 1.2 (2H, H^{21}; 2H, H^{22}; 3H, H^{25}; 3H, H^{28}); 1.8 (2H, H^{20}); 1.9 – 2.1 (3H, H^{2}; 3H, H^{10}; 2H, H^{24}; 1H, H^{26}); 2.6 (2H, H^{6}; 2H, H^{23}); 2.8 (2H, H^{27}); 2.9 – 3.1 (3H, H^{1}; 2H, H^{12}; 2H, H^{8}; 2H, H^{17}; 2H, H^{30}); 3.3 – 3.6 (4H, H^{3}; 2H, H^{4}); 3.7 (1H, H^{9}; 2H, H^{7}); 4.03 (2H, H^{18}); 4.2 (2H, H^{5}); 4.5 (1H, H^{19}); 7.2 (1H, H^{13}; 1H, H^{31}); 7.8 (1H, H^{14}; 1H, H^{15}; 1H, H^{32}; 1H, H^{33})

Signals corresponding to H^{11}, H^{16}, H^{29} were overlapped by the signal of the solvent.

HPLC (10-90%, 30 min): R_t = 10.91.

ESI-MS: m/z 856.8 [(m(n=8) + $2H^+$)/2]; 899.4 [(m(n=9) + $2H^+$)/2]; 941.8 [(m(n=10) + $2H^+$)/2]; 984.2 [(m(n=11) + $2H^+$)/2]; 1026.9 [(m(n=12) + $2H^+$)/2]; 1069.4 [(m(n=13) + $2H^+$)/2]; 1111.9 [(m(n=14) + $2H^+$)/2]; 878.8 [(m(n=8) + $2Na^+$)/2]; 921.2 [(m(n=9) + $2Na^+$)/2]; 963.8 [(m(n=10) + $2Na^+$)/2]; 1006.3 [(m(n=11) + $2Na^+$)/2]; 1049 [(m(n=12) + 2 Na^+)/2]; 1091.4 [(m(n=13) + $2Na^+$)/2]; 1134 [(m(n=14) + $2Na^+$)/2]; 867.7 [(m(n=8) + H^++ Na^+)/2]; 910.3 [(m(n=9) + H^+ + Na^+)/2]; 952.7 [(m(n=10) + H^+ + Na^+)/2]; 995.6 [(m(n=11) + H^+ + Na^+)/2]; 1037.9 [(m(n=12) + H^+ + Na^+)/2]; 1080.1 [(m(n=13) + H^+ + Na^+)/2]; 1122.9 [(m(n=14) + H^+ + Na^+)/2].

6.3.6 Coupling between P(MeOx)-Ter-MalIm and test peptide PEP3 (PPC4)

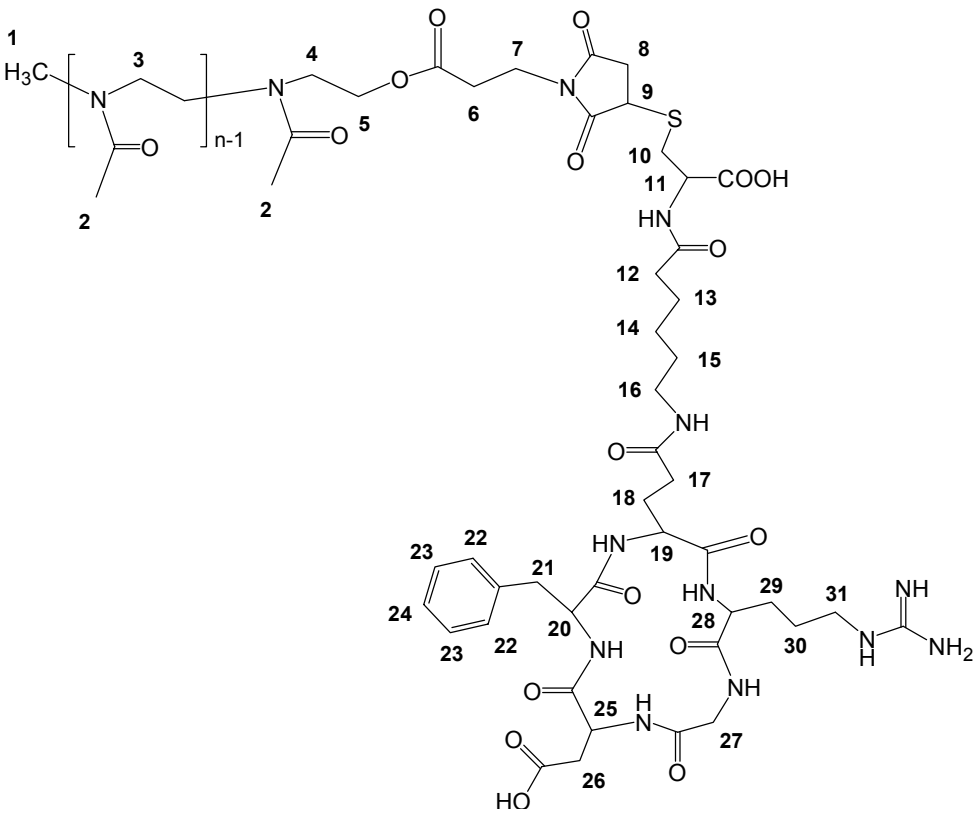

PEP3 (6 mg, 0.0086 mmol) was dissolved in 24 mL phosphate buffer (0.1 M, pH = 6.6) and 9 mg (0.0108 mmol) of **P(MeOx)-Ter-MalIm** were added. The mixture was stirred for one day at room temperature. The solvent was evaporated and the remaining solid was dissolved in methanol and filtrated. The solution was concentrated and the remaining solid was purified by HPLC. Yield = 5 mg (35%)

^{1}H-NMR (CD_3OH): δ in ppm = 1.09 – 1.2 (2H, H^{13}; 2H, H^{14}; 2H, H^{15}; 2H, H^{30}); 1.7 (2H, H^{29}); 1.8 – 2.2 (2H, H^{18}; 2H, H^{17}; 2H, H^{12}; 3H, H^2); 2.5 – 2.6 (2H, H^{31}; 2H, H^6); 2.7 (2H, H^{26}); 2.9 (2H, H^{10}; 3H, H^1; 2H, H^8); 3.1 – 3.4 (2H, H^{21}; 4H, H^3; 2H, H^4; 2H, H^{16}); 4.1 (2H, H^{27}); 4.3 (2H, H^5); 4.5 (1H, H^{19}; 1H, H^{28}); 7.1 (2H, H^{21}); 7.3 (2H, H^{23}; 1H, H^{24})
The signals corresponding to the protons H^7, H^{11}, H^9, H^{20}, H^{25} overlap with the signal of the solvent.

ESI-MS: m/z 885.9 [(m(n=9) + $2H^+$)/2]; 928.2 [(m(n=10) + $2H^+$)/2]; 970.8 [(m(n=11) + $2H^+$)/2]; 1013.3 [(m(n=12) + $2H^+$)/2]; 1055.8 [(m(n=13) + $2H^+$)/2].

6.2 Aminooxy ligation

6.4.1 Synthesis of Benzyl 1-piperazinecarboxylate (1)

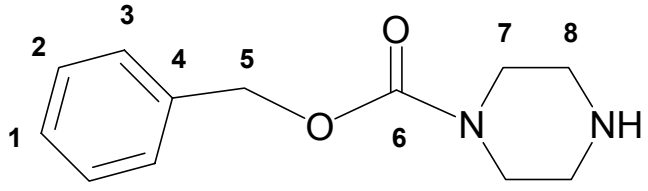

Piperazine (7.64 g, 0.908 mol) was dissolved in a 1:1 mixture of methanol and water. In order to adjust the pH to 3.7, HCl_{conc} was added until the pH indicator bromphenol blue turned from blue to yellow. Then, a solution of 10.06 g (0.045 mol) of benzyl chloroformate in 150 mL toluene and 4 N $NaOH_{aq}$ were added dropwise and simultaneously to maintain the pH.

After the addition was completed, the reaction mixture was stirred for 1 h before most of the solvent was removed. The pH was adjusted with HCl_{conc} to 3.0 and benzyl 1,4-piperazine-dicarboxylate was extracted with toluene. The remaining aqueous solution was adjusted with 12.5 N NaOH to pH = 13. Benzyl-1-piperazine-carboxylate **(1)** was extracted with toluene. The organic phase was dried over Na_2SO_4 and the solvent was evaporated and the remaining yellow oil was collected. Yield = 5.5 g (55%)

^{1}H-NMR ($CDCl_3$): δ in ppm = 2.86 (4H, H^8); 3.53 (4H, H^7); 5.23 (2H, H^5); 7.43 (5H, $H^{1,2,3}$)

^{13}C-NMR ($CDCl_3$): δ in ppm = 48.5 (C^7); 44.99 (C^8); 66.16 (C^5); 127.6 ($C^{1,2,3}$); 135.99 (C^4); 154.41 (C^6)

6.4.2 Synthesis of 4-(2,2-Diethoxy-ethyl)-piperazine-1-carboxylic acid benzyl ester (2)

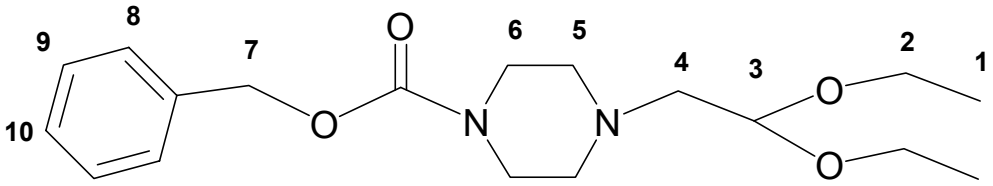

Benzyl-1-piperazinecarboxylate **(1)** (2.6 g, 0.0118 mol) was dissolved in ethanol and 2,33 g (0.0118 mol) of 2-bromo-1,1-diethoxyethane together with 1.79 g (0.0177 mol) TEA were added under stirring. The solvent was refluxed for 20 h. The mixture was evaporated under reduced pressure and purified by column chromatography (silica gel) eluting with a dichloromethane/ethanol (95:5) to give yellow oil. Yield = 3.4 g (85%)

^{1}H-NMR ($CDCl_3$): δ in ppm = 1.14 (6H, H^1); 2.46 (2H, H^4; 2H, H^5); 3.43 (4H, H^2); 3.59 (2H, H^6); 4.56 (1H, H^3); 5.20 (2H, H^7); 7.4 (5H, $H^{8,9,10}$)

6.4.3 Synthesis of 1-(2,2-Diethoxy-ethyl)-piperazine (Pip-Acetal)

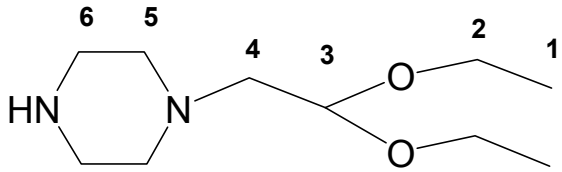

4-(2,2-diethoxy-ethyl)-piperazine-1-carboxylic acid benzyl ester (2.2 g, 0.00654 mol) was dissolved in methanol, Pd/C was added and the suspension reacted at 40 °C for one day. The catalyst was filtrated and the solvent evaporated. The remaining yellow oil was lyophilized. Yield 1.83 g (83.27 %).

^{1}H-NMR ($CDCl_3$): δ in ppm = 1.14 (6H, H^1); 2.48 (2H, H^4); 2.60 (2H, H^5); 2.95 (2H, H^6); 3.48-3.60 (4H, H^2); 3.6 (4H, H^7); 4.56 (1H, H^3)

6.4.4 Synthesis of P(MeOx)-Ter-Acetal

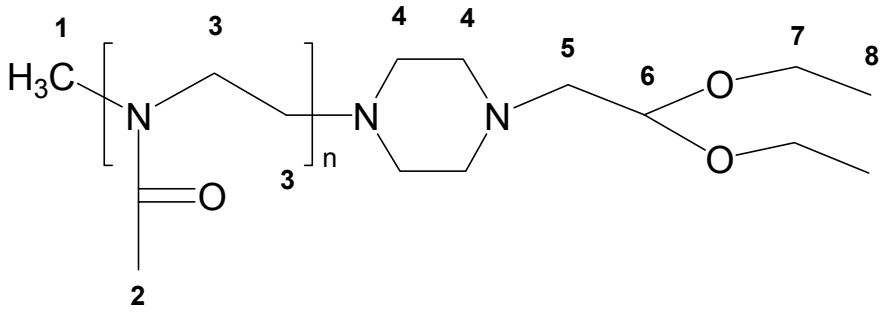

2-Methyl-2-oxazoline (1.211 g, 0.01425 mol) was dissolved in 28 mL ACN and MeOTf (0.234 g, 0.001425 mol) was added under stirring and under a dry nitrogen atmosphere. The mixture was heated to 80 °C for 15 h. 1-(2,2-diethoxy-ethyl)-piperazine (0.865 g, 0.004275 mol) was added at 0 °C and the solution reacted for 18 h at room temperature. The solvent was evaporated and the solid residue was dissolved in dichloromethane and dry K_2CO_3 was added. The suspension was stirred for another 15 h. K_2CO_3 was removed by filtration and the solution was concentrated. The

remaining solid was dissolved in chloroform and precipitated in diethylether. The solid part was collected by filtration and dried in a vacuo. Yield = 1.29 g (86%).

^{1}H-NMR ($CDCl_3$): δ in ppm = 1.15 (6H, H^8); 2.0 – 2.1 (3H, H^2); 2.48 (8H, H^4; 2H, H^5); 2.9 – 3.0 (3H, H^1); 3.3 – 3.5 (4H, H^3); 3.6 (4H, H^7); 4,56 (1H, H^6)

n = 8; M_n = 896.94 g/mol

GPC ($CDCl_3$): M_n = 604 g/mol; M_w = 659 g/mol; MP = 729 g/mol; PDI = 1.09.

ESI-MS: m/z 642.6 [m(n=5) + H^+]; 727.6 [m(n=6) + H^+]; 812.6 [m(n=7) + H^+]; 897.6 [m(n=8) + H^+]; **982.6 [m(n=9) + H^+]**; 1067.6 [m(n=10) + H^+]; 1152.6 [m(n=11) + H^+]; 1237.6 [m(n=12) + H^+]; 1322.6 [m(n=13) + H^+]; 1407.6 [m(n=14) + H^+]; 1492.6 [m(n=15) + H^+]

6.4.5 Synthesis of (Piperazin-1-yl-methyleneaminooxy)-acetic acid (6)

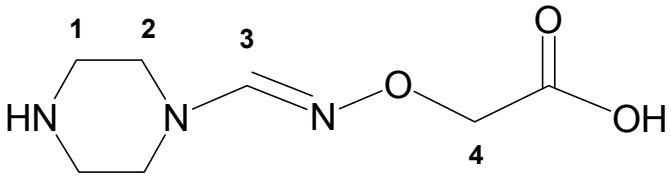

N-formyl piperazine (0.1 g) was dissolved in 1 mL of 95 %-wg. TFA and aminooxy acetic acid hydrochloride was added under stirring. The solution was stirred for 15 h and the solvent was evaporated and substituted with deuterated water as solvent for the ^{1}H-NMR characterization.

^{1}H-NMR (D_20): δ in ppm = 2.82 (4H, H^2); 3.28 (4H, H^1); 4.27 (2H, H^4); 7.59 (1H, H^3)

ESI-MS: m/z 186.2 $[m - H]^-$

6.4.6 Synthesis of P(MeOx)-Ter-FAld

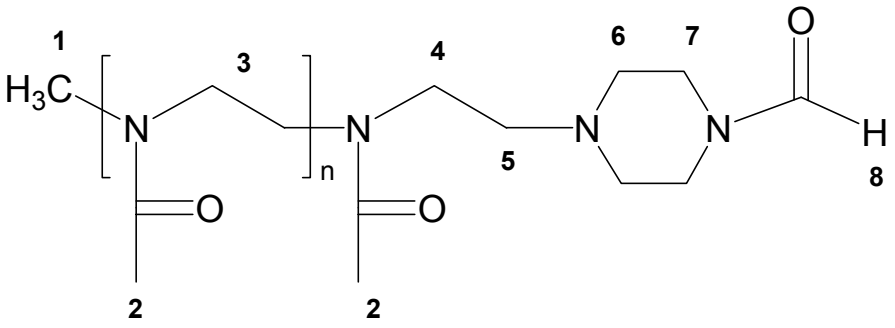

2-Methyl-2-oxazoline (0.767 g, 0.00903 mol) was dissolved in 18 mL ACN and MeOTf (0.249 g, 0.0009 mol) was added under stirring and under a dry nitrogen atmosphere. 0.618 g (0.00542 mol) of N-formyl piperazine was added under stirring at 0 °C. The solution was stirred for 12 h and then the solvent was evaporated in vacuo. The remaining solid was dissolved in dichloromethane and dry K_2CO_3 was added. The suspension reacted for 15 h and then K_2CO_3 was removed by filtration. The solution was concentrated and the remaining solid was dissolved in chloroform and precipitated in diethylether. The solid part was collected by filtration and dried in a vacuo at 50 °C. A yellow solid was collected. Yield = 0.87 g (87%).

^{1}H-NMR ($CDCl_3$): δ in ppm = 1.9 – 2.1 (3H, H^2); 2.3 – 2.4 (4H, H^6; 2H, H^5); 2.8 (4H, H^7); 2.9 – 3.0 (3H, H^1); 3.2 – 3.4 (4H, H^3; 2H, H^4); 7.99 (1H, H^8).

n = 8; M_n = 808.85 g/mol

ESI-MS: m/z 299.4 [m(n=2) + H^+]; 384.4 [m(n=3) + H^+]; 469.5 [m(n=4) + H^+]; 554.5 [m(n=5) + H^+]; 639.5 [m(n=6) + H^+]; **724.5 [m(n=7) + H^+]**; 809.5 [m(n=8) + H^+]; 894.5 [m(n=9) + H^+]; 979.5 [m(n=10) + H^+]; 1064 [m(n=11) + H^+]; 1149.6 [m(n=12) + H^+]

6.5 Isothiocyanate coupling

6.5.1 Polymer modification of P(MeEstOx) with diethyldiamine

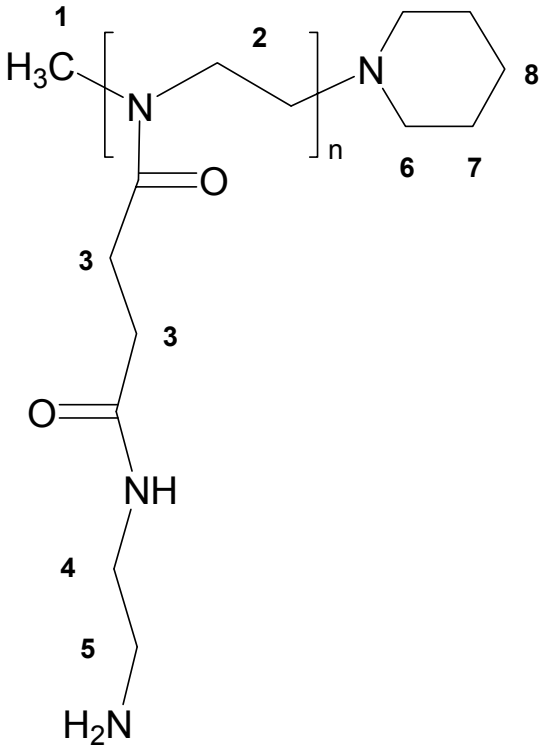

P(MeEstOx) (0.1 g, 0.006 mmol) was dissolved in 0.15 mL methanol and the solution was added to 20 mL ethyldiamine. The mixture was stirred for 3 days. Ethyldiamine was evaporated and the remaining solid was lyophilized. Yield = 0.114 g (80%).

^{1}H-NMR (DMSO): δ in ppm = 1.4 (4H, H^7; 2H, H^8); 2.1 – 2.3 (4H, H^3; 4H, H^6); 2.9 (3H, H^1); 3.2 – 3.4 (4H, H^2; 2H, H^4); 7.7 (1H, NH)

n = 6; M_n = 1208.83 g/mol

GPC (DMAc): M_n = 1899 g/mol, M_w = 2087 g/mol, MP = 2072 g/mol; PDI = 1.1

6.5.2 Synthesis of P(MeOx)-Ter-Pipaz

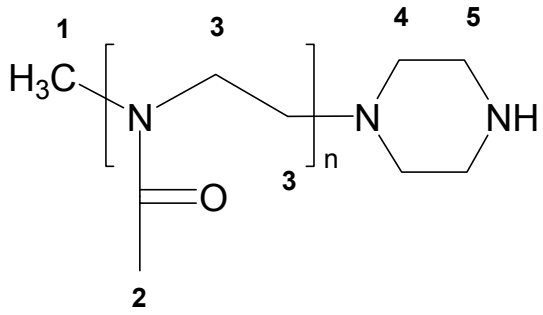

2-Methyl-2-oxazoline (1.849 g, 0.02175 mol) was dissolved in 29 mL ACN and MeOTf (0.238 g, 0.00145 mol) was added under stirring and under a dry nitrogen atmosphere. The mixture was heated at 80 °C for 15 h. A solution of piperazine (3.045 g, 0.03625 mol) in chloroform was added at 0 °C and stirred at room temperature for 13 h. The solvents were evaporated in vacuo. The remaining solid was dissolved in dichloromethane and dry K_2CO_3 was added. The suspension was stirred for other 15 h at room temperature before K_2CO_3 was removed by filtration. The solution was concentrated and the remaining solid was dissolved in chloroform and precipitated in diethylether three times in order to remove the excess of piperazine from the polymer. The solid was collected by filtration and lyophilized. Yield = 1.17 g (85%).

^{1}H-NMR ($CDCl_3$): δ in ppm = 2.0 – 2.1 (3H, H^2); 2.4 (4H, H^4); 2.6 (4H, H^5); 3.0 (3H, H^1); 3.4 – 3.6 (4H, H^3)

n = 6; M_n = 610.62 g/mol

GPC ($CDCl_3$): M_n = 652 g/mol; M_w = 700 g/mol; MP = 776 g/mol; PDI = 1.07

ESI-MS: m/z 611.6 [m(n=6) + H^+]; 696.6 [m(n=7) + H^+]; 781.6 [m(n=8) + H^+]; 866.6 [m(n=9) + H^+]; 951.6 [m(n=10) + H^+]; **1036.7 [m(n=11) + H^+]**; 1121.7 [m(n=12) + H^+]; 1206.7 [m(n=13) + H^+], 1291.7 [m(n=14) + H^+]; 1376.8 [m(n=15) + H^+]; 1461.9 [m(n=16) + H^+]

6.5.3 Synthesis of (N-Boc-5-amino pentyl)-2-oxazoline ((AmineOx)Mmer)

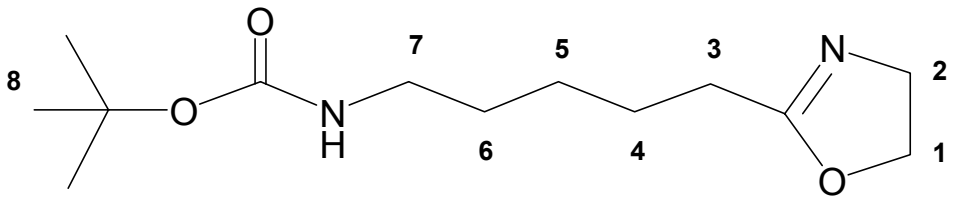

NaH was suspended in THF and a solution of 1 g (0.00341 mol) of [4-(2-chloro-ethylcarbamoyl)-pentyl]carbamic acid *tert*-butyl ester in methanol (6 mL) and THF (70 mL) was slowly added. The solution was stirred at room temperature for 6 h. The salts were filtered and the solution was concentrated. The resulting residue was purified by column chromatography (silica gel) using EtAc : TEA : DCM (15 : 1 : 2). Yield = 0.339 g (40%).

^{1}H-NMR ($CDCl_3$): δ in ppm = 1.2 – 1.4 (9H, H^8; 2H, H^4; 2H, H^5); 1.49 (2H, H^3); 2.12 (2H, H^6); 2.96 (2H, H^7); 3.68 (2H, H^1); 4.09 (2H, H^2)

HPLC-RP (10-90%, 30 min): R_t = 5.8 – 6.2; R_t = 6.47 – 6.78

ESI-MS: m/z 257 [m + H^+]; 201 [(m – ^{t}Bu + H^+)]; 157 [m – Boc + H^+]

6.5.4 Synthesis of 2-methyl-2-oxazolinium triflate

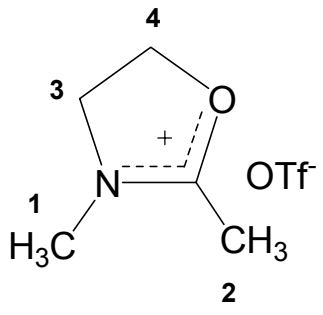

2-Methyl-2oxazoline (3 g, 0.0352 mol) was dissolved in 30 mL of dry ethyl ether and added dropwise at 0 °C to a solution of 6.9 g (0.0423 mol) of MeOTf dissolved in 30 mL of dry diethyl ether. The mixture was stirred for further 2 h at 0 °C. The obtained colorless solid was filtrated and washed with diethyl ether, dried in vacuo and stored under nitrogen atmosphere. A colorless solid was obtained. Yield = 7.62 g (87 %).

^{1}H-NMR (CD_3OH): δ in ppm = 2.43 (3H, H^2); 3.35 (3H, H^1); 4.17 (2H, H^3); 4.93 (2H, H^4).

6.5.5 Polymerization of the amino functionalized monomer (P(BocAmineOx))

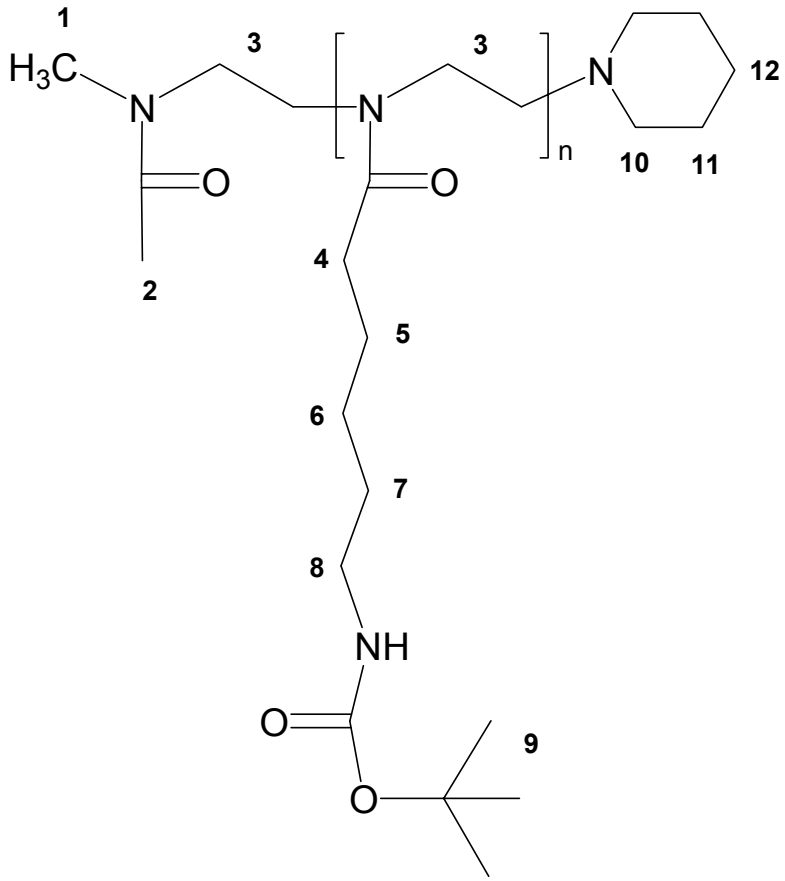

(AmineOx)Mmer (0.5 g, 0.00195 mol) and MeOxOTf (0.048 g, 0.000195 mol) were dissolved in 4 mL ACN and 4 mL chlorobenzene. The solution was stirred for 30 h at 80 °C. Piperidine (0.049 g, 0.00058 mol) was added at 0 °C. The mixture was stirred for 13 h and then the solvent was evaporated. The solid residue was dissolved in dichloromethane, dry K_2CO_3 was added and the suspension reacted for 15 h. K_2CO_3 was removed by filtration and the solution was concentrated. The solid residue was dissolved in chloroform and precipitated in diethylether. Yield = 0.43 g (80%).

^{1}H-NMR ($CDCl_3$): 1.3 – 1.5 (9H, H^9; 4H, H^{11}; 2H, H^{12}; 2H, H^5; 2H, H^6); 2.04 – 2.3 (2H, H^4;3H, H^2; 2H, H^7); 2.6 (4H, H^{10}); 3.06 (2H, H^8; 3H, H^1); 3.4 – 3.6 (4H, H^3)

GPC ($CDCl_3$): M_n = 1928 g/mol; M_w = 2218 g/mol; MP = 2356 g/mol; PDI = 1.15

6.5.6 Cleavage of the Boc protecting group (P(AmineOx))

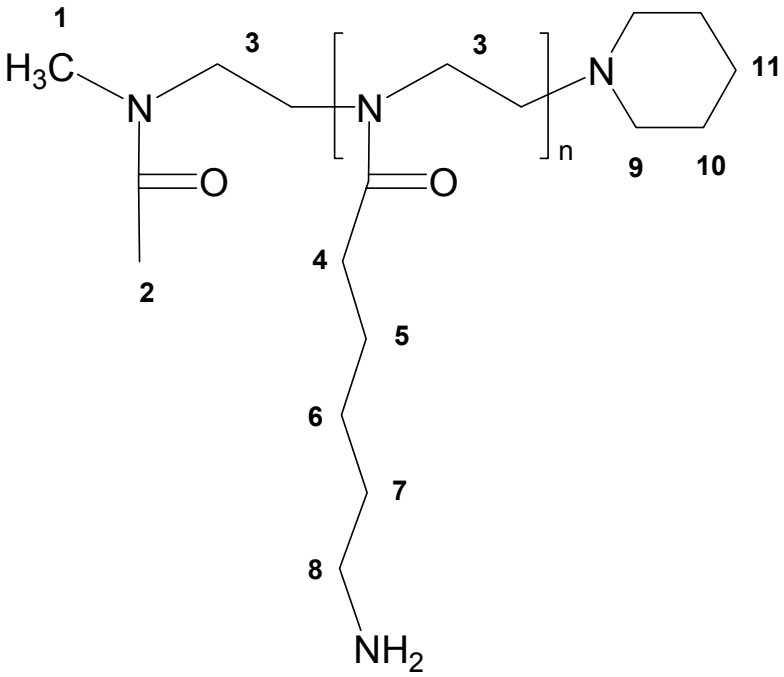

P(BocAmineOx) was dissolved in 50 % TFA-dichloromethane and the solution was stirred for 15 h. The solvent was evaporated and the remaining solvent was collected. Yield = 0.179 g (89 %).

^{1}H-NMR (CD_3OH): 1.3 – 1.5 (4H, H^{10}; 2H, H^{11}; 2H, H^{5}; 2H; H^{6}); 1.9 (3H, H^{2}); 2.2-2.4 (2H, H^{4}; 2H, H^{7}; 4H, H^{9}); 2.8 – 3.0 (2H, H^{8}; 3H, H^{1}); 3.4 – 3.6 (4H, H^{3})

n = 8; M_n = 1433.19 g/mol

7 Literature

[1] J. M. Harris, R. B. Chess, *Nature Rev. Drug Discov.* **2003**, *2*, 214.

[2] M.-A. Zanta, O. Boussif, A. Adib, J.-P. Behr, *Bioconj. Chem.* **1997**, *8*, 839.

[3] M.-A. Zanta, P. Belguise-Valladier, J.-P. Behr, *Proc. Natl. Acad. Sci. USA* **1999**, *96*, 91.

[4] M. Dubber, J. M. J. Fréchet, *Bioconj. Chem.* **2003**, *14*, 239.

[5] P. Ferruti, M. A. Marchisio, R. Duncan, *Macromol. Rapid Commun.* **2002**, *23*, 332.

[6] R. Duncan, *Nature Rev. Drug Discov.* **2003**, *2*, 347.

[7] R. Duncan, J. Kopecek, P. Rejmanova, J. B. Lloyd, *Biochim. Biophys. Acta* **1983**, *755*, 518.

[8] S. Hellman, E. E. Vokes, *Spektrum der Wissenschaft* **1996**, *Spezial 5*, 59.

[9] B. Alberts, D. Bray, J. Lewis, M. Raff, K. Roberts, J. D. Watson, *Molecular Biology of the Cell*, 3rd ed., Garland Publishing, New York, **1994**.

[10] S. M. Albelda, S. A. Mette, D. E. Elder, R. M. Stewart, L. Damjanovich, M. Herlyn, C. A. Buck, *Cancer Res.* **1990**, *50*, 6757.

[11] C. L. Gladson, D. A. Cheres, *J. Clin. Invest.* **1991**, *88*, 1924.

[12] J. F. Marshall, S. A. Nesbitt, M. H. Helfrich, M. A. Horton, K. Polakova, I. R. Hart, *Int. J. Cancer* **1991**, *49*, 924.

[13] R. M. Lafrenie, S. Gallo, T. J. Podor, M. R. Buchanan, F. W. Orr, *Eur. J. Cancer* **1994**, *14*, 2151.

[14] R. Haubner, H. J. Wester, W. A. Weber, M. Schwaiger, *Quar. J. Nuc. Med.* **2003**, *47*, 189.

[15] J. Folkman, M. Klagsbrun, *Science* **1987**, *235*, 442.

[16] L. A. Liotta, P. S. Steeg, W. G. Stetler-Stevenson, *Cell* **1991**, *64*, 327.

[17] J. Folkman, K. Watson, D. Ingber, D. Hanahan, *Nature* **1989**, *339*, 58.

[18] R. O. Hynes, *Cell* **1992**, *69*, 11.

[19] M. Takeichi, *Annu. Rev. Biochem.* **1990**, *59*, 237.

[20] M. Takeichi, *Science* **1991**, *251*, 1451.

[21] A. F. Williams, A. N. Barclay, *Annu. Rev. Immunol* **1988**, *6*, 381.

[22] T. Hunkapiller, L. Hood, *Adv. Immunol.* **1989**, *44*, 1.

[23] M. Bevilacqua, E. Butcher, B. Furie, M. Gallatin, M. Gimbrone, J. Harlan, K. Kishimoto, L. Lasky, R. McEver, J. Paulson, S. Rosen, S. Seed, M. Sigelmann, T. Springer, L. Stoolman, T. Tedder, A. Varki, D. Wagner, I. Weisman, G. Zimmerman, *Cell* **1991**, *67*, 233.

[24] S. Koepper, *Nachr. Chem. Tech. Lab.* **1995**, *43*, 421.

[25] J. Samanen, A. Jonak, D. Rieman, T.-L. Yue, *Curr. Pharm. Des.* **1997**, *3*, 545.

[26] M. A. Arnaout, S. L. Goodman, J.-P. Xiong, *Curr. Opin. Cell Biol.* **2002**, *14*, 641.

[27] M. J. Humphries, *Biochem. Soc. Trans.* **2000**, *28*, 311.

[28] J. Bella, H. M. Berman, *Structure* **2000**, *8*, R121.

[29] S. Suzuki, Y. Naitho, *EMBO J.* **1990**, *9*, 757.

[30] J.-O. Lee, P. Rieu, M. A. Arnaout, R. C. Liddington, *Cell* **1995**, *80*, 631.

[31] F. G. Giancotti, E. Ruoslahti, *Science* **1999**, *285*, 1028.

[32] J. A. Varner, D. A. Cheresh, *Curr. Opin. Cell Biol.* **1996**, *8*, 724.

[33] A. F. Horwitz, *Spektrum der Wissenschaft* **1998**, *Jan 1998*, 86.

[34] M. Mammen, S.-K. Choi, G. M. Whitesides, *Angew. Chem.* **1998**, *110*, 2908.

[35] M. D. Pierschbacher, E. Ruoslahti, *Nature* **1984**, *309*, 30.

[36] E. Ruoslahti, M. D. Pierschbacher, *Science* **1987**, *238*, 491.

[37] P. Schaffner, M. M. Dard, *CMLS, Cell. Mol. Life Sci.* **2003**, *60*, 119.

[38] E. Ruoslahti, *Annu. Rev. Cell Dev. Biol.* **1996**, *12*, 697.

[39] M. D. Pierschbacher, E. Ruoslahti, *Proc. Natl. Acad. Sci. USA* **1984**, *81*, 5985.

[40] A. Hautanen, J. Gailit, D. M. Mann, E. Ruoslahti, *J. Biol. Chem.* **1989**, *264*, 1437.

[41] M. D. Pierschbacher, E. Ruoslahti, *J. Biol. Chem.* **1987**, *262*, 17294.

[42] S. J. Bogdanowich-Knipp, S. Chakrabarti, T. D. Williams, R. K. Dillman, T. J. Siahaan, *J. Pept. Res.* **1999**, *53*, 530.

[43] T. Geiger, S. Clarke, *J. Biol. Chem.* **1987**, *262*, 785.

[44] K. C. Nicolaou, J. I. Trujillo, B. Jandeleit, K. Chibale, M. Rosenfeld, B. Diefenbach, D. A. Cheresh, S. L. Goodman, *Bioorg. Med. Chem.* **1998**, *6*, 1185.

[45] M. Gurrath, G. Müller, H. Kessler, M. Aumailley, R. Timpl, *Eur. J. Biochem.* **1992**, *210*, 911.

[46] M. Gurrath, G. Müller, H. Kessler, R. Timpl, *Angew. Chem. Int. Ed.* **1992**, *31*, 385.

[47] M. Pfaff, K. Tangemann, B. Müller, M. Gurrath, G. Müller, H. Kessler, R. Timpl, J. Engel, *J. Biol. Chem.* **1994**, *269*, 20233.

[48] L. Tranqui, A. Andrieux, G. Hudry-Clergeon, J. J. Ryckewaert, S. Soyez, A. Chapel, M. H. Ginsberg, E. F. Plow, G. Marguerie, *J. Cell. Biol.* **1989**, *108*, 2519.

[49] R. Haubner, R. Gratias, B. Diefenbach, S. L. Goodman, A. Jonczyk, H. Kessler, *J. Am. Chem. Soc.* **1996**, *118*, 7461.

[50] B. P. Feuston, J. C. Culberson, M. E. Duggan, G. D. Hartman, C.-T. Leu, S. B. Rodan, *J. Med. Chem.* **2002**, *45*, 5640.

[51] G.A.G. Sulyok, C. Gibson, S.L. Goodman, G. Hölzemann, M. Wiesner, H. Kessler, *J. Med. Chem.* **2001**, *44*, 1938.

[52] P. C. Brooks, A. M. P. Montgomery, M. Rosenfeld, R. A. Reisfeld, T. Hu, G. Klier, D. A. Cheresh, *Cell* **1994**, *79*, 1157.

[53] P. C. Brooks, R. A. F. Clark, D. A. Cheresh, *Science* **1994**, *264*, 569.

[54] W. D. Klohs, J. M. Hamby, *Curr. Opin. Biotech.*. **1999**, *10*, 544.

[55] A. Matter, *Drug Discov. Today* **2001**, *6*, 1005.

[56] R. O. Hynes, B. L. Bader, K. Hodivala-Dilke, *Braz. J. Med. Biol. Res.* **1999**, *32*, 501.

[57] S. Stromblad, D. A. Cheresh, *Chem. Biol.* **1996**, *3*, 881.

[58] J. S. Kerr, R. S. Wexler, S. A. Mousa, C. S. Robinson, E. J. Wexler, S. Mohamed, M. E. Voss, J. J. Devenny, P. M. Czerniak, A. J. Gudzelak, A. M. Slee, *Anticancer Res.* **1999**, *19*, 959.

[59] P. C. Brooks, S. Stromblad, R. Klemke, D. Visscher, F. H. Sarkar, D. A. Cheresh, *J. Clin. Invest.* **1995**, *96*, 1815.

[60] J. Haier, U. Goldmann, B. Hotz, N. Runkel, U. Keilholz, *Clin. Exp. Metastasis* **2002**, *19*, 665.

[61] S. Liu, D. S. Edwards, *Bioconj. Chem.* **2001**, *12*, 7.

[62] W. Wolf, J. Shani, *Nucl. Med. Biol.* **1986**, *13*, 319.

[63] R. A. Fawwaz, T. S. T. Wang, C. Srivastava, M. A. Hardy, *Nucl. Med. Biol.* **1986**, *13*, 429.

[64] P. A. Schubiger, R. Alberto, A. Smith, *Bioconj. Chem.* **1996**, *7*, 165.

[65] J. D. Chapman, J. D. Bradley, J. F. Eary, R. Haubner, S. M. Larson, J. M. Michalski, P. G. Okunieff, H. W. Strauss, Y. C. Ung, M. J. Welch, *Int. J. Radiation Oncology Biol. Phys.* **2003**, *55*, 294.

[66] R. Haubner, H.-J. Wester, W. A. Weber, C. Mang, S. I. Ziegler, S. L. Goodman, R. Senekowitsch-Schmidtke, H. Kessler, M. Schwaiger, *Cancer Res.* **2001**, *61*, 1781.

[67] P. Brust, R. Haubner, A. Friedrich, M. Scheunemann, M. Anton, O.-N. Koufaki, M. Hauses, S. Noll, B. Noll, U. Haberkorn, G. Schackert, H. K. Schackert, N. Avril, B. Johannsen, *Eur. J. Nucl. Med.* **2001**, *28*, 721.

[68] M. Ogawa, K. Hatano, S. Oishi, Y. Kawasumi, N. Fujii, M. Kawaguchi, R. Doi, M. Imamura, M. Yamamoto, K. Ajito, T. Mukai, H. Saji, K. Ito, *Nucl. Med. Biol.* **2003**, *30*, 1.

[69] M. Bock, F. Burcherseifer, R. Haubner, R. Senekowitsch-Schmidtke, H. Kessler, M. Schwaiger, H. J. Wester, *J. Nucl. Med.* **2000**, *41*, 41P.

[70] M. D. Jong, P. M. Vantlagen, W. A. Breeman, H. F. Bernard, M. Schaar, A. V. Gameren, A. Srinivasam, M. Schmidt, J. E. Bugaj, E. P. Krenning, *J. Nucl. Med.* **2000**, *41*, 232P.

[71] R. Haubner, H. J. Wester, M. Bock, R. Senekowitsch-Schmidtke, M. Herz, U. Keuning, B. Diefenbach, G. Stocklin, H. Kessler, M. Schwaiger, *J. Labelled Compods Radiopharm.* **1999**, *42*, S36.

[72] G. B. Sivolapenko, D. Skarlos, D. Pectasides, E. Stathopoulou, A. Milonakis, G. Sirmalis, A. Stuttle, N. S. Courtenay-Luck, S. Nigels, K. Kostantinides, A. A. Epenetos, *Eur. J. Nucl. Med.* **1998**, *25*, 1383.

[73] M. L. Janssen, W. J. Oyen, I. Dijkgraaf, L. F. Massuger, C. Frielink, D. S. Edwards, M. Rajopadhye, H. Boonstra, F. H. Corstens, O. C. Boerman, *Cancer Res.* **2002**, *62*, 6146.

[74] H. Ringsdorf, *J. Polymer Sci.: Symposium* **1975**, *51*, 135.

[75] T. Yamaoka, Y. Tabata, Y. Ikada, *J. Pharm. Sci.* **1994**, *83*, 601.

[76] M. J. Keating, R. Holmes, S. Lerner, H. D. Ho, *Leuk. Lymphoma* **1993**, *10*, 153.

[77] L. T. Liang, *Am. Intern. Med.* **2000**, *132*, 296.

[78] A. M. Gillinov, B. W. Lytle, *J. Card. Surg.* **2001**, *16*, 255.

[79] R. Ferland, D. Mulani, P. K. Campbell, *Human Reprod* **2001**, *16*, 2718.

[80] P. A. Vasey, S. B. Kaye, R. Morrison, C. Twelves, P. Wilson, R. Duncan, A. H. Thomson, L. S. Murray, T. E. Hilditch, T. Murray, S. Burtles, D. Fraier, E. Frigerio, J. Cassidy, *Clinical Cancer Res.* **1999**, *5*, 83.

[81] S. M. Morgan, V. Subr, K. Ulbrich, J. F. Woodley, R. Duncan, *Int. J. Pharm.* **1996**, *128*, 99.

[82] R. Satchi, T. Connors, R. Duncan, *Brit. J. Cancer* **2001**, *85*, 1070.

[83] Y. Matsumura, H. Maeda, *Cancer Res.* **1986**, *6*, 6387.

[84] T. Konno, H. Maeda, *Neoplasm of the liver*, Springer New York, **1987**.

[85] K. Iwai, H. Maeda, T. Konno, *Cancer Res.* **1984**, *44*, 2114.

[86] H. Maeda, T. Konno, *Neocarzinostatin*, Springer Berlin, **1997**.

[87] R. K. Jain, *Adv. Drug Deliv. Rev.* **1997**, *26*, 71.

[88] S.-E. Stiriba, H. Kautz, H. Frey, *J. Am. Chem. Soc.* **2002**, *124*, 9698.

[89] P. Ferruti, S. Knobloch, E. Ranucci, R. Duncan, E. Gianasi, *Macromol. Chem. Phys.* **1998**, *199*, 2565.

[90] H. Dautzenberg, *Langmuir* **2001**, *17*, 3096.

[91] D. A. Tomalia, H. Baker, J. Dewald, M. Hall, G. Kallos, S. Martin, J. Roeck, J. Ryder, P. Smith, *Polym. J.* **1985**, *17*, 117.

[92] J. M. J. Frechet, *J. Mater. Sci. Pure Appl. Chem.* **1996**, *83*, 1399.

[93] M. Pechar, K. Ulbrich, V. Subr, L. W. Seymour, E. H. Schacht, *Bioconj. Chem.* **2000**, *11*, 131.

[94] F. Chaves, J. C. Calvo, C. Carvajal, Z. Rivera, L. Ramirez, M. Pinto, M. Trujillo, F. Guzman, M. E. Patarroyo, *J. Pept. Res.* **2001**, *58*, 307.

[95] S. Forster, T. Plantenberg, *Angew. Chem. Int. Ed.* **2002**, *41*, 688.

[96] B. V. Robinson, *J. Biomed. Mat. Res.* **1987**, *21*, 1341.

[97] M. Szwarc, *Nature* **1956**, *178*, 1168.

[98] K. Aoi, M. Okada, *Prog. Polym. Sci.* **1996**, *21*, 151.

[99] S. Kobayashi, *Prog. Polym. Sci.* **1990**, *15*, 751.

[100] S. Kobayashi, S. Iijima, T. Igarashi, T. Saegusa, *Macromolecules* **1987**, *20*, 1729.

[101] S. Kobayashi, H. Uyama, N. Higuchi, T. Seagusa, *Macromolecules* **1990**, *23*, 54.

[102] P. Goddard, L. E. Hutchinson, J. Brown, L. J. Brookman, *J. Controll. Rel.* **1989**, *10*, 5.

[103] S. Zalipsky, *Bioconjugate Chem.* **1995**, *6*, 150.

[104] R. C. Schulz, A. Dworak, *Macromol. Symp.* **1994**, *85*, 203.

[105] A. Dworak, R. C. Schulz, I. Panchev, B. Trzebicka, R. Velitshkova, *R. Polym. Int* **1994**, *34*, 157.

[106] P. I. C. Guimaraes, A. P. Monteiro, J. L. Mazzei, *Eur. Polym. J.* **1995**, *31*, 1251.

[107] S. C. Lee, Y. Chang, J.-S.-. Yoon, C. Kim, I. C. Kwon, Y.-H. Kim, S. Y. Jeong, *Macromolecules* **1999**, *32*, 1847.

[108] P. Guinot, L. Bryant, T. Y. Chow, T. Saegusa, *Macromol. Chem. Phys.* **1996**, *197*, 1.

[109] G. Cai, M. H. Litt, *J. Polym. Sci. Polym. Chem.* **1996**, *34*, 2679.

[110] S. Kobayashi, H. Uyama, Y. Narita, *Macromolecules* **1992**, *25*, 3232.

[111] S. Kobayashi, H. Uyama, Y. Narita, *Macromolecules* **1990**, *23*, 353.

[112] M. Grasmüller, J. C. Rueda-Sanchez, B. Voit, O. Nuyken, *Macromol. Symp.* **1998**, *127*, 109.

[113] G. Sinai-Zingde, A. Verma, Q. Liu, A. Brink, J. M. Bronk, H. Marand, J. E. McGrath, J. S. Riffle, *Chem. Macromol. Symp.* **1991**, *42/43*, 329.

[114] G. Hochwimmer, O. Nuyken, U. S. Schubert, *Macromol. Rapid Commun.* **1998**, *19*, 309.

[115] S. Kobayashi, H. Uyama, T. Mori, Y. Narita, *Chem. Lett.* **1991**, *10*, 1771.

[116] M. Einzmann, W. H. Binder, *J. Polym. Sci. Polym. Chem.* **2001**, *39*, 2821.

[117] R. Jordan, K. Martin, H. J. Räder, K. K. Unger, *Macromolecules* **2001**, *34*, 8858.

[118] R. Jordan, A. Ulman, *J. Am. Chem. Soc.* **1998**, *120*, 243.

[119] R. Weberskirch, O. Nuyken, *J. Macromol. Sci. - Pure Appl.* **1999**, *36*, 843.

[120] J. M. Rodriguez-Parada, V. Percec, *J. Polym. Sci., Polym. Chem. Ed.* **1987**, *25*, 2269.

[121] G. Cai, M. H. Litt, *J. Polym. Sci., Polym. Chem.* **1992**, *30*, 671.

[122] T. Kotre, O. Nuyken, R. Weberskirch, *Macromol. Chem. Phys.* **2002**, *205*, 1187.

[123] D. Schönfelder, R. Weberskirch, O. Nuyken, *Polym. Prep., Am. Chem. Soc.* **2004**, *45*, 450.

[124] P. Persigehl, *Dissertation*, TU-München, **2000**.

[125] P. Persigehl, R. Jordan, O. Nuyken, *Macromolecules* **2000**, *33*, 6977.

[126] M. T. Zarka, O. Nuyken, R. Weberskirch, *Chem. Eur. J.* **2003**, *9*, 3228.

[127] T. B. Bonne, K. Lüdtke, R. Jordan, P. Stepanek, C. M. Papadakis, *Colloid and Polym. Sci.* **2004**, *282*, 833.

[128] Y. Chujo, E. Ihara, T. Seagusa, *Macromolecules* **1989**, *22*, 2044.

[129] T. Kagiya, T. Matsuda, M. Nakato, R. Hirata, *J. Macromol. Sci., Chem.* **1972**, *A6*, 1631.

[130] S. Kobayashi, H. Uyama, H. Shirasaka, *Macromol. Chem., Rapid Commun.* **1990**, *11*, 11.

[131] M. Miyamoto, Y. Sano, Y. Kimura, T. Saegusa, *Macromolecules* **1985**, *18*, 1641.

[132] O. Nuyken, G. Maier, A. Groß, H. Fischer, *Macromol. Chem. Phys.* **1996**, *197*, 83.

[133] S. Kobayashi, E. Masuda, D. Shoda, Y. Shimano, *Macromolecules* **1989**, *22*, 2878.

[134] P. Deslongchamps, S. Dube, C. Lebreux, D. R. Patterson, R. J. Taillefer, *Can. J. Chem.* **1975**, *53*, 2791.

[135] M. J. Kurth, E. G. Brown, O. H. W. Decker, *J. Org. Chem.* **1985**, *50*, 4984.

[136] G. H. Hsiue, A. X. Swamikannu, M. H. Litt, *J. Polym. Sci. Polym. Chem.* **1988**, *26*, 3043.

[137] S. Kobayashi, H. Uyama, *Macromolecules* **1991**, *24*, 5473.

[138] M. K. Kaloustaian, M. I. A.-L. d. Gutierrez, R. B. Nader, *J. Org. Chem.* **1979**, *44*, 666.

[139] M. Dreme, P. L. Perchec, J. Garapon, B. Sillion, *Tetrahedron Lett.* **1982**, *23*, 73.

[140] M. Dreme, S. Brunel, M. F. Llauro, P. L. Perchec, J. Garapon, B. Sillion, *Tetrahedron* **1984**, *40*, 349.

[141] S. Brunel, B. Fixari, P. L. Perchec, B. Sillion, *Tetrahedron Lett.* **1985**, *26*, 1013.

[142] S. Büchel, *Dissertation*, TU-München, **2001**.

[143] A. Groß, *Dissertation*, Bayreuth, **1994**.

[144] U. Hersel, C. Dahmen, H. Kessler, *Biomaterials* **2003**, *24*, 4385.

[145] M. Morpurgo, E. A. Bayer, M. Wilchek, *J. Biochem. Biophys. Methods* **1999**, *38*, 17.

[146] A. Kondoh, K. Makino, T. Matsuda, *J. Appl. Polym. Sci.* **1993**, *47*, 1983.

[147] M. R. Kim, J. H. Jeong, T. G. Park, *Biotechn. Prog.* **2002**, *18*, 495.

[148] P. Banarjee, D. J. Irvine, A. M. Mayes, L. G. Griffith, *J. Biomed. Mat. Res.* **2000**, *50*, 331.

[149] Y. W. Tong, M. S. Shoichet, *J. Biomed. Mat. Res.* **1998**, *42*, 85.

[150] S. P. Massia, J. A. Hubbell, *J. Biomed. Mat. Res.* **1991**, *25*, 223.

[151] K. Nilsson, K. Mosbach, *Methods Enzymol* **1984**, *104*, 56.

[152] S. P. Massia, J. A. Hubbell, *Ann. NY Acad. Sci.* **1990**, *589*, 261.

[153] J. P. Tam, Q. Yu, Z. Miao, *Biopolymers* **1999**, *51*, 311.

[154] G. Tuchscherer, *Tetrahedron Lett.* **1993**, *34*, 8419.

[155] F. Wahl, M. Mutter, *Tetrahedron Lett.* **1996**, *37*, 6861.

[156] J. P. Tam, C. Rao, C.-F. Liu, J. Shao, *Int. J. Peptide Protein Res.* **1995**, *45*, 209.

[157] P. E. Dawson, S. B. H. Kent, *J. Am. Chem. Soc.* **1993**, *115*, 7263.

[158] D. L. Elbert, J. A. Hubbell, *Biomacromolecules* **2001**, *2*, 430.

[159] M. Kantlehner, P. Schaffner, D. Finsinger, J. Meyer, A. Jonczyk, B. Diefenbach, B. Nies, G. Hölzemann, S. L. Goodman, H. Kessler, *ChemBioChem* **2000**, *1*, 107.

[160] R. A. Stile, K. E. Healy, *Biomacromolecules* **2001**, *2*, 185.

[161] T. Hamma, P. S. Miller, *Bioconjugate Chem.* **2003**, *14*, 320.

[162] L. Scheibler, P. Dumy, M. Boncheva, K. Leufgen, H.-J. Mathieu, M. Mutter, H. Vogel, *Angew. Chem. Int. Ed.* **1999**, *38*, 696.

[163] G. Thumshirn, U. Hersel, S. L. Goodman, H. Kessler, *Chem. Eur. J.* **2003**, *9*, 2717.

[164] A. Mayer, S. Neuenhofer, *Angew. Chem.* **1994**, *106*, 1097.

[165] W. H. Velander, R. D. Madurawe, A. Subramanian, G. Kumar, G. Sinai-Zingde, J. S. Riffle, C. L. Orthner, *Biotechn. Bioeng.* **1992**, *39*, 1024.

[166] A. Levy, M. Litt, *J. Polym. Sci. Polym. Chem.* **1968**, *6*, 1883.

[167] M. B. Foreman, J. P. Coffman, M. J. Murcia, S. Cesana, R. Jordan, G. S. Smith, C. A. Naumann, *Langmuir* **2003**, *19*, 326.

[168] D. Christova, R. Velichova, E. J. Goethals, *Macromol. Rapid Commun.* **1997**, *18*, 1067.

[169] M. Miyamoto, Y. Sano, Y. Kimura, T. Saegusa, *Macromolecules* **1989**, *22*, 1604.

[170] C. D. Eisenbach, E. Stadler, *Macomol. Chem. Phys.* **1995**, *196*, 833.

[171] R. Barbaro, L. Betti, M. Botta, F. Corelli, G. Giannaccini, L. Maccari, F. Manetti, G. Strappaghetti, S. Corsano, *J. Med. Chem.* **2001**, *44*, 2118.

[172] T. Saegusa, H. Ikeda, H. Fujii, *Macromolecules* **1972**, *5*, 359.

[173] L. L. Kiessling, J. E. Gestwicki, L. E. Strong, *Curr. Opin. Cell Biol.* **2000**, *4*, 696.

Appendix

Molecular structure of the peptides

C(-R(Pbf)GD(O^{t}Bu)fK-)-piperidine (**PEP1**)

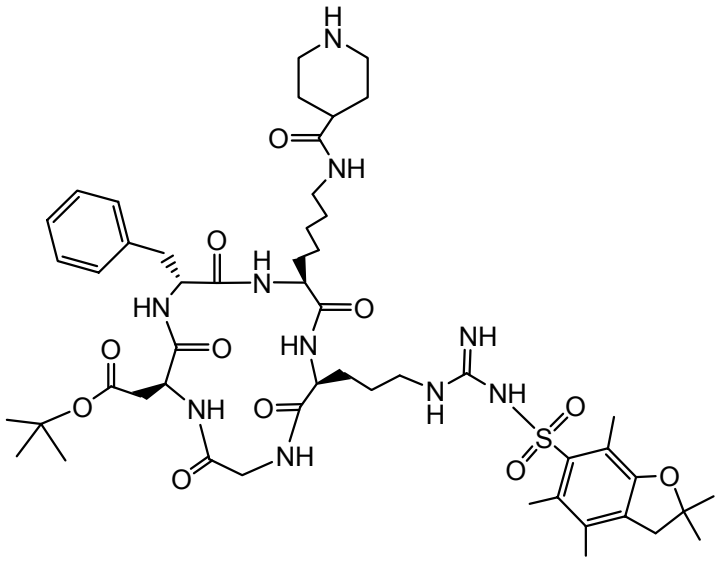

c(-R(Pbf)GD(O^{t}Bu)yK-) (**PEP2**)

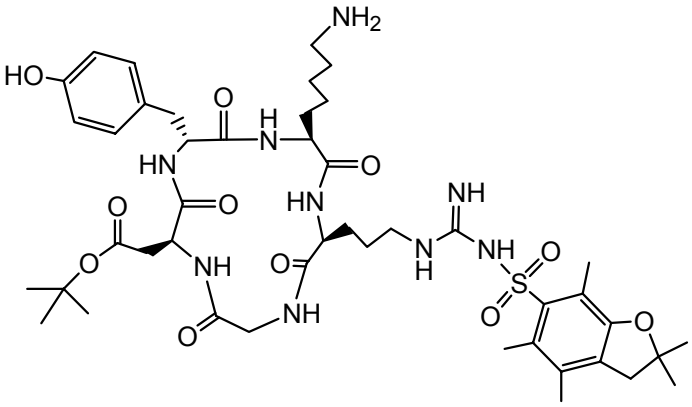

c(-RGDfE-)-Ahx-C (**PEP3**)

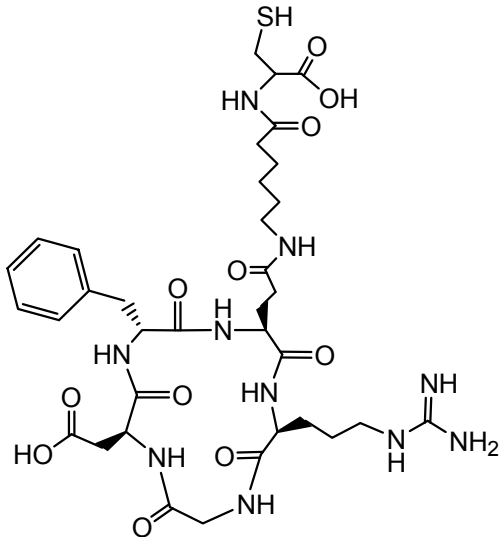

c(-R(Pbf)GD(O^{t}Bu)fK-)-Ahx-Ahx-Ahx-NCS (**PEP4**)

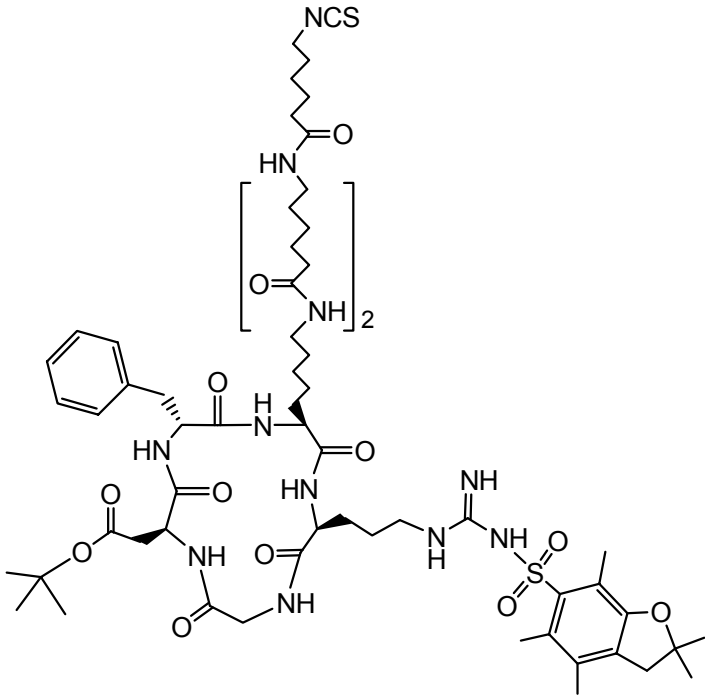

FCGKF (**PEP5**)

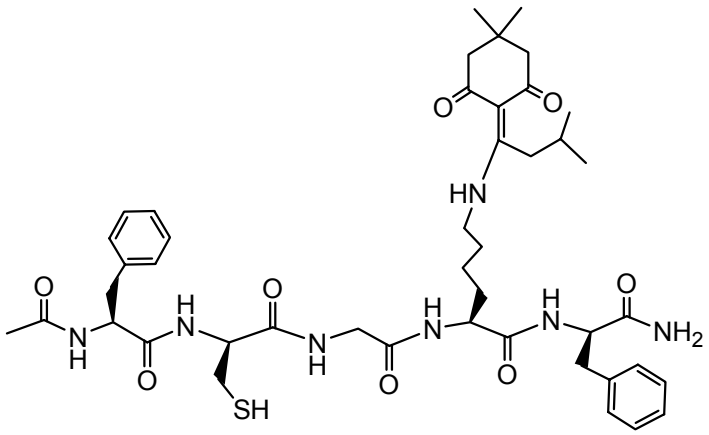

Monomers

2-(2-methoxycarbonylethyl)-2-oxazoline (**(MeEstOx)Mmer**)

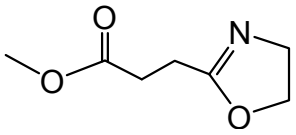

(N-Boc-5-amino pentyl)-2-oxazoline (**(AminoOx)Mmer**)

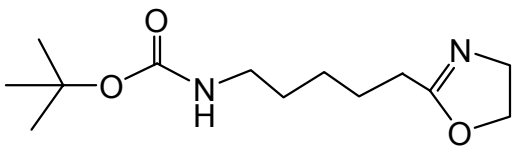

Terminating agent

1-(2,2-diethoxy-ethyl)-piperazine (**Pip-Acetal**)

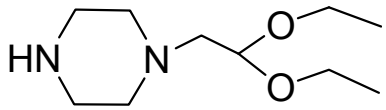

Functionalized polymers

Poly(2-methyl-2-oxazoline) terminated ethyl ester (**P(MeOx)-Ter-EtEst**)

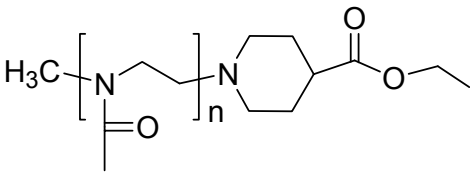

Poly(2-methyl-2-oxazoline) terminated carboxylic acid (**P(MeOx)-Ter-CarAc**)

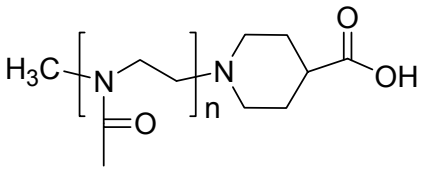

Poly(2-methyl-2-oxazoline) terminated acrylic acid (**P(MeOx)-Ter-AcrAc**)

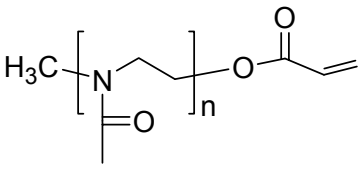

Poly(2-methyl-2-oxazoline) terminated maleimide (**P(MeOx)-Ter-MalIm**)

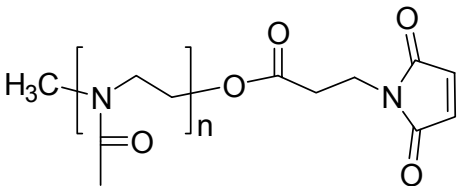

Poly(2-methyl-2-oxazoline) terminated acetal (**P(MeOx)-Ter-Acetal**)

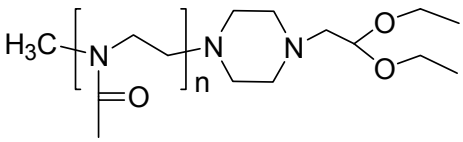

Poly(2-methyl-2-oxazoline) terminated formaldehyde (**P(MeOx)-Ter-Acetal**)

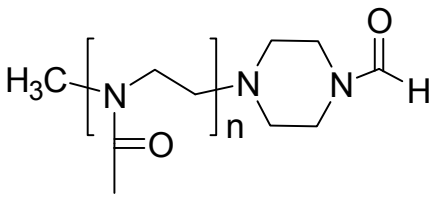

Poly(2-methyl-2-oxazoline) terminated piperazine (**P(MeOx)-Ter-Pipaz**)

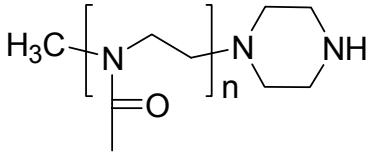

Poly(2-methoxycarbonylethyl)-2-oxazoline) (**P(MeEstOx)**)

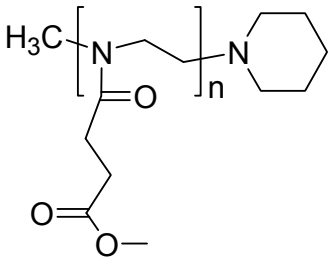

Poly[(2-methyl-2-oxazoline)-*stat*-(2-(2-methoxycarbonylethyl-2-oxazoline))]
(**P[(MeOx)-*stat*-(MeEstOx)]**)

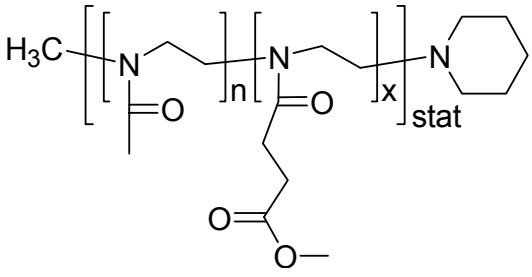

Poly[(2-methyl-2-oxazoline)-*stat*-(2-(2-propionic acid ethyl -2-oxazoline))] (**P[(MeOx)-*stat*-(CarAcOx)]**)

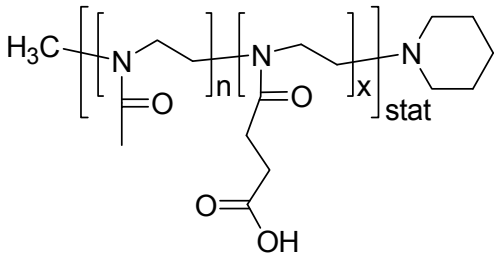

Poly[(2-methyl-2-oxazoline)-*b*-(2-(2-methoxycarbonylethyl-2-oxazoline))] terminated methyl ester (**P[(MeOx)-*b*-(MeEstOx)]-Ter-MeEst**)

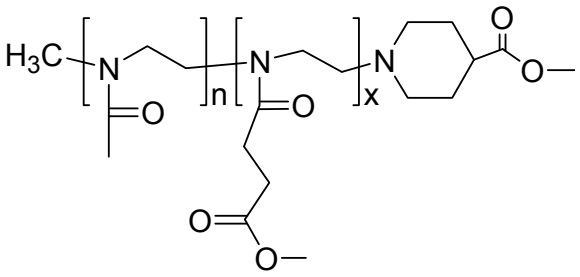

Poly[(2-methyl-2-oxazoline)-*b*-(2-(2-propionic acid ethyl-2-oxazoline))] terminated carboxylic acid (**P[(MeOx)-*b*-(CarAcOx)]-Ter-CarAc**)

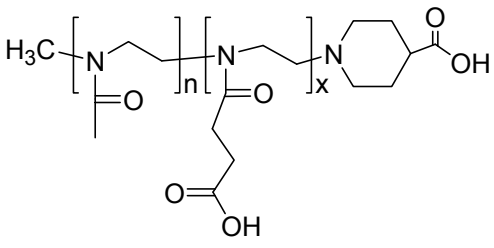

Poly(2-methoxycarbonylethyl)-2-oxazoline) modified diethyldiamine (**P(MeEstOx) mod. diethyldiamine**)

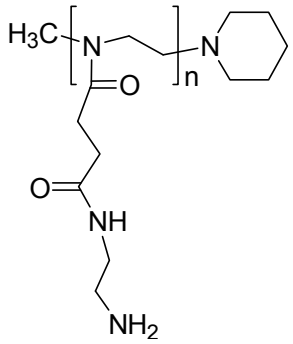

Poly(N-Boc-5-amino pentyl-2-oxazoline) (**P(BocAmineOx)**)

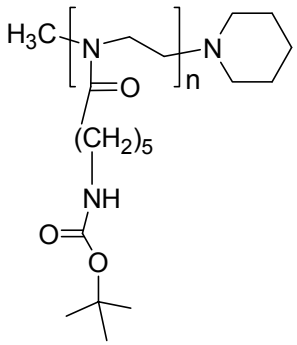

Poly(5-amino pentyl-2-oxazoline) (**P(AmineOx)**)